Fakultät für Medizin

Institut für Molekulare Immunologie

Chemically modified mRNA Therapeutics for Bone Regeneration

Wen Zhang

Vollständiger Abdruck der von der Fakultät für Medizin der Technischen Universität München zur Erlangung des akademischen Grades eines

Doctor of Philosophy (Ph.D.)

genehmigten Dissertation.

Vorsitzende/r: Prof. Dr. Roland M. Schmid

Betreuer/in: Prof. Dr. Christian Plank

Prüfer der Dissertation:

1. Prof. Dr. Martijn van Griensven

2. Priv.-Doz. Dr. Carsten Rudolph

Die Dissertation wurde am 26. Juni 2019 bei der Fakultät für Medizin der Technischen Universität München eingereicht und durch die Fakultät für Medizin am 13. August 2019 angenommen.

Table of contents

1. Abstract

Five to 10% of bone fractures fail to heal, leaving patients with debilitating handicaps and society with a socio-economic burden of billons of Euros. Recombinant BMP-2 protein is used in the management of bone fractures. However, due to the short half-life of the protein, supraphysiological doses are applied, which is associated with side effects including heterotopic bone formation. It was the aim of this thesis, to establish an mRNA-based therapeutic technology for bone healing and to demonstrate proof of concept of its potency in a critical size femoral bone defect model in rats.

For this purpose, the concept of an osteo-inductive transcript-activated matrix (o-TAM) was adopted and optimized. The o-TAM developed here consists of a lipidoid nanoparticle formulation of chemically modified mRNA (cmRNA) construct encoding bone morphogenetic protein (BMP)-2 loaded on collagen sponges. The o-TAM was designed to be placed within a bone defect in order to be colonized by cells which would be transfected within the o-TAM matrix and thus produce the encoded BMP protein. This would induce osteogenic differentiation in an autocrine and paracrine manner and result in improved bone healing.

Thus, a new chemically modified mRNA (cmRNA) construct encoding bone morphogenetic protein (BMP)-2 with improved osteogenic features was designed and manufactured by in vitro transcription. An upstream open reading frame in the 5'UTR and a polyadenylation element together with an AU-rich tract in the 3'UTR of the human wild type sequence were removed. Instead of the wild type 5’UTR, a translation initiator of short UTRs (TISU) was placed upstream of the coding sequence and 5-iodo-modified pyrimidine nucleotides were introduced into the sequence to minimize the immunogenicity of the mRNA.

The new TISU BMP-2 cmRNA displayed robust BMP-2 production in vitro in cell lines (HEK293 and MC3T3) and primary cells (muscle-derived mesenchymal stem cells). Stem cells

additionally showed upregulation of both osteogenic and angiogenic genes upon TISU BMP-2 cmRNA transfection. The in vivo osteogenic properties of TISU BMP-2 cmRNA were explored in a critical-size femoral bone defect in the rat. Animals treated with TISU BMP-2 cmRNA displayed superior bone formation that appeared to recapitulate endochondral ossification while the bone defects in control groups did not bridge at all. The higher of the two doses examined in this model showed significantly greater new tissue formation. Furthermore, improved vascularization was also detected in the healing area of TISU BMP-2 cmRNA-treated animals. Based on a tendency for a dose effect was observed, we decided to investigate the dose-response over a greater range (5 µg, 10 µg, 25 µg, 50 µg), with TISU BMP-2 cmRNA directly loaded on collagen sponge before surgery without freeze-drying. The micro-computed tomography results clearly demonstrated dose-dependent bone formation. Not only did the 50 µg TISU group display the best bone healing among all the groups, even more bone formation was detected compared with the application of 11 µg recombinant BMP-2 protein at the end of the 8-week observation period. These findings were confirmed by histological analysis. When a luciferase-encoding TAM was placed within the bone defect, bioluminescence imaging demonstrated that the mRNA was restricted to the defect area. Cytokine expression after surgery showed no significant immunogenicity of TISU BMP-2 cmRNA compared to the negative control group.

In summary, the results of this thesis constitute a promising technology for the treatment of non-healing bone defects and a promising alternative to recombinant BMP-2 or gene therapy-based approaches for bone regeneration.

1. Zusmmenfassung

Fünf bis zehn Prozent der Knochenbrüche heilen nicht, so dass Patienten an schwersten Behinderungen und Einschränkungen ihrer Lebensqualität leiden und die Gesellschaft eine sozioökonomische Belastung in Höhe von Milliarden Euro zu tragen hat. Das rekombinante BMP-2-Protein wird bei der Behandlung von Knochenbrüchen eingesetzt. Aufgrund der kurzen Halbwertszeit des Proteins werden jedoch supraphysiologische Dosen angewendet, was mit Nebenwirkungen wie heterotopem Knochenaufbau verbunden ist. Es war das Ziel dieser Arbeit, eine mRNA-basierte therapeutische Technologie für die Knochenheilung zu etablieren und den Wirksamkeitsnachweis in einem kritischen femoralen Knochendefektmodell bei Ratten zu erbringen.

Zu diesem Zweck wurde das Konzept einer osteoinduktiven transkript-aktivierten Matrix (o-TAM) übernommen und optimiert. Die hier entwickelte o-TAM besteht aus einer Lipidoid-Nanopartikelformulierung eines chemisch modifizierten mRNA (cmRNA)-Konstrukts, das für das nnochenmorphogenetische Protein (BMP)-2 kodiert, das auf Kollagenschwämme geladen ist. Die o-TAM wurde so konzipiert, dass sie in einen Knochendefekt eingebracht wird, um von Zellen besiedelt zu werden, die innerhalb der o-TAM-Matrix transfiziert werden und so das kodierte BMP-Protein produzieren. Dies würde zu einer osteogenen Differenzierung auf autokrine und parakrine Weise und zu einer verbesserten Knochenheilung führen.

Daher wurde ein neues chemisch modifiziertes mRNA (cmRNA)-Konstrukt, das für das Knochenmorphogenetische Protein (BMP)-2 mit verbesserten osteogenen Eigenschaften kodiert, entworfen und durch in vitro-Transkription hergestellt. Ein stromaufwärts gelegener offener Leserahmen in der 5'-UTR und ein Polyadenylierungselement sowie ein AU-reicher Trakt in der 3'-UTR der menschlichen Wildtypsequenz wurden entfernt. Anstelle der Wildtyp-5'-UTR wurde ein Translationsinitiator von kurzen UTRs (TISU) stromaufwärts der kodierenden Sequenz platziert und 5-Jodo-modifizierte Pyrimidin-Nukleotide in die Sequenz eingeführt, um die Immunogenität der mRNA zu minimieren.

Im ersten Teil dieser Arbeit zeigte die neue TISU BMP-2 cmRNA eine robuste BMP-2-Produktion in vitro in Zelllinien (HEK293 und MC3T3) und Primärzellen (aus Muskel isolierte mesenchymale Stammzellen). Die Stammzellen zeigten zusätzlich eine Hochregulation sowohl osteogener als auch angiogener Gene bei der TISU BMP-2 cmRNA-Transfektion. Die in vivo osteogenen Eigenschaften der TISU BMP-2 cmRNA wurden in einem kritisch großen femoralen Knochendefekt bei der Ratte untersucht. Tiere, die mit TISU BMP-2 cmRNA behandelt wurden, zeigten eine überlegene Knochenbildung, die die endochondrale Ossifikation zu rekapitulieren schien, während die Knochendefekte in den Kontrollgruppen überhaupt keine Brücke bildeten. Die höhere der beiden in diesem Modell untersuchten Dosen zeigte eine signifikant größere Neubildung von Gewebe. Darüber hinaus wurde auch im Heilungsbereich von TISU BMP-2 cmRNA-behandelten Tieren eine verbesserte Vaskularisation festgestellt.

Da im ersten Teil der Studie eine Tendenz zu einer Dosiswirkung beobachtet wurde, haben wir uns entschieden, die Dosis-Wirkungsbeziehung über einen größeren Bereich (5 µg, 10 µg, 25 µg, 50 µg) zu untersuchen, wobei TISU BMP-2 cmRNA vor der Operation direkt auf Kollagenschwamm geladen wurde, ohne die o-TAM gefrierzutrocken. Die Ergebnisse der Mikro-Computertomographie zeigten deutlich die dosisabhängige Knochenbildung. Die 50 µg TISU-Gruppe zeigte nicht nur die beste Knochenheilung unter allen Gruppen, sondern es wurde auch noch mehr Knochenbildung festgestellt als bei der Anwendung von 11 µg rekombinantem BMP-2-Protein. Diese Ergebnisse wurden durch histologische Analysen bestätigt. Als eine Luziferase-kodierendes TAM innerhalb des Knochendefektes platziert wurde, zeigte die Biolumineszenz-Bildgebung, dass die mRNA auf den Defektbereich beschränkt war. Die Zytokinexpression nach der Operation zeigte keine signifikante Immunogenität der TISU BMP-2 cmRNA im Vergleich zur Negativkontrollgruppe.

Zusammenfassend lässt sich feststellen, dass die Ergebnisse dieser Arbeit eine vielversprechende Technologie für die Behandlung von nicht heilenden Knochendefekten und eine vielversprechende Alternative zu rekombinantem BMP-2 oder gentherapeutischen Ansätzen zur Knochenregeneration darstellen.

2. Introduction

2.1 Bone tissue regeneration

For a considerable time, clinical researchers have been attempting to solve various bone healing problems that arise from severe trauma, bone tumors, fractures, and osteoporosis. One of the current treatments is autograft implantation. In this procedure, pieces of bone taken from the patient's iliac crest are transplanted to the defective site. Indeed, autografting remains the gold-standard graft material, because it naturally possesses both osteoinductive and osteoconductive properties and is associated with a low risk for rejection [1, 2]. However, there are several disadvantages associated with an autograft, including limited source, increased surgery time, limited donor-site availability, and donor-site pain — with rates that vary significantly in the literature [3-7]. All these limitations mean that autologous bone graft is not an optimal treatment. To overcome these problems, different forms of bone grafts have been investigated [8]. Table1 provides a summary of the advantages and disadvantages of possible different bone grafts [9].

Table 1. Advantages and disadvantages of different bone grafts [10].

	Advantages	**Disadvantages**
Autograft	• Osteogenic • Osteoconductive • Osteoinductive	• High patient morbidity: pain and infection at donor site, possible visceral injury during harvesting • Lack of vascularization • Limited availability and quantity
Allograft or xenograft	• Osteoconductive • Osteoinductive • High availability • No donor site morbidity	• Lack of osteogenicity and vascularization • Relatively higher rejection risk • Risk of disease transmission • High cost

	Advantages	Disadvantages
Engineered grafts	• Capability to integrate growth factors and stem cells for osteogenicity and graft incorporation improvement • Shaped to fit site defects • No donor site morbidity	• Osteogenicity limited by material porosity (due to manufacturing process) • Variable biodegradability of different materials • Poor neovascularization • Unknown immune response • Limited mechanical properties

With the development of engineered grafts, the concept of tissue engineering has encompassed the combination of therapeutic molecules, biomaterials, and/or cells. Recent studies have shown that culturing cells using three-dimensional (3D) scaffolds more closely resembles the *in vivo* situation regarding cell signaling and cellular behavior, which can further influence cellular gene expression [11, 12].

2.1.1 3D matrices

3D matrices for cell culture can be considered as scaffolds used as 3D structures for cells to attach, grow, migrate, and proliferate [13, 14]. Ultimately, it is important that such matrices can also support cell differentiation. As scaffolds/biomaterials have gained ever greater attention, metals, glasses, polymers, and ceramics were studied as 3D scaffolds for cell culture. Among these, polymers have gained the greatest interest because of the potential to adapt their chemical and structural properties. Polymer matrices can be further subdivided into synthetic (e.g. poly glycolic acid (PGA) and poly lactic acid (PLA)) and natural polymers (e.g. collagen and chitosan) [15, 16].

A critical requirement for all biomaterial scaffolds is to provide an extracellular matrix environment for supporting cell growth. Additionally, an ideal 3D scaffold for clinical purposes

should be biocompatible and biodegradable. Natural sources of polymers, including collagen, fulfill the requirements indicated above [17].

2.1.1.1 Collagen as natural polymer of choice

Collagen is one of the most frequently used and highly biocompatible natural polymers for 3D cell culture. Because of the characteristics of collagen sponges, they can not only modify cell migration, attachment, adhesion, and distribution [18], but also possibly facilitate cellular differentiation through differential functional gene expression in the cells as well as provide mechanical support [19]. Among many reported types of collagen, collagen type I (Col I) (located in skin and bone), Col II (cartilage), and Col III (blood-vessel walls) are still considered as the best potential candidates [16, 19].

Collagen-based implants have been evaluated for dermal tissues and burn wounds [20, 21], bone regeneration [22, 23], blood vessels and heart valves[24, 25], periodontal tissues[26], and peripheral nerve regeneration[27]. Additionally, collagens have been successfully used in gene and drug delivery in the forms of films, shields, sponges, gels, and tablets [19, 28-31]. Indeed, collagen is currently the only FDA-approved carrier for recombinant bone morphogenetic protein 2 (BMP-2), which is used for bone healing [32].

2.1.1.2 Collagen sponges for sustained cmRNA delivery

Over recent years, finding an approach to achieve sustained gene or drug delivery has become an increasing focus for researchers. Collagen sponges as a sustained delivery system may lead to a better acceptance as a therapeutic approach in patients [33, 34]. In the case of cmRNA therapy, this sustained delivery system can be particularly suitable when aiming for long-term protein expression. Therefore, collagen sponges were tested for the first time as matrices for sustained cmRNA delivery both *in vitro* and *in vivo* [35]. The results showed that vacuum-dried cmRNA-loaded collagen sponges, known as transcript-activated matrices (TAMs), enable

steady protein production for up to 6 days and substantial residual expression until day 11 post-transfection [35]. Based on these findings, the collagen sponge was chosen for sustained cmRNA delivery for this thesis, both *in vitro* and *in vivo*.

2.1.2 Therapeutic Molecules

2.1.2.1 Bone morphogenetic proteins (BMPs)

Since Hanamura and Urist[36] first identified the ectopic osteogenesis factors in the decalcified bone matrix as BMPs, at least 15 BMPs (BMP1–15) have been cloned. BMPs are a group of secreted, hydrophobic, and acidic glycoproteins, with the exception of BMP-1, which belong to the TGF-β (transforming growth factor-beta) superfamily [37]. This group of proteins can induce the formation of bone, cartilage, and bone-related connective tissue via paracrine and autocrine forms *in vivo* [38]. There is already a great body of research focusing on the multi-functions and biomedical applications of BMPs.

2.1.3 Stem and progenitor cells: BMPs Signaling System

The critical factors for tissue regeneration are actually the proliferation and differentiation of immature precursor cells. These immature precursor cells include mesenchymal stem cells (MSCs), which are a group of cells possessing the potential to differentiate and proliferate. To determine the development of these MSCs, several different signaling pathways always operate together. Rather than angiogenesis, here we mainly focused on the osteogenesis potentiality [39] and BMPs signaling.

There are two forms of transmembrane serine/threonine kinase receptors: BMP-I receptor (BMPR-I) and BMP-II receptor (BMPR-II). BMPR-I can be further divided into BMPR-IA and BMPR-IB. The former receptor is widely expressed in many cell types *in vitro*, including

MC3T3-E1 fibroblasts, C2C12 myoblasts, and C3H10T1/2 pluripotent mesenchymal cells [40]. All the receptors play different roles during transduction of BMPs. It has been confirmed that there are at least two signal transduction pathways for BMP-2 activation, that is, the Smad and MAPK pathways[41].

2.1.3.1 Smad pathway

Following BMP-2 association with BMPR-II/BMPR-I complexes, BMPR-II activation can further facilitate phosphorylation of the GS domain of BMPR-I, which continues acting on downstream Smads [42]. Smads can be classified into three groups: receptor-activated Smads (R-smads); co-mediated Smad (common-mediated smad, C-smad); inhibitory Smads (I-smads). The R-smads, Smad1, Smad5, and Smad8 are direct substrates of BMPR-I. The complex formed by these three activated R-Smads binds with Smad4 and translocate into the nucleus to combine with different DNA-binding proteins, including co-activators and inhibitors. This causes further transcription of downstream BMP-related genes, thereby regulating cell differentiation [43].

2.1.3.2 MAPKs pathway

When BMP-2 binds to BMPR-I with high affinity to form a complex at the cell surface [44], free BMPR-II in the cytoplasm can be recruited to form heteromeric BISC (BMP-2 induced signaling complex) via the BMPR-I complex. BMPR-Is indirectly linked to transforming growth factor beta-activated kinase1(TAK1) can activate p38 MAPK, which transduces the signaling pathway of BMPs. Studies have shown that p38 MAPK inhibition also inhibits the expression levels of alkaline phosphatase and bone calcium, leading to delayed osteogenic differentiation [45]. When p38 MAPK is not inhibited, it activates downstream genes by direct phosphorylation of runt-related transcription factor 2 (RUNX2) and Osterix (Osx) [46], or

indirectly via other kinases to express osteogenic molecules, including among others alkaline phosphatase, osteocalcin (OCN), and bone sialoprotein (BSP) [47].

2.1.3.3 Other important regulating factors

Some important transcription factors that regulate BMP signaling pathways have been discovered during recent years, including the positive regulatory factors RUNX2, and Osx, and negative regulatory factors. The positive factor RUNX2 can recognize the osteoblast-specific cis-acting element 2, which appears in some osteogenic-specific gene promoter regions of Col I and osteopontin (OPN) [48]. In C3H10T1/2 fibroblast cells, BMP-2 and BMP-7 can induce Cbfa1 expression, which can further induce the expression of osteogenic marker protein [49]. Another positive factor, Osx, is expressed by osteoblasts in mice and its homologue is also known as Sp7. Sp7/Osx, first discovered in BMP-2-induced myoblast C2C12, can regulate the expression of many important osteogenic genes, including OCN, OPN, and Col I [50, 51]. BMP-2 can up-regulate Sp7/Osx expression. Runx2 may be located upstream of Sp7/Osx to regulate osteogenesis differentiation [52]. Therefore, it is believed that Sp7/Osx plays an important role in the terminal differentiation and maturation of osteoblasts. Dlx5 and 6 are expressed during the late stage of osteoblast differentiation, and are mainly responsible for regulating the expression of two types of collagens and OCN, causing calcification of extracellular matrix. BMP-2 can induce Dlx5 expression in osteoblasts, chondrocytes, and non-bone cells [52].

BMPs can not only induce RUNX2, Osx, Dlx, and other transcription factors that promote osteogenesis, but also induce some negative regulation of osteogenesis by osteogenesis-deficient transcription factors. Such negative regulation by BMPs also has a greatly significant influence on both physiological and pathological phenomena.

2.2 Controversy in clinical applications of BMPs

In addition to stimulating MSC differentiation to osteoblasts and chondroblasts, BMPs can also induce endochondral ossification based on the microenvironment where cells are located. Therefore, they have been considered to be among the most important physiological mediatory factors in the healing process of bone fractures and defects. Following the sequencing and cloning of all the BMP genes in the early 1990s, large-scale production of different BMPs became feasible. In the past decade, 20 individual human recombinant BMPs (rhBMPs) possessing various bone- and cartilage-stimulation characteristics were identified [53]. Pre-clinical and clinical studies showed that rhBMP-2/ rhBMP-7-loaded absorbable gelatin sponges can be implanted into the fracture site to induce bone formation and act as a replacement for autologous transplantation [54, 55]. Subsequently, in a multicenter follow-up study, InFUSE Bone Graft/LT-CAGE Lumbar Tapered Fusion Device (Medtronic Sofamor Danek, Memphis, TN) and autograft were compared for clinical and radiographic fusion following anterior lumbar interbody fusion (ALIF), with a significant increase in radiographic fusion being achieved in the rhBMP-2 loaded group at the 2-year follow-up [3]. On the basis of this pilot work, the FDA granted approval in 2003 for rhBMP-2 use in conjunction with the LT-CAGE™ Lumbar Tapered Fusion Device for ALIF. However, from 2006 onwards, independent research groups started to report serious side effects of rhBMP-2 use, with complication rates ranging from 20 to 70% [4]. The most notable complications included retrograde ejaculation, seroma formation, bone overgrowth, osteolysis, and an increased risk for cancer.

As for another well-studied BMP, several independent studies demonstrated superior bone formation with BMP-7 (known as OP-1) versus autograft alone in different models [56, 57]. However, an FDA approved study including 4,000 patients [58] actually showed lower bone formation in OP-1-treated patients than the autograft-treated group in an up to 3-year follow-up, which finally led to the rejection of Pre-Market Approval of OP-1 by the FDA in 2009.

Although this has been considered as a significant setback for the clinical application of BMPs, it still indicates the huge potentiality of the application of BMPs in orthopedics.

The risks for uncontrolled bone formation, anti-BMP antibody formation, bone resorption, immunogenicity, urethrogenital complications, and malignancies have yet to be fully characterized. All of this on the recent backdrop of research controversy makes it difficult for clinicians to understand the proper use of BMP in a clinical setting. However, this controversy has in the meantime became the stimulus for novel treatment studies instead of conventional protein therapy.

2.2.1 Gene Therapy

To generate functional, and eventually clinical biological substitutes in tissue engineering and regenerative medicine, the utilization of technologies derived from chemistry, material science, stem cell biology, and therapeutic molecule engineering have been applied. The most increasingly investigated therapy is therapeutic molecule engineering. Gene and protein therapies have been developed for a variety of medical indications, ranging from hereditary or acquired metabolic diseases to regenerative medicine. Despite the progress that has been made in these two therapies, there remained considerable complications. In contrast to the risks for insertional mutagenesis in gene therapy and the consequent induction of aberrant endogenous gene expression, protein therapy has several safety concerns regarding immunogenic responses, high costs, and relative short storage among others [59-61]. With the increased understanding of mRNA's essential role in gene expression, the alternative treatment of transcript therapy using mRNA as a new therapeutic approach has been developed.

2.2.2 Transcript Therapy

mRNA transcript therapy is technically and conceptually similar to gene therapy, however it uses mRNA as the active pharmaceutic ingredient instead of plasmid DNA or viral constructs.

The advantages of mRNA therapeutics are: i) the ability to bypass the barrier of the nuclear membrane for successful gene transfer by directly delivering mRNA into the cytoplasm and transfecting non-dividing or non-mitotic cells, ii) rapid, transient and predictable protein expression kinetics, which allows temporal regulation, iii) no risk of genomic integration, and iv) utility with non-viral delivery technologies in cancer immunotherapy [62, 63], vaccine development [64-66], etc. All the advantages indicated above predict the significant potentiality of mRNA therapy or transcript therapy in tissue engineering.

2.3 Messenger RNA: Definitions and therapeutic applications

When mRNA was first discovered in 1960, it was described as the middle product during the process from DNA to protein. By definition, mRNA is a single-strand transcript containing the coding sequence of a given gene, transferring the genetic information from the nucleus to the ribosome, where the genetic information is translated to a specific protein (Fig. 1).

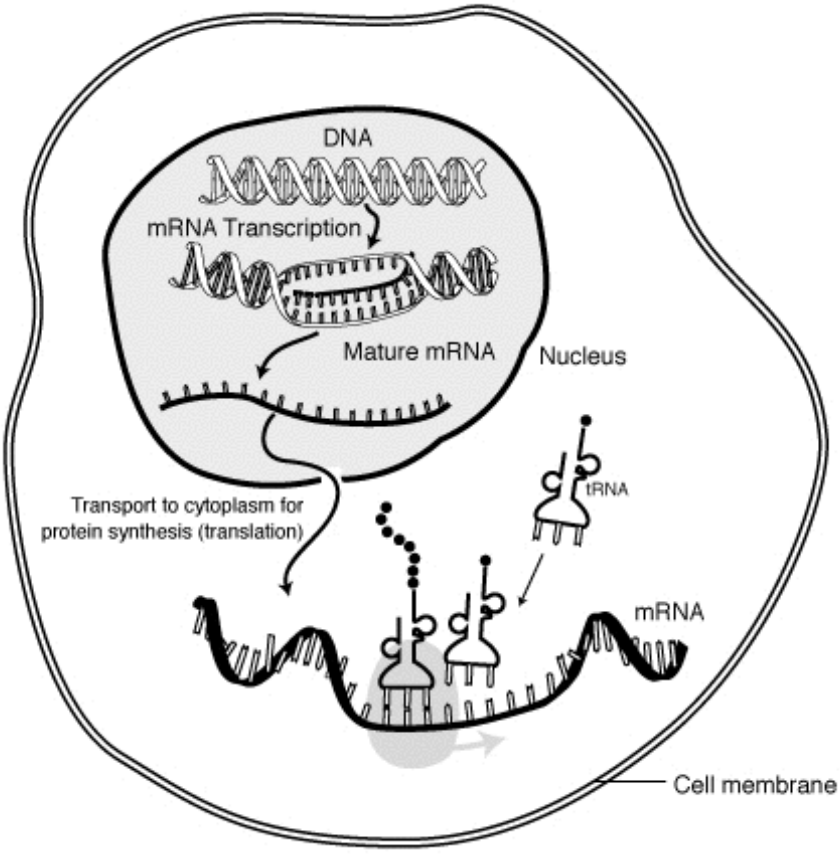

Fig.1. Transcription and translation: From DNA to protein (resource: National Human Genome Research Institute)

2.3.1 The structure of mRNA

A mature mRNA consists of a 5' cap, 5' untranslated region (5'-UTR), coding region, 3'-UTR, and poly (A) tail. The genetic information for protein production is located within the coding sequence, also known as the open reading frame (ORF). The ORF starts with the start codon, AUG, and terminates with one of the stop codons, UAA, UAG, or UGA. Other regions cannot be translated into amino acids. The 5'- and the 3'-end of the mRNA body are called untranslated regions (UTRs), known as the regulatory regions. Decades earlier, there was little understanding regarding the function of these UTR regions. However, as more research has been performed regarding these regions, this has since revealed their important roles in mRNA stability and translational efficiency [67, 68]. (The general structure shown in Fig. 2)

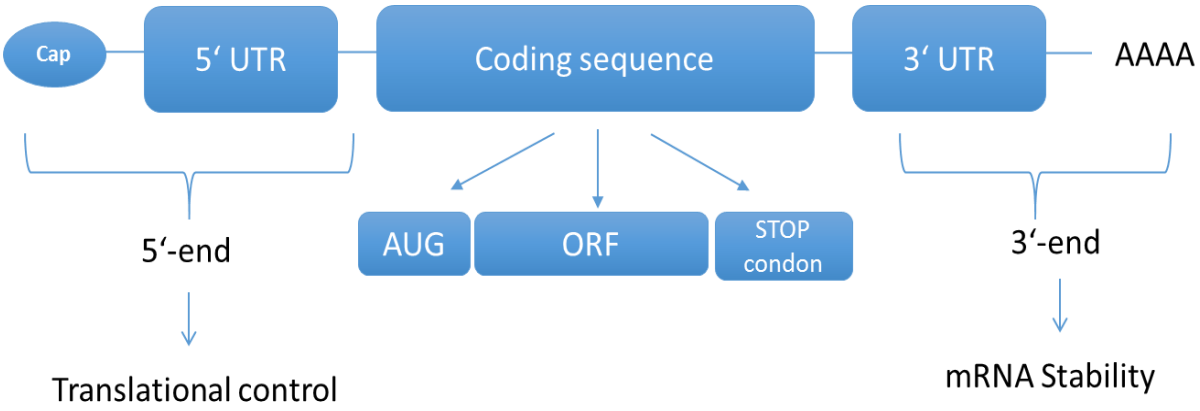

Fig.2. Structure of a mature eukaryotic mRNA.

2.3.2 Untranslated region of mRNA

UTRs, as known, do not have a direct effect on the amino acid sequence of translated protein, but do greatly influence mRNA stability as well as the efficiency of its translation. This is due to the regulation of mRNA stability by certain regulatory elements, which are localized within the mRNA structure [69]. Some examples of regulatory elements are upstream ORFs (uORFs), the poly(A) tail , and the AU-rich elements.

In 5'-UTRs of eukaryotic mRNAs, uORFs are increasingly recognized as important elements that regulate cellular protein synthesis. These uORFs can either be translated or skipped by the scanning machinery pre-initiation complex [70]. The potential regulatory functions of uORFs have been studied in the context of numerous individual genes [71, 72]. Translation of these uORFs can lead to decreased protein synthesis from the main ORF in most studied examples [73]. uORFs have frequently been implicated as translational repressors; a good example of an uORF activity study is for GCN4, in which uORFs repressed translation of the main ORF [74].

The length of the poly (A) tail is known to be related to mRNA stability. Many studies have revealed the protective nature of the poly (A) tail in mRNA via deadenylation during the mRNA degradation pathway [75, 76]. In addition to protecting mRNA from degradation, the poly (A)

tail is also involved in the precursor mRNA's transportation from the nucleus to the cytoplasm and facilitating translation [77, 78]. For *in vitro*-transcribed mRNA (IVT mRNA), the poly (A) tail can be added via an enzymatic post-adenylation reaction or genetical insertion into the DNA template. In the case of post-adenylation, the length of the poly (A) tail is determined by the incubation time of the Escherichia coli poly (A) polymerase I enzyme.

Regarding the AU-rich elements, which are mainly responsible for mRNA instability, these are only located at the 3'-UTR. This destabilizing effect was demonstrated by experimental insertion of an AU-rich element from the RNA coding region for granulocyte/macrophage colony-stimulating factor (GM-CSF) into the 3'-UTR of beta-globin [79, 80].

2.3.3 Modifications to mRNA structure

Under natural conditions, mRNA compared to other RNAs, including tRNA and rRNA, clearly displays less stability. Cells can readily regulate the protein expression level via regulation of mRNA stability. mRNA being an essential member of the protein production machinery, its stability is closely associated with gene expression regulation. The above-mentioned structural elements all correlate with mRNA stability.

Another aspect restricting mRNA use as a therapeutic molecule is the induction of an innate immunogenic response. *In vitro* transcription (IVT) mRNAs are always recognized as exogenous RNAs, like viral RNAs, which subsequently activate the innate immune response, finally leading to the suppression of protein expression [81-83]. The question of how to resolve the immunogenic characteristic of IVT mRNAs has started to gain ever greater attention. Up to date, various chemical modifications have been incorporated into mRNAs applied in a wide range of studies. One of the most common modifications involves utilizing modified nucleosides. One example is pseudouridine (Ψ), with Ψ being a naturally occurring modified nucleoside produced by enzymatic isomerization, which can greatly reduce the immune

response and enhancing the translation efficiency of mRNAs [81]. Following the introduction of different chemical modifications into different mRNAs, Li et al. observed an improved protein expression level [84]. Subsequently, this improved protein expression was found to be highly dependent on the cell type, modification conditions, and encoding sequences. Similarly, Uchida and co-workers observed that various mRNA modifications displayed varied translation efficiency and immunogenicity in different cell lines [85]. In addition to potentially generating elevated protein expression levels, another advantage of chemically modified IVT mRNA is the reduction in immunogenicity. One study demonstrated that a replacement of 25% of the uridine and cytidine with 2-thiouridine and 5-methyl-cytidine, respectively, synergistically decreased mRNA binding to recognition receptors, including toll-like receptor 3 (TLR3), TLR7, and TLR8 and retinoid-inducible gene 1 (RIG-1), with substantially decreased activation of the innate immune system *in vitro* and *in vivo* [86].

2.3.3.1 Translation initiator of short UTR (TISU)

As studies of mRNA modification continued, scientists started to notice that the secondary structure has a very important role in determining mRNA functions. To avoid the loss of mRNA function and binding efficiency after incorporating modified nucleotides [86], the need for effective independent "shorter" UTRs has increased. Up to date, the major part of the related research has been performed using a Kozak element as a translational regulator. As these studies continued, a unique TISU present in approximately 5% in genes with short UTRs [87] was identified. Previous studies have shown that certain coding sequences have very short 5'-UTRs harboring a consensus sequence, namely the TISU-element [88].

As a greater understanding of mRNA, both structurally and functionally, has been achieved during recent decades, ever more attention has been directed towards the potentiality of mRNA as a therapeutic tool in gene transfer application.

2.3.3.2 *In Vitro* Transcribed mRNA

Because of the characteristics of being unstable, pro-inflammatory, and cytotoxic, native mRNA is unsuitable for repeated administration duration and higher level of protein expression. To overcome these challenges, cmRNA has been developed. Previous research identified several alterations to mRNA that address one or more of its limitations that prevent it from becoming a therapeutic agent [86, 89, 90]. For example, extending the 3' poly (A) tail to 120 nucleotides increases the metabolic stability of RNA [90]. Pyrimidine substitution inhibits the interaction of the RNA with TLRs and RIG-1, thereby reducing inflammation [86]. As was first demonstrated elegantly by Kariko et al. [91], Ψ -substituted mRNA displays reduced binding to TLRs. Our group also reported that substituting 25% of uridine and cytidine with 2-thiouridine and 5-methylcytidine, respectively, decreased mRNA interactions with TLRs and RIG-1 in human peripheral blood mononuclear cells (PBMCs) [86]. Another modification of interest includes the use of non-native 5'- and 3'-UTRs. In our previous study, we demonstrated that the use of human cellular cytochrome b-245 alpha polypeptide (CYBA) UTR sequence increased mRNA translation while maintaining stability of the recombinant RNA transcripts [89]. Previous publications already explored the use of cmRNA as an agent of osteogenesis [35, 92].

2.3.4 Current clinical uses of mRNA

Therapeutic applications of mRNA have proven to be promising in cancer immunotherapy, vaccination, and replacement therapy. One of the first attempts to use mRNA as a therapeutic application was in metastatic prostate cancer, whereby patients were administered dendritic cells exposed to mRNA encoding prostate-specific antigen (PSA) [93]. In all nine patients, PSA-specific T-cells were detected. This proved the ability to modulate the T-cell immune

response in humans using mRNA. Later, further clinical trials were performed based on applying multiple antigen-encoding mRNAs to treat melanoma and prostate cancer [94-96].

In another attempt to use mRNA-based vaccines, a more universal immune response was found. Compared to antibody recognition on certain viral types, the activation of humoral and T-cell-mediated immune responses confirmed the potentiality of mRNA vaccination [97, 98]. Since the first report that mRNA encoding influenza virus protein could induce a virus-specific T-cell immune response in mice [98], several further combinations of mRNAs have been applied in different animal models [99, 100]. There was even an attempt to create anti-HIV mRNA vaccine [101].

With the ongoing development of mRNA therapy, the therapeutic application of cmRNA has considerable potential. Despite the improvement of mRNA transfection efficiency and stabilization, the means of mRNA delivery is another key problem in mRNA therapy.

2.4 Delivery of cmRNA

Like for all nucleic acid therapies, mRNA delivery remains the major challenge for applications in a broad spectrum of therapeutic areas. The highly anionic character of mRNA and the ubiquitous presence of RNases are the main obstacles to successful direct delivery of mRNA to cells. Therefore, a delivery reagent that is designed for efficient mRNA encapsulation using carriers that possess effective cell-penetrating properties is required. Naked mRNA has also been successfully transfected into dendritic cells *in vitro* [102]. However, most publications demonstrated cationic lipids to be efficient non-viral vectors for mRNA delivery [103, 104]. For gene delivery of plasmid DNA into lung tissue, cationic polymers have proven to be effective reagents [105]. For any successful nucleic acid (gene or mRNA) delivery, a key parameter that determines the transfection efficiency is an acid dissociation constant (pKa) in a pH range of 6.2 to 6.5. Within this range, endosomal escape of the carrier complex into the

cytoplasm is hypothesized to be enhanced [106-108]. Because oligoalkylamine-based carriers are well-known effective delivery systems [109-111], a small diverse set of tri- (2-2, 3-3) and tetramines bearing ethylene (2-2-2) and/or propylene spacers (2-3-2, 3-3-3) were compared at a defined buffering capacity by potentiometric titration to predict their potency in mRNA delivery. The best performing lipid - N, N′ -Bis (2-aminoethyl)-1, 3-propanediamine modified with C12 alkylchains (C12-(2-3-2)) - had the highest protein translation level. Therefore, this C12-(2-3-2) was chosen as our mRNA carrier used in this thesis [112].

3. Thesis objectives

It was the main objective of this thesis to establish an optimized mRNA-based therapeutic technology for bone healing and to demonstrate proof of concept of its potency in a critical size femoral bone defect model in rats.

Building on previous work of the research group, improvements and optimizations were to be achieved by engineering the mRNA construct, by applying an optimized lipidoid nanoparticle formulation for mRNA delivery and by generating an optimized way of applying o-TAMs in bone defects. In order to implement these objectives, a new chemical modification was applied, substituting 35% of uridines in the mRNA construct with 5-iodo-uridine and 7.5% of cytidines with 5-iodo-cytidine. Furthermore, the 5' UTR of the previous development stage was replaced with a TISU sequence to improve translational efficiency. In addition, an uORF in the 5' UTR and an extra polyadenylation signal followed by an AU-rich region in the 3' UTR were removed.

Employing an optimized lipidiod nanoparticle formulation for generating o-TAMS, the main goals of this thesis were: First, to investigate and demonstrate the capacity to improve BMP-2 production by the TISU BMP-2 cmRNA construct in cell lines and primary cells; second, to describe the *in vitro* immunogenicity in human PBMCs after exposure to the TISU BMP-2 cmRNA; third, to demonstrate the osteogenic properties of this new construct *in vitro* and *in vivo*; and finally and importantly, to demonstrate the dose-dependent therapeutic potency of the o-TAM technology in a bone healing model in rats.

4. Materials and Methods

4. 1 Cell lines and primary cells

The osteoblastic cell line MC3T3-E1 and the human embryonic kidney HEK293 cell line were cultured using Dulbecco's Modified Eagle's Medium (DMEM, Sigma-Aldrich, St. Louis, USA), low glucose supplied with 10% fetal bovine serum (FBS, Sigma-Aldrich) and 1% penicillin/streptomycin (P/S, Sigma-Aldrich, USA). C2C12 mouse myoblasts were cultured in complete alpha Minimum essential medium (α-MEM) supplemented with 10% FBS and 1% P/S.

Rat muscle-derived mesenchymal stem cells (rMMSCs) isolated from rat hind limb muscles were kindly provided by Prof. Chris Evans' Musculoskeletal Gene Therapy Research Laboratory at the Mayo clinic (Rochester, MN, USA). These cells were cultured in DMEM high glucose containing 20% FBS, 10% heat-inactivated horse serum (HS; HyClone, USA), 1% chicken embryo extract (CEE; USBiological, USA), and 1% P/S.

Dulbecco's phosphate-buffered saline without calcium or magnesium (DPBS) and 0.05% trypsin-ethylenediaminetetraacetic acid (EDTA, Gibco by Life Technologies GmbH, Germany) were used for splitting of all cell types. MC3T3-E1 and HEK293 cells were split every three to four days 1:5 to 1:10, and were used until passage 15. All MSCs were expanded at a density of 1000–3000 cells/cm2, and were used between passages 2 and 4 in this project. All cells were cultured at 37 °C under 5% CO2 in an incubator.

4. 2 Generation of cmRNAs used in the study

cmRNAs encoding BMP-2 with different UTRs were generated for this thesis.

BMP-2 cmRNA was produced from the plasmid pVAXA120 BMP-2, which contained codon-optimized human BMP-2 sequence (optimized using Gene Optimizer, Thermo Fisher

Scientific, MA, USA) as reported in our previous studies [35, 89, 92]. However, this sequence also included undesirable features: a uORF in the 5'UTR and a cytoplasmic polyadenylation element together with an additional AU-rich region in the 3'UTR (Fig. 3B). In the present study, the BMP-2-coding sequence (corresponding to the annotation in the NCBI database: NM_001200.2) was used in combination with different 5'UTR elements, namely a minimal UTR BMP-2 cmRNA (Fig. 3B) [113, 114] and the TISU BMP-2 cmRNA (Fig. 3C) [87]. The recombinant constructs were synthesized and cloned into BamHI-EcoRI sites of pUC-57-Kana Vector by GeneScript.

In addition to the BMP-2-coding construct, a negative control was also needed. Another plasmid pVAXA120 containing a non-coding sequence was produced. Within this plasmid, the Kozak element (GCCACC) was scrambled (CGCACC) and all in-frame ATGs were converted to stop codons (TGA). This same pVAXA120 plasmid backbone was used for manufacturing the BMP-2-encoding cmRNA in this study.

IVT was applied in the production of all chemically modified mRNAs in this study. Plasmids were linearized and purified using chloroform – ethanol. IVT reactions were performed using T7 RNA Polymerase (Thermo Fisher Scientific), following the manufacturer's instructions.

To obtain the cmRNAs, chemically modified ribonucleotides were added to the IVT mix. Therefore, 35% of uridine residues were replaced with 5-iodo-uridine and 7.5% of cytidine residues with 5-iodo-cytidine in both minimal UTR BMP-2 and TISU BMP-2; these constructs are referred to as 5IU (0.35) 5IC (0.075).

In addition, for comparison purposes, a cmRNA was produced using our previously published PVAXA120 BMP-2, with 25% of pyrimidines substituted with 2-thiouridine and 5-methylcytosine (s2U (0.25) m5C (0.25)) [35, 89, 92]. For investigating the localization of cmRNA post treatment, a Luciferase cmRNA was produced with the same replacement of 35%

of uridine residues into 5-iodo-uridine and 7.5% of cytidine residues into 5-iodo-cytidine, and same TISU element was incorporated into the final constructs.

The chemically modified nucleotides were obtained from Jena Biosciences (Jena, Germany). Following incubation for 2h at 37°C, 0.01 U/µl DNase I (Thermo Fisher Scientific) was added into the incubated complete-IVT mix for 45 min to remove the plasmid template. The resulting RNAs were precipitated with ammonium acetate at a final concentration of 2.5 M, followed by two washing steps with 70% ethanol. A C1-m7G cap structure was added to the 5' end using Vaccinia Virus Capping Enzyme (New England Biolabs, MA, USA), while the 3' end was subjected to enzymatic polyadenylation of approximately 120 nucleotides using E. coli poly(A) polymerase after the pellet was re-suspended in aqua ad injectabilia. Because all RNA constructs were incubated for an equal time, they had comparable poly (A) tails. The concentration and quality of all the produced cmRNAs were determined on a NanoDrop2000C (Thermo Fisher Scientific). The purity and correct size were confirmed by automated capillary electrophoresis (Fragment Analyzer, Advanced Analytical, IA, USA). A schematic representation of the structure of the cmRNAs generated for the study is shown in Fig. 3.

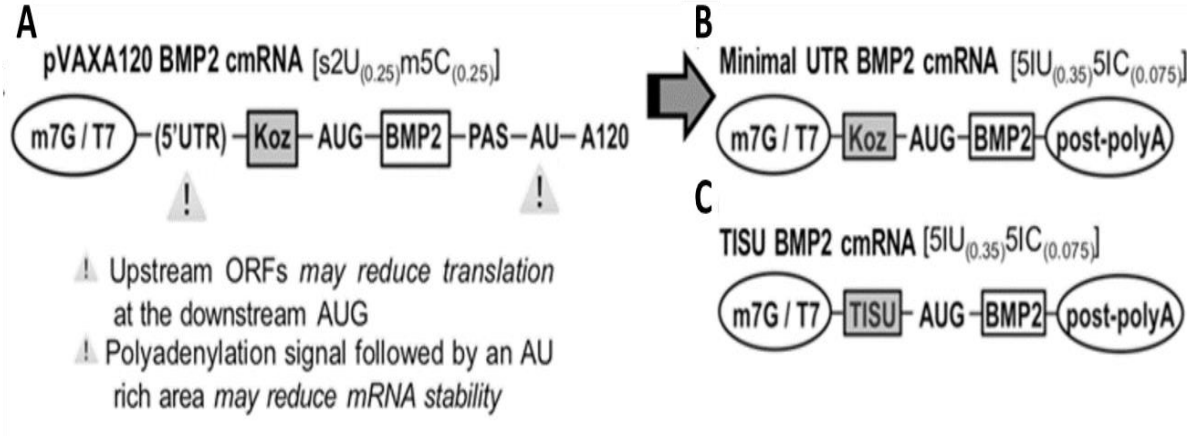

Fig.3. Schematic diagram of cmRNA constructs based on the sequence of the BMP-2 cmRNA previously produced and tested in a pVAXA120 plasmid. (**A**) demonstration of not only the general mRNA structural elements, but also undesirable features such as upstream ORF in the 5'UTR, polyadenylation element and AU-rich trac1t in the 3'UTR are indicated. New BMP-2

cmRNAs constructs used here: inclusion of 5-iodo modified nucleotides and different 5'UTR elements, either Minimal UTR (**B**) or TISU element(**C**). Figure reproduced from Zhang et al [115]with permission from Mary Ann Liebert, Inc.

4. 3 BMP-2 cmRNA transfection screening in HEK293 and MC3T3 cell lines

To perform screening experiments, HEK293 cells was transfected with different dosages of 7.8, 15.625, 31.25, 62.5, 125, 250, and 500 ng/well of mRNAs to evaluate dose-dependent effects. To confirm the transfection efficiency in different cell lines, 500 ng/well was added to MC3T3-E1 cells. The experimental set-up was as follows: $2x10^4$ HEK293 or $1x10^4$ MC3T3-E1 cells in 200 µl complete medium were seeded per well in 96-well plates and transfected for 24h post-seeding, using the commercial transfection reagent Lipofectamine® 2000 (Thermo Fisher Scientific). Complexes were prepared at a ratio of 2 µl Lipofectamine® 2000/µg mRNA. Following 20 min of incubation at room temperature (RT), the complexes were added to the cells and incubated for 24h, 48h, and 72h. During the incubation, cell culture supernatant was collected for BMP-2 quantification by enzyme-linked immunosorbent assay (ELISA) at each time point (R&D Systems, MN, USA) following the manufacturer's instructions.

4. 4 Formation and characterization of a self-assembled cmRNA-lipidoid nanoparticle formulation

The lipoplex formulation used in this project has been patented by Ethris GmbH. The non-viral transfection reagent used comprised a cationic lipid N, N´-Bis(2-aminoethyl)-1,3-propanediamine modified with C12 alkyl chains (C12-(2-3-2)) together with 1,2-dipalmitoyl-sn-glycero-3-phosphocholine (DPPC) and cholesterol as helper lipids. Moreover, 1,2-dimyristoyl-sn-glycerol methoxy polyethylene glycol (DMG-PEG2k) was included as a PEGylated lipid. The preparation methodology for this transfection reagent has been described elsewhere[112,114]. A molar ratio of amino groups of the lipid to phosphate groups of cmRNA

of 8 was used. Complexes was formed via self-assembling by rapid injection of lipid complexes into the aqueous phase containing cmRNA using insulin syringes followed by 15s vortex at the highest speed and 30 min incubation at RT. The generated lipoplexes were dialyzed against double-distilled water using dialysis cassettes with a molecular weight cut-off of 7 kDa (Pierce™, Thermo Fisher Scientific) with a single water exchange after 30min followed by overnight dialysis. The final cmRNA concentration was adjusted to 200 μg/mL. The particle sizes, polydispersity index, and electro kinetic potential of the obtained lipoplexes were determined by dynamic light scattering (DLS) using a Zetasizer Nano ZS (Malvern Instruments, Worcester, UK) (Table 2).

Table 2. Characteristic size, polydispersity index and electrokinetic potential of the TISU BMP-2 cmRNA and NC cmRNA lipoplexes. Each value represents the mean ± SD.

Lipoplex (LF92)	Assembling medium	Mean hydrated diameter Dh (nm)	Polydispersity index, PdI	Electrokinetic potential ξ (mV)
TISU BMP-2 cmRNA	Water	80.89 ± 1.09	0.211 ± 0.007	+18.1 ± 3.7
TISU NC-BMP-2 cmRNA		82.45 ± 0.44	0.209 ± 0.001	+20.0 ± 4.2

Finally, the cmRNA-lipoplex formulation was adjusted to the required concentration and volume for the following experiments and aliquots were stored at −20 °C.

4. 5 Loading of BMP-2 cmRNA lipoplexes on collagen sponges to obtain o-TAMs

Following formulation, the BMP-2 mRNA lipoplexes were loaded on collagen sponges. The collagen biomaterial used was KOLLAGEN resorb™ (equine origin) from Resorba Medical GmbH (Nuremberg, Germany) and was applied in both *in vitro* and *in vivo* studies. The methodology used for the loading of the BMP-2 mRNA lipoplexes into the sponge has been published previously [35]. Briefly, 50 μl lipoplexes in 2% sucrose (lyo-protective) were added

drop-wise onto 6-mm collagen disks punched from the original collagen sponge in 96-well plates and incubated for 30 mins at RT. Once the sponges were completely soaked with the lipoplexes, the BMP-2 mRNA loaded sponges were dried under high vacuum for a minimum of 2h at 0.05 mbar, after which the o-TAMs were ready to use for *in vitro* and *in vivo* applications. First, two BMP-2 cmRNA loading doses were used to produce the o-TAMs, a low dose containing 1.25 μg cmRNA/sponge and a high dose with 5 μg cmRNA/sponge; while for the control groups: the non-coding BMP-2 group was also 5 μg cmRNA/sponge while the other group was the empty sponge alone. The o-TAMs structure and surface topography were characterized using a VHX-900F microscope (Keyence, USA) with its software (version 1.6.1.0) and the VHZ20R objective. Then, in the dose-response study, four different dosages of BMP-2 cmRNAs of 5 μg, 10 μg, 25 μg and 50 μg were used per rat femur defect; in addition to the negative controls of empty sponge and non-coding BMP-2 (50 μg/defect), there was a positive-control group using rhBMP-2 protein (11 μg/defect). The lipoplexes used in the dose-response experiments were formulated following the same procedure but directly applied on the sponge without freeze drying. In this case, the loading of lipoplexes into the collagen sponges was performed 30 mins prior to the surgery. For the dose-response experiments, a new type of collagen sponge "Helistat" (Integra LifeScience Corpporation, USA) was applied.

4. 6 Isolation of human peripheral blood mononuclear cells (hPBMCs) for Immunogenicity evaluation of BMP-2 cmRNA o-TAMs

To investigate the immunogenicity of the lipoplexes, hPBMCs were isolated from fresh human blood (n=3 donors). Isolation of the hPBMCs was performed in accordance with approval # 5870/13 by the ethical committee of the Faculty of Medicine at the Technical University of Munich and with the most recent guidelines of the declaration of Helsinki.

hPBMCs isolation was performed using Lymphocyte Separation Medium (LSM, density 1077 kg/m3, Biowest, Nuaillé, France) following the manufacturer's recommendations. Subsequently, hPBMCs were re-suspended in RPMI-GlutaMax containing 10% FBS and 1% P/S and were incubated with o-TAMs containing BMP-2 cmRNA or with its unmodified mRNA homologue at two different concentrations (low dose (1.25 μg) and high dose (5 μg)). Cells were seeded on the loaded sponges (o-TAMs) at $1x10^5$ cells/sponge. The supernatant was collected at 6 h, 12 h, and 24 h time points for detection of cytokines produced by hPBMCs as a result of lipoplex stimulation. Cytokines such as tumor necrosis factor-alpha (TNF-α), Interferon-gamma (IFN-γ), Interleukin-1 alpha (IL-1 α) and IL-6) were evaluated by ELISA. All ELISA kits were purchased from PeproTech (NJ, USA) and used following the manufacturer's instructions.

4. 7 BMP-2 cmRNA transfection in rat muscle-derived mesenchymal stem cells

Three different o-TAMs were used to transfect rMMSCs, that is, collagen sponges loaded with non-coding cmRNA (5 μg NC cmRNA), low dose BMP-2 cmRNA (1.25 μg BMP-2 cmRNA), or high dose BMP-2 cmRNA (5 μg BMP-2 cmRNA). A total of $1x10^5$ cells suspended in 50 μl non-supplemented DMEM were seeded per sponge and incubated under normal cell culture conditions for 2h, followed by the addition of 200 μl supplemented DMEM (5% FBS + 5% HS + 0.5% CEE + 1% P/S) to each well. Cell culture supernatants were collected 6, 12, 24, 48, and 72 h post-transfection; at 6 days post-transfection, both cell culture supernatants and cell lysates were harvested. Samples were stored at –80°C until further examination. ELISA was performed to quantify the amount of BMP-2 produced by the cells using a commercial kit (R&D Systems) following the manufacturer's instructions; the results are reported as ng/mL sample.

4. 8 Expression of osteogenic and angiogenesis markers by transfected rat, muscle-derived MSCs

Two different groups were established in this functional assay, that is, plain collagen sponges (without cmRNA) and low-dose BMP-2 cmRNA o-TAMs. The culture medium was supplemented with 10 mM β-glycerophosphate and 50 μg/mL L-ascorbic acid (both reagents from Sigma Aldrich, MO, USA). Culture media was renewed every two to three days.

After 7, 14, and 21 days of cell culture, cells were examined for the expression of osteogenic markers, CD31, and vascular endothelial growth factor (VEGF) genes by RT-PCR.

To extract total RNA, cell-seeded sponges were collected in TRI-reagent (Life Technologies, Darmstadt, Germany) and total RNA was isolated by the phenol/chloroform method. RNA concentration and purity were determined spectrophotometrically using a BioPhotometer plus UV spectrophotometer (Eppendorf AG, Hamburg, Germany). Total RNA was reverse-transcribed using a First Strand cDNA Synthesis Kit (Thermo Scientific, MA, USA) with random primers. SoFast Eva Green Supermix (Bio-Rad Laboratories, CA, USA) was used and the PCR reactions were performed in a Bio-Rad CFX96 thermal cycler (Bio-Rad Laboratories).

Here, both markers of osteogenesis and angiogenesis were evaluated: Runx2, collagen type I (Col I), OCN, OPN, CD31, and VEGF (sequence in the Table.3). The expression levels of target genes mentioned above were normalized to that of rat beta-tubulin, a housekeeping gene, and results were reported relative to untransfected rMMSCs seeded onto plain collagen sponges by means of the 2-ΔΔCT method.

Table 3. **Primers for bone regeneration experiment on MSCs.**

Gene	Forward primer	Reverse primer

RUNX2	TGCCTAGGCGCCATTTCAGGTGC	TGAGGTGACTGGCGGGGTGT
OPN	CTCCATTGACTCGAACGACTC	CGTCTGTAGCATCAGGGTACTG
OCN	CCAGCGTGCAGAGTCCAGC	GACACCCTAGACCGGGCCGT
Col I	AGCGGACGCTAACCCCCTCC	CAGACGGGACAGCACTCGCC
VEGF	ATCTTCAAGCCATCCCTGTGTGC	GCTCACCGCCTCGGCTTGT
CD31	GATAGCCCCGGTGGATGA	GTTCCATCAAGGGAGCCTTC
β-tubulin	GAGGGCGAGGACGAGGCTTA	TCTAACAGAGGCAAAACTGAGCACC

4. 9 Rat critical size femoral bone defect model

To investigate the potentiality of accelerating bone healing using o-TAMs, a critical-size femoral bone defect model was used. This model has been established and optimized for the study described in this thesis by Prof. Chris Evans' Musculoskeletal Gene Therapy Research Laboratory at the Mayo clinic (Rochester, MN, USA). Permission to conduct these experiments was obtained from the Mayo Clinic Institutional Animal Care and Use Committee (#A00002349-16). All rats used in this thesis were purchased from Charles River Laboratory (Wilmington, MA, USA). They were housed with 12 h light cycles and provided with sterile food and water ad libitum in a central animal facility at the Mayo clinic.

Prior to surgery, the rats were anesthetized with 2.5% isoflurane inhalation (induction and maintenance) at 1 L/min of oxygen flow. All surgeries were performed under sterile conditions.

First, a 4 cm incision was made in the right posterolateral thigh of the rats. Then the lateral intermuscular septum was dissected to expose the diaphysis of the femur while carefully preserving the periosteum and the surrounding soft tissues.

Before making a 5 mm critical defect, four holes were drilled along the mid-diaphysis using a 0.79 mm drill guided by a polyacetal plate (Special Designs, TX, USA). A 5 mm osteotomy was made precisely using a 0.22 mm Gigli wire saw (RISystem AG, Davos, Switzerland) and a precision saw guide. Following the osteotomy, the plate was secured carefully to the femur using four hand-driven 0.9 mm threaded K-wires (MicroAire Surgical Instruments, VA, USA). This fixation allowed the construct to function in localized area. Finally, the site was washed with saline and the defect was left either empty or filled with o-TAMs. Collagen sponges loaded with NC cmRNA (5 μg), low- (1.25 μg), or high-dose (5 μg) BMP-2 cmRNA was placed in the 5 mm gap. In the following dose-response study, the defect was loaded with an empty sponge, o-TAMs loaded with NC cmRNA (50 μg), or TISU BMP-2 cmRNA (5 μg, 10 μg, 25 μg and 50 μg), or human recombinant BMP-2 protein as a positive control. The adjacent muscles were used to create a soft-tissue pouch to ensure the localization of the o-TAMs in the defect area. The wound was closed using 4-0 Vicryl sutures and the incision site closed using 9 mm wound clips. The animals were allowed to recover at 37°C in a recovery box before being returned to their cages. Analgesic treatment were administered subcutaneously pre- and post-operatively using slow release Buprenorphine at a dose of 0.6 mg/kg. Eight weeks after surgery, the animals were sacrificed and the right femora were harvested. Bone explants were fixed in 10% v/v neutral buffered formalin (Thermo Fisher Scientific) for 48h. Subsequently, the samples were stored in 70% ethanol at 4°C until further processing.

Images in Fig. 8A show the polyacetal plate used for stabilization as well as the bone defect. The experimental outline together with the experimental groups included in the study are presented in Fig. 8B. Six animals were included in each experimental group.

In vivo study of two doses comparison, rats (n=24) were 14-weeks-old at the time of surgery; in the following dose-response *in vivo* study, rats of the same age (n=72) were operated.

4. 10 Radiographic evaluation

The whole *in vivo* bone-healing process was monitored by obtaining radiographic images of the right femur using a digital x-ray cabinet (Faxitron Bioptics, AZ, USA) under general isoflurane inhalation anesthesia over 8 weeks. Rats were ventrally positioned inside the chamber with the hind limbs abducted at a 90° angle from the body. Radiographs were obtained on days 10, 28, and 56 with 42 kV energy and 10 seconds exposure time. Two independent observers analyzed the images, looking for fractures, failure of fixation, and bone formation.

4. 11 Micro-computed tomography (µ-CT) analysis

Following completion of the observation period, the entire bone section sample containing the critical bone defect area was excised. All the bone explants were scanned using a Skyscan 1176 µCT (Bruker, Kontich, Belgium) with settings of 65 kV voltage, 385 uA current, and 9 µm voxel size. Image reconstruction and analysis were performed sequentially using NRecon (Bruker, Version1.7.3) and CTAn (Bruker, Version 1.13). Briefly, after reconstructing all the scans, a region of interest (ROI) was selected, representing the entire area of the defect. This was followed by implementation of global thresholding for the binarization of the images. Finally, using a built-in algorithm in CTAn, the bone volume (BV, cm3), tissue volume (TV, cm3), and the ratio BV/TV (%) were calculated for each sample.

4. 12 Histology and immunohistochemistry (IHC)

To further detect events in the defect area, tissue histology was performed. Following µCT, femoral bone samples were subjected to decalcified tissue histology. The samples were decalcified in 10% buffered EDTA (Sigma Aldrich), dehydrated in an ascending ethanol series, and embedded in paraffin.

4. 12. 1 Hematoxylin and Eosin (H & E) staining and Masson-Goldner Trichrome staining

For both stainings, the sections were deparaffinized and subsequently rehydrated using decreasing alcohol concentrations (100%, 90%, 70%, and 50%). In H&E staining, sections was performed in hematoxylin (Carl Roth GmbH, Karlsruhe, Germany) for 10min and the sections washed for 10min under running tap water until they became "blue". Subsequently, the sections were stained in Eosin Y (Carl Roth GmbH) for 5min with a subsequent washing step under tap water for 1–5minand dehydrated in solutions with increasing alcohol concentrations and finally in xylene. The sections were mounted in mounting media (Carl Roth GmbH). Following overnight drying under a safety hood, the samples were ready for microscopic observation.

Longitudinal cross-sections of 7μm thickness were stained using a Masson-Goldner Trichrome kit (Carl Roth GmbH, Karlsruhe, Germany) following the manufacturer's instructions.

4. 12. 2 Immunohistochemistry (IHC) staining

Following deparaffinization and rehydration, the sections were first incubated for 15 min in 3% hydrogen peroxide (Sigma Aldrich) to block endogenous peroxidase activity. Depending on the different staining processes applied, the antigen retrieval methods varied. In this thesis, sections stained for collagens and CD31 were incubated with proteinase K (Dako, Glostrup, Denmark) for 7 min at RT, while for CD45 staining, the sections were heated for 20 min at 90°C in 10 mM citrate buffer (pH 6). Following washing with Tris-HCl and blocking in 2% bovine serum albumin (Sigma Aldrich) for 60 min, all the sections were incubated with the respective primary antibody solution in blocking buffer overnight at 4°C. Primary antibodies and the dilutions used in this thesis as follows: Col I, ab34710, 1:200; Col II, ab34712, 1:200; Col III, ab7778, 1:200; CD31, ab182981, 1:1000; CD45, ab10558, 1:1000; rabbit isotype control IgG, ab27478, 1:200 (all purchased from Abcam, Cambridge, UK). Subsequently, primary antibodies were detected by incubation with EnVision+ Dual Link System-HRP Rabbit/Mouse (Dako) for 1h at RT.

Liquid diaminobenzidine chromogen (Dako) was added to visualize the localization of different staining and sections were counterstained with Mayer's hematoxylin (Carl Roth GmbH).

To observe the localization of luciferase mRNA, after permeabilization and antigen retrieval, sections were blocked with donkey serum for 1 h, RT. After blocking, sections were incubated with primary anti-luciferase antibody in the dilution of 1:200(Promega, USA). The secondary antibody, donkey anti-Goat IgG (Promega), was applied according to the manufacturer's instructions.

All stained slides were observed and photographed using a microscope (Biorevo BZ9000, Keyence, Osaka, Japan) at 10x and 20x magnifications. A general image of the entire histological section was generated using the software BZ-II Viewer and BZ-II Analyzer (Keyence).

4. 13 Bioluminescence Imaging

For detecting the cmRNA localization, after rats (n=6/ group) were anesthetized with 2.5% isoflurane inhalation (induction and maintenance) at 1 L/min of oxygen flow, same surgery procedures have been applied. o-TAMs loaded with NC cmRNA (50 μg) and Luciferase cmRNA (50 μg) were transplanted into the defect areas. Bioluminescence imaging was performed on the same animals at indicated time points up to 4 days. Animals were anesthetized during the imaging. An IVIS (Xenogen, Hopkinton, MA) was used to image the animals. Each animal was scanned until the peak total flux signal was obtained, then the radiance was recorded from regions of interest. Radiance was quantified in photons per second per centimeter squared per steradian.

4. 14 Osteoimmunogenic study *in vivo*

Blood was collected at days 1, 3, and 10 after implantation of the TAMs in a rat femur defect. Tubes containing blood were immediately placed on a roller for up to 35 min prior to

centrifugation for 15 min (approx. 1500 g, 20℃). Plasma was transferred into 1.5 mL Eppendorf tubes and was stored at −80°C.

To further investigate the immunogenic response to cmBMP-2 lipids-loaded TAMs *in vivo*, the cytokine level was evaluated using ELISA multiplex technology to measure the secretion of a variety of 14 cytokines: G-CSF/CSF-3, GM-CSF, IFN-γ, IL-1 α, IL-10, IL-12p70, IL-13, IL-17A, IL-1β, IL-2, IL-4, IL-5. The experiment was performed using the ProcartaPlex Multiplex Immunoassay (Invitrogen, USA) following the manufacturer's instructions.

4. 15 Statistical analysis

All *in vitro* cell transfection experiments were performed in triplicate. Transfections of rMMSCs and hPBMCs using the 3D o-TAMs were performed using three individual donors. For each donor, the experiments were performed in triplicate. Results are shown as the mean ± standard deviation. Statistical analysis was performed using GraphPad Prism Version 7.00 (GraphPad Software, CA, USA). The comparison of multiple groups was conducted by one- and two-way ANOVA. A p value $\leqslant 0.05$ was considered significant. P values reported in this thesis are described as the following: $p>0.05$ was considered non-significant and indicated with "ns", $p\leqslant 0.05$ was indicated with *, $p\leqslant 0.01$ was indicated with **, $p\leqslant 0.001$ was indicated with *** and $p\leqslant 0.0001$ was indicated with ****.

5. Results

5. 1 BMP-2 cmRNA transfected cells secrete high levels of hBMP-2

In a first set of experiments, the new constructs harboring a TISU or minimal UTR were compared to the previous, non-optimized pVAXA120 BMP-2 cmRNA.

Cells transfected with either of the two modified BMP-2 constructs (i.e. TISU and minimal UTR) displayed significantly higher BMP-2 expression compared to the cells transfected with the pVAXA120 BMP-2 cmRNA construct ($p<0.0001$) in both cell types (Fig. 5A and B). Moreover, the inclusion of the TISU sequence considerably enhanced BMP-2 expression ($p<0.0001$). From EC50, TISU BMP-2 cmRNA showed more than 4 times as effective as minimal UTR BMP-2 cm RNA. TISU BMP-2 cmRNA constructs were modified with 5IU (0.35) 5IC (0.075), while minimal UTR BMP-2 cmRNA included s2U(0.25) m5C(0.25) and had no TISU element. The NC BMP-2 construct showed no expression as with the untransfected group (Fig. 4A). In the kinetic experiments of up to 72 h, BMP-2 expression was detected in both HEK293 and MC3T3-E1 cells (Fig. 4B). On the basis of the different cell types, the level of protein synthesis differed, but the same tendency was observed as with the 24 h transfection. In both experiments, clear dose-response and time effects were observed.

Because TISU BMP-2 cmRNA appeared to have outperformed the minimal UTR BMP-2, it was therefore selected for further experiments.

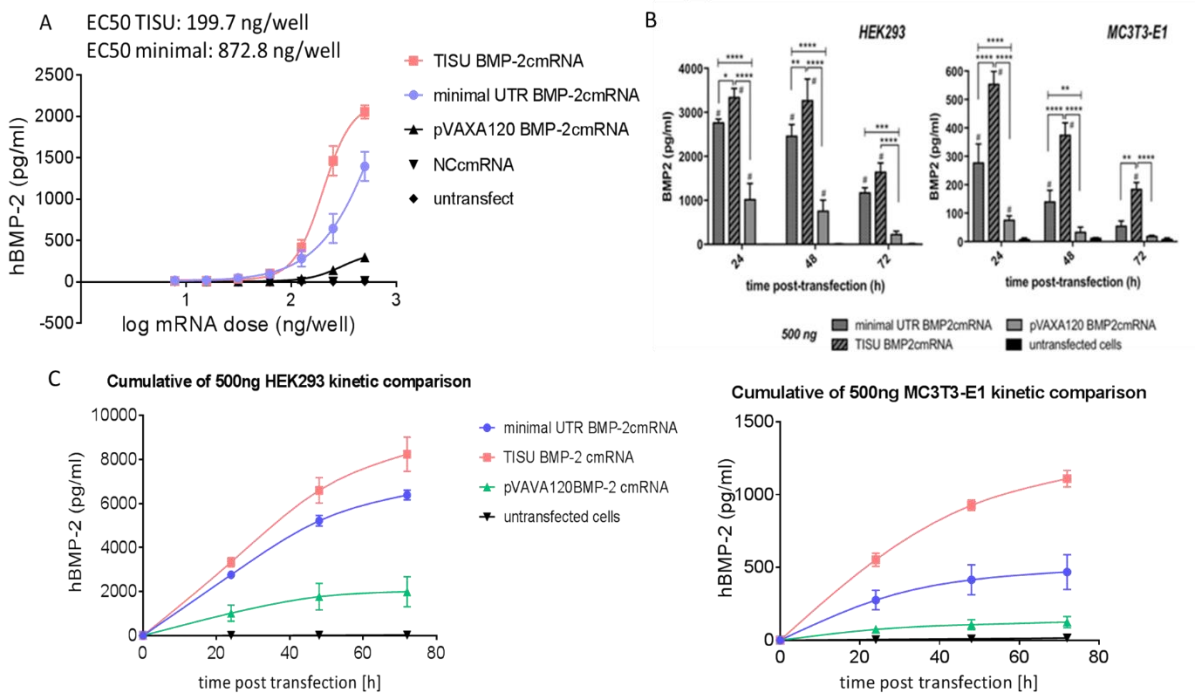

Fig.4 Transfection screening of candidate cmRNAs. (**A**) BMP-2 production 24 hours post HEK293 transfection in the concentration scale of 7.8 ng - 500 ng BMP-2 cmRNAs/well. (**B**) BMP-2 production over 72h for transfection in HEK293 and MC3T3-E1 (500 ng/well). (**C**)Cumulative kinetic expression comparison over 72h for transfection in HEK293 and MC3T3-E1 (500 ng/well). In all transfections, NC cmRNA transfected and untransfected cells were analyzed as controls. P-values are indicated as follows: *p≤0.05, **p≤0.01, ***p≤0.001 and ****p≤0.0001. In addition, the symbol # is used to indicate p-values ≤0.05 obtained when analyzed groups were compared with untransfected cells. n=3, mean ± SD. Figure reproduced from Zhang et al [115] with permission from Mary Ann Liebert Inc.

5. 2 o-TAMs loaded with TISU BMP-2 cmRNA

Generated BMP-2 cmRNA contained modifications including the TISU element was formulated in lipoplex and subsequently loaded into a 3D collagen sponge. Sucrose was added as lyo-protection reagent and the sponges were dried by vacuum drying. The schematic image in Fig. 5A shows the appearance of the cmRNA-loaded collagen sponges. The lipoplexes used for loading were approximately 80 nm in diameter and had a positive charge (Table 2). The o-TAMs obtained had a cylinder-like structure of 6 mm diameter and 3mm height (Fig. 5B), with

relatively smooth surfaces (Fig. 5C and D). Under a digital light microscope, a clear porous structure was observed in the interior of the o-TAMs from the longitudinal section (Fig. 5E and F).

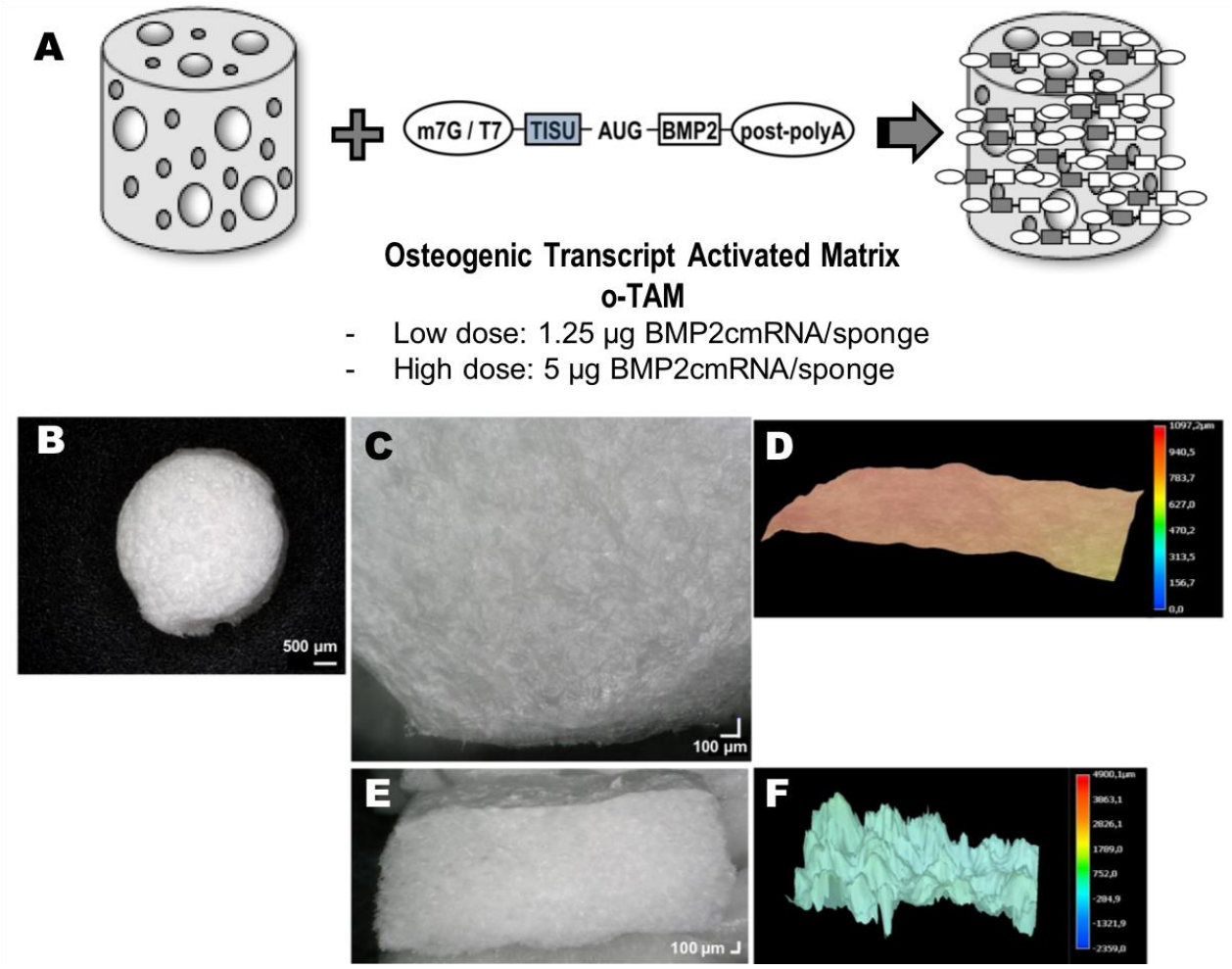

Fig. 5. Demonstration of osteogenic transcript activated matrix (o-TAM) and surface characterization of sponges used here. (**A**) Schematic graph of the o-TAM, collagen sponges, loaded with two doses of TISU BMP-2 cmRNA. Two different dosages loaded o-TAM, low dose (1.25 μg) or high dose (5 μg) cmRNA-lipocomplex, were produced. (**B, C**) Digital light microscopy images showing the appearance of the obtained o-TAMs. (**D**) Surface characteristics of the o-TAMs. (**E, F**) Transversal section showing higher porosity features that characterizes the interior of the o-TAMs. Figure reproduced with permission from Zhang et. al. [115] with permission from Mary Ann Liebert Inc.

5. 3 Reduced immunogenicity of TISU BMP-2 cmRNA in Human PBMCs

Two doses of o-TAMs loaded with TISU BMP-2 cmRNA and unmodified BMP-2 mRNA (5 µg/sponge and 1.25 µg/sponge) were incubated with hPBMCs. There was a clear reduction in cytokine production as result of cmRNA stimulation in the TISU BMP-2 group compared to unmodified BMP-2 mRNA (Fig. 6). In most cases, a dose-dependency was observed in the induction of cytokines by both TISU BMP-2 cmRNA and unmodified BMP-2 mRNA.

When considering the individual growth factors, a gradually decreasing expression of TNF-α and IFN-γ was observed over a 24h period in both the TISU BMP-2 cmRNA and modified RNA groups (Fig. 6A and B). A significant difference ($p<0.001$) was observed in the comparison of cmRNA and unmodified mRNA in the high dose 5 µg/sponge for IFN-γ. Interestingly, when hPBMCs were incubated with low-dose cmRNA, the low TNF-α and IFN-γ expression levels (<200 pg/mL) remained constant over time ($p>0.05$). In contrast to TNF-α and IFN-γ, increasing IL-1 and IL-6 production was detected during the same time as result of the unmodified mRNA transfection (Fig. 6C and D), while the cmRNA group mostly remained at the same low level (<100 pg/mL IL-1). Concentrations >600 pg/mL were detected for both these cytokines at 24h post-exposure of hPBMCs in the unmodified group. Notably, no significance differences were found between low- and high-dose cmRNA regarding IL-1 and IL-6 induction ($p>0.05$).

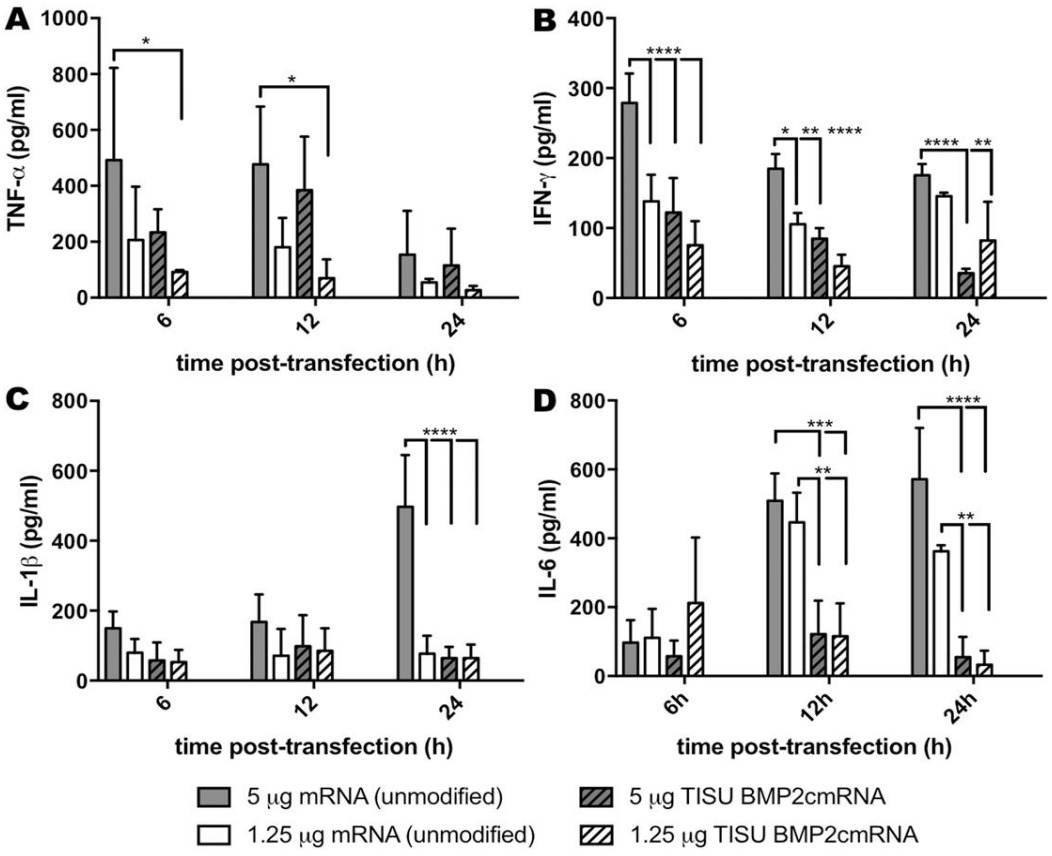

Fig. 6. Inflammatory cytokine expression by hPBMCs *in vitro* up to 24 hours post-exposure to low or high dose TISU BMP-2 cmRNA o-TAMs. Unmodified BMP-2 cmRNA, also loaded into collagen sponges, was used as control. (**A**) TNF-α, (**B**) IFN-γ, (**C**) IL-1β and (**D**) IL-6 were evaluated. Obtained p-values are indicated as follows: *p≤0.05, **p≤0.01, ***p≤0.001 and ****p≤0.0001. N=3 donors and n=3 triplicate for each donor, mean ± SD. Figure reproduced from Zhang et. al. [115] with permission from Mary Ann Liebert Inc.

5. 4 Transfection of rat, muscle-derived MSCs with TISU BMP-2 cmRNA o-TAM

Significantly higher BMP-2 expression was detected in the rMMSCs incubated with either dose of TISU BMP-2 cmRNA o-TAMs than NC cmRNA o-TAMs (Fig. 7A, $p<0.01$). Remarkably, BMP-2 production could still be shown by ELISA detection at the end of the evaluation of 6 days. Interestingly, from the cell culture supernatant, the higher dose TISU BMP-2 cmRNA o-TAMs resulted in significantly less BMP-2 expression than the lower dose between 12 h and

72 h post-transfection ($p<0.0001$). There were no significant differences in terms of BMP-2 secretion between the cmRNA doses ($p>0.05$) at 6 days post-transfection. By contrast, in the lysates of cells transfected with the high dose, a greater amount of BMP-2 could be detected in comparison to the low dose at 6 days ($p<0.01$).

5. 5 TISU BMP-2 cmRNA o-TAM promotes the expression of osteogenic genes by rat, muscle-derived MSCs

The persistent BMP-2 expression for up to 6 days provided the basis for *in vitro* differentiation. Here, RT-PCR was performed to quantify the expression of osteogenesis- and angiogenesis-related gene markers (Fig. 7B–G). Among the selected osteogenesis markers, Runx2, Col I, and OPN, were significantly induced by BMP-2 cmRNA, but not OCN. Runx2 and Col I upregulation that occurred at 14 days post-transfection was consistent with their characteristics as the early-middle expression markers during osteogenesis (14). Of particular interest were the results for OPN, a well-known later osteogenesis marker, whereby a significant OPN induction ($p<0.05$) occurred as early as 7 days post-transfection. In accordance with osteogenesis, VEGF and CD31 expression also increased with time, although neither reached statistical significance (Fig. 7.F and G). In the non-coding group, no inductive effects on both osteogenesis and angiogenesis were observed. (Results not shown here).

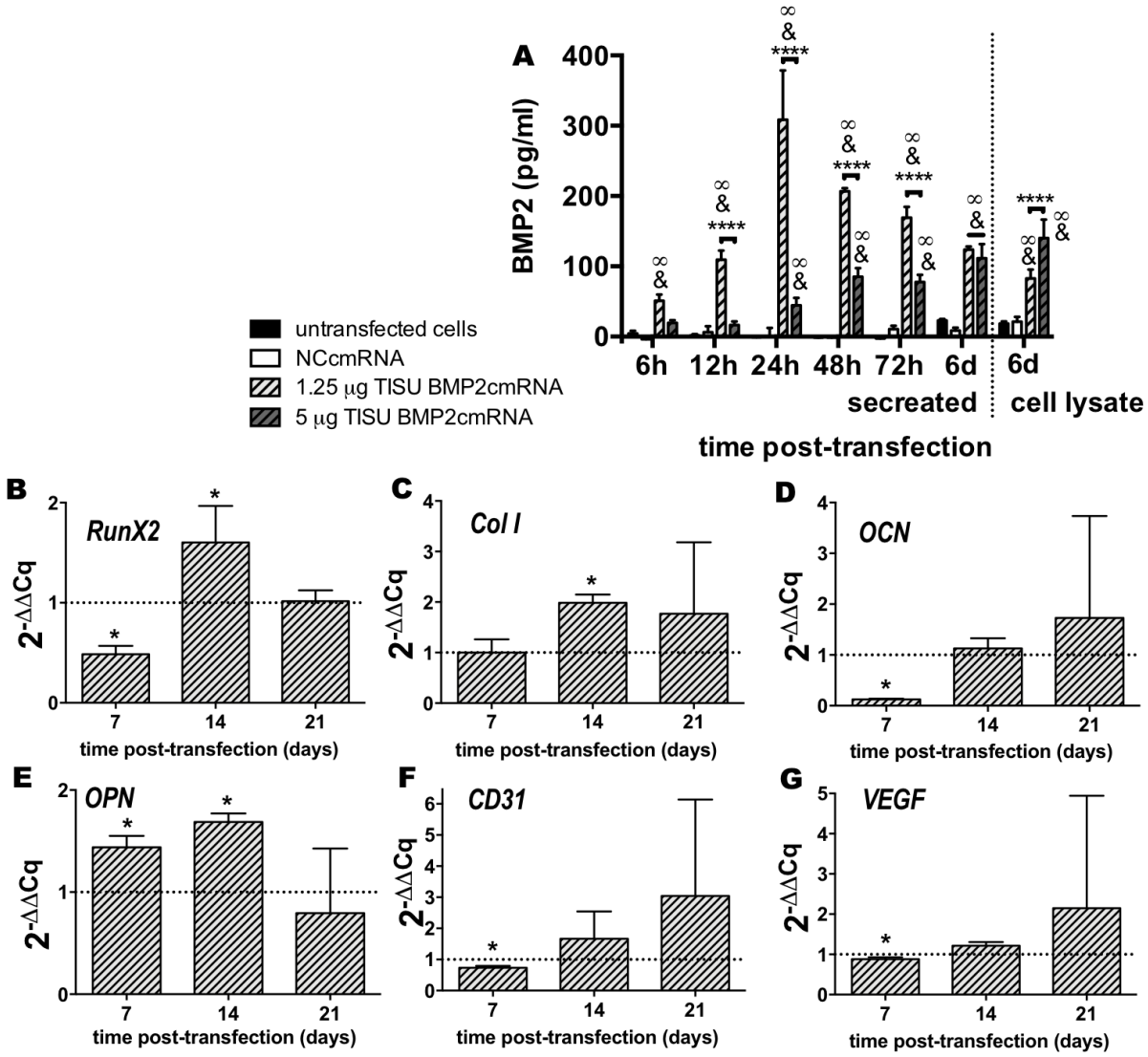

Fig. 7. Osteogenese capacity of TISU BMP-2 cmRNA o-TAM transfection on rat, muscle-derived MSCs. (**A**) BMP-2 production is shown for up to 6 days post-transfection. low dose (1.25 μg/sponge) and high dose (5 μg/sponge) TISU BMP-2 cmRNA as well as NC cmRNA (1.25 μg/sponge) as a negative control were used for transfection. Untransfected cells were also evaluated as controls. Obtained p-values are indicated as ****p≤0.0001. In addition, the symbol & is used to indicate p-values ≤0.05 obtained when TISU BMP-2 cmRNA was compared with NC cmRNA. Similarly, the symbol ∞ is used to indicate p-values ≤0.05 obtained when TISU BMP-2 cmRNA was compared with untransfected cells. N=3 donors and n=3 triplicate for each donor mean ± SD. Expression of osteogenic [(**B**) RunX2, (**C**) Col I, (**D**) OCN and (**E**) OPN] and angiogenic genes [(**F**) CD31 and (**G**) VEGF] at 7, 14 and 21 days post-TISU BMP-2 cmRNA transfections by using the low dose o-TAM. p≤0.05 is indicated as *. Results are normalized to the housekeeping gene (rat β-tubulin) and to the untransfected cells. N=3 donors

and n=3 triplicate for each donor, mean ± SD. Figure reproduced from Zhang et. al. [115] with permission from Mary Ann Liebert Inc.

5. 6 Osteogenic properties of TISU BMP-2 cmRNA *in vivo*

5. 6. 1 Bone formation as evaluated by μCT

Following evaluation of the imaging of all the bone samples, both the X-ray and μCT data clearly showed more abundant neo-tissue formation within the defects treated with the TISU BMP-2 cmRNA o-TAMs (Fig. 8C and D). The higher TISU BMP-2 cmRNA dose (15 μg/defect) produced approximately twice as much new bone as the lower dose (3.75 μg/defect) (Fig. 8D, BV/TV %). A relatively lower BV/TV was also clearly demonstrated here in the NC BMP-2 group (15 μg/defect) compared to the non-treated control. Almost completely bridged bone healing was shown in the representative 3D reconstructed image of the high-dose TISU BMP-2 cmRNA group (Fig. 8D).

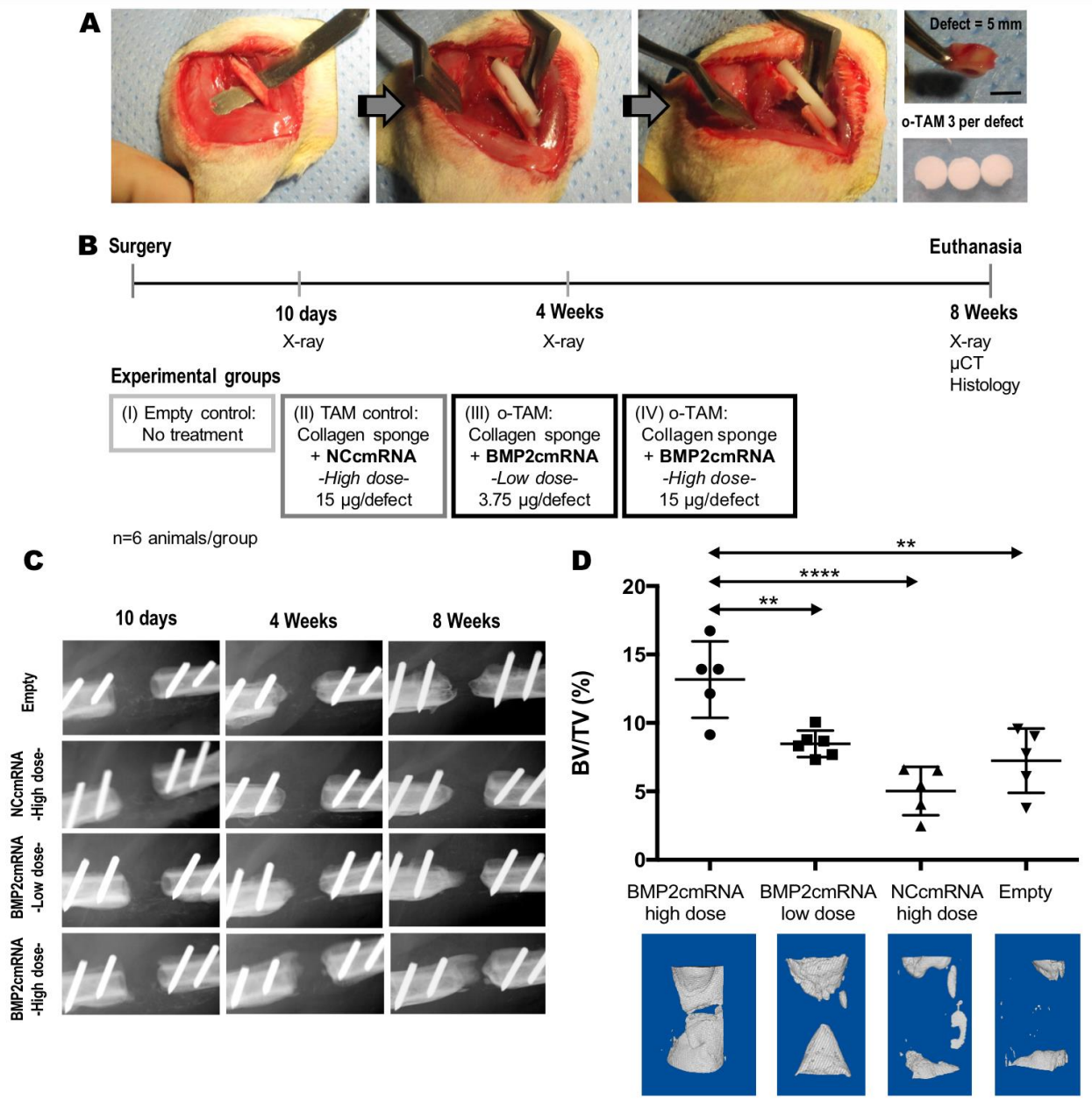

Fig. 8. Schematic representation of surgery plans and results from *in vivo* experiments.

(**A**) surgical approach and (**B**) surgery time line and experimental groups tested *in vivo* in a femoral critical-sized defect in rats. (**C**) X-ray were evaluated at 10 days, 4 weeks and 8 weeks after treatment. (**D**) Representative 3D reconstruction of the µCT images obtained for each group at 8 weeks after treatment. BV/TV (%) as calculated by the CTAn software. The values obtained for each individual sample are shown. Obtained p-values are indicated as **p≤0.01 and ****p≤0.0001. N=6 animals per group. Figure reproduced from Zhang et. al. [115] with permission from Mary Ann Liebert Inc.

In the dose-response *in vivo* experiments, the highest dose used (50 μg/defect) showed bridged bone healing inside of the defect area, as occurred in the positive control 11 μg rhBMP-2 group. A clear dose-dependent increasing neo-bone formation was observed in the TISU BMP-2 cmRNA-treated groups for the 4 weeks and 8 weeks observation times (range from 5 μg to 50 μg/defect) (Fig. 9A).The quantitative calculation of BV/TV confirmed the reconstruction images. In the 5 μg, 10 μg, and 25 μg groups, bone formation increased non-significantly. When comparing the higher-dose group, that is, 50 μg, with all the other cmRNA dosage groups, the enhanced BV/TV values were found to be strongly significant. At 4 weeks, there was no significant difference between 50 μg cmRNA and 11 μg rhBMP-2, even though greater bone formation was obsrved in the cmRNA group. By 8 weeks, the difference had become significant, because of less bone formation in the recombinant protein group. Bone formation in the NC cmRNA group was negligible and comparable to the empty sponge group (Fig. 9B).

Interestingly, there was a tendency for a decreasing BV/TV in the rhBMP-2 group at 8 weeks, whereas in the cmRNA-treated groups, bone formation remained high.

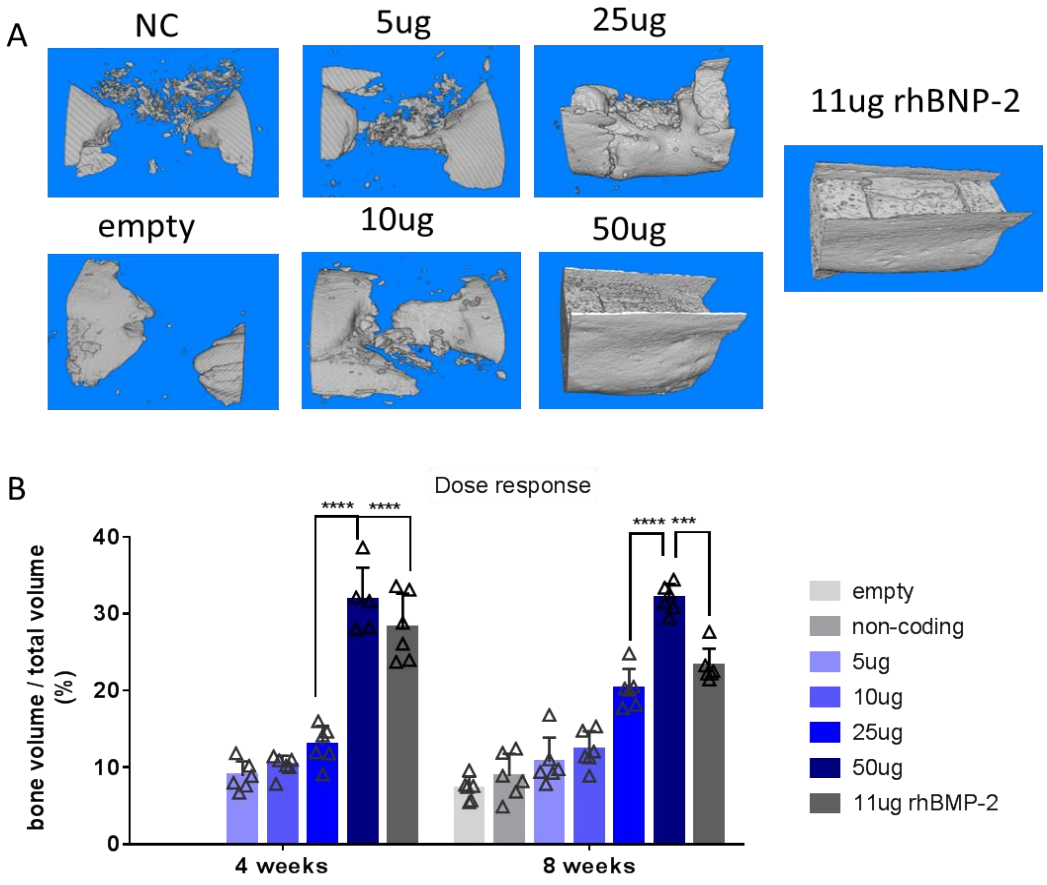

Fig.9. Bone regeneration results from dose-response *in vivo*. (**A**) Representative 3D reconstruction of the µCT images obtained for all groups at 4&8 weeks after treatment. (**B**) BV/TV (%) as calculated by the CTAn software. The values obtained for each individual sample are shown. Obtained p-values are indicated as ***p≤0.001 and ****p≤0.0001. N=6 animals per group.

5. 6. 2 Representative histological stainings

5. 6. 2. 1 Masson trichrome staining

Masson trichrome staining results were consistent with the µCT data in that bone tissue (compact green) was only detected in the presence of TISU BMP-2 cmRNA (Fig. 10). By contrast, in the two negative control groups, the empty and NC BMP-2 groups, the formation of new bone tissue was negligible (Fig. 10A and B). Interestingly, a cartilage-like tissue was observed at the bridging point of the bone defects when treated with the high-dose TISU BMP-

2 cmRNA (Fig. 10D, 10x and 20x magnifications). A gradient of mineralizing tissue (stained as solid green) was observed from the bridging area towards the old bone, which was consistent with the quantitative results.

In dose-response experiments, the same mineralization pattern was found in the lower-dose cmRNA groups (Fig.11 B, C, D) as well as the control groups (Fig.11 F and G). Interestingly, however, a strong green stained region was detected on the outer layer of the defect area. Between the two layers of strongly green-stained tissue, a net-like spongy structure (also intensely green stained) was detected (Fig.11 A and E).

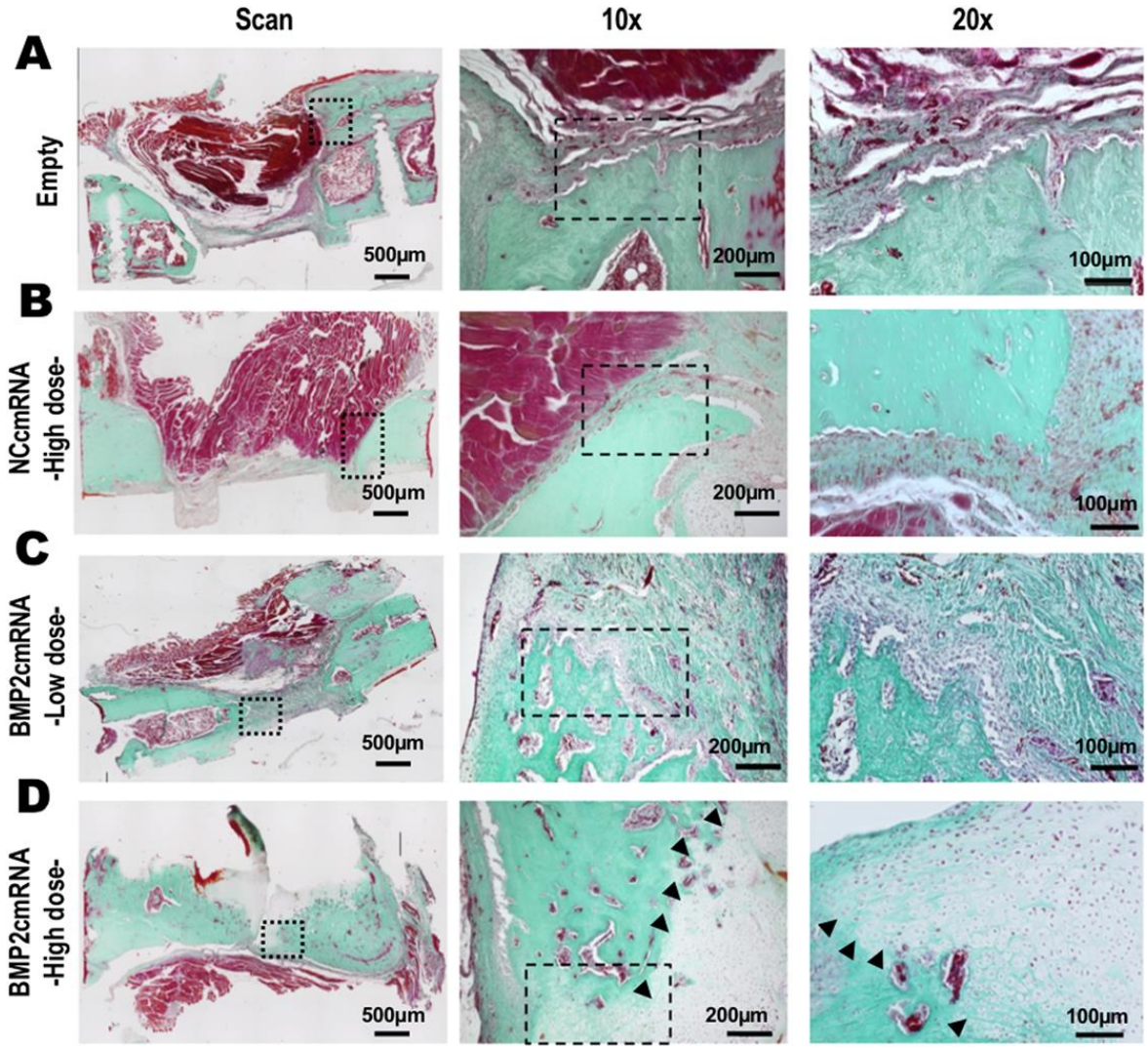

Fig. 10. Representative images of Masson Trichrome staining of bone defects after 8 weeks. (**A**) Empty and (**B**) NC cmRNA control groups together with (**C**) low dose BMP-2 cmRNA (3.75

μg/defect) and (**D**) high dose BMP-2 cmRNA (15 μg/defect) are organized in panel view. From left to right, a general scan of the entire section, 10x and 20x magnifications images are displayed. Red staining = muscle, Green staining = collagen (bony tissue). Figure reproduced from Zhang et. al. [115] with permission from Mary Ann Liebert Inc.

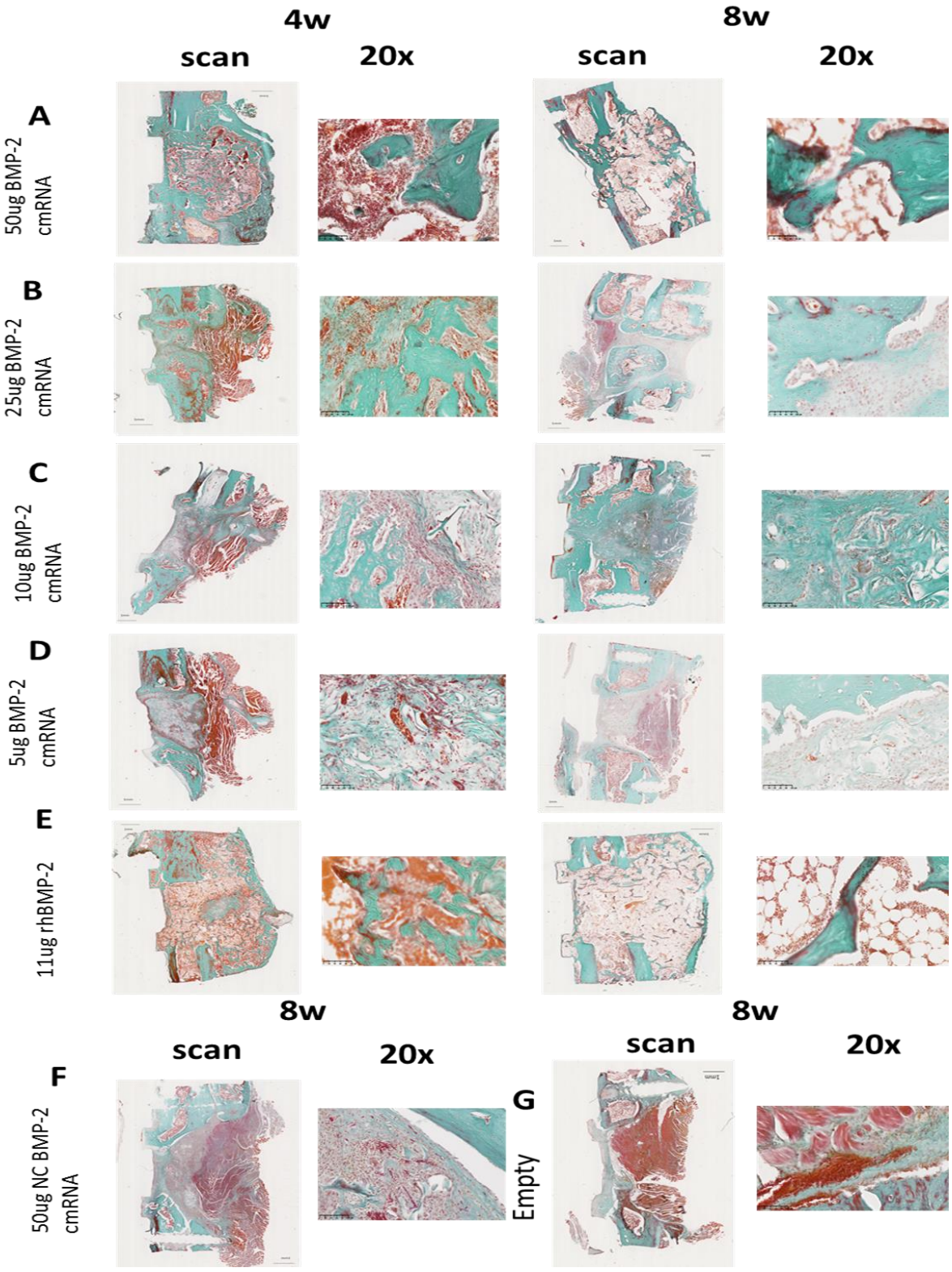

Fig. 11. Masson Trichrome staining of bone defects from dose-response experiments collected at 4 weeks and 8 weeks. for (**A**) 50 μg/defect BMP-2 cmRNA, (**B**) 25 μg/defect BMP-2 cmRNA, (**C**) 10 μg/defect BMP-2 cmRNA , (**D**) 5 μg/defect BMP-2 cmRNA groups as well as (**F**) 50 μg/defect NC BMP-2 cmRNA control group(8 weeks) and (**G**) Empty group(8 weeks); (**E**) is the 11μg/defect rhBMP-2 positive group. From left to right, a general scan of the entire section, and 20x magnifications images are displayed. Red staining = Muscle tissue, Green staining = collagen (bony tissue)

5.6.2.2 Immunohistochemistry

To determine the deposition of different types of collagen, IHC for Col I, Col II, and Col III was performed. There was a clear correlation between TISU BMP-2 cmRNA dosage and Col I deposition (Left panels, Fig.12C and D). The most intense deposition was localized in the newly formed bone area. By contrast, Col I staining of the NC cmRNA group mostly showed deposition in the native bone region (Fig. 12B). Moreover, many vessel-like structures were observed in the fibrous tissue filled in the defect area that were positive for Col I in the empty group (Fig. 12A). The fracture area showed the same dose-dependent relationship for Col II deposition (middle panels, Fig. 12C and D) in the TISU BMP-2 cmRNA groups (Fig. 12C and D). Considerably less Col II was present in the NC cmRNA and empty groups (Fig. 12A and B). The pattern for Col III was similar to that of Col II (Right panels, Fig. 12C and D).

In the dose-response study, the representative images showed that Col I staining was widely distributed in the sample even in the fibrosis tissue area. By contrast, Col II and III were more localized to a specific area in the defect. The cmRNA-treated groups displayed more intense staining and a dose-dependent deposit pattern compared with the control groups. For Col II and III, the 50 μg cmRNA/defect and 11 μg rhBMP-2/defect showed a similar intense staining localization (Fig.13).

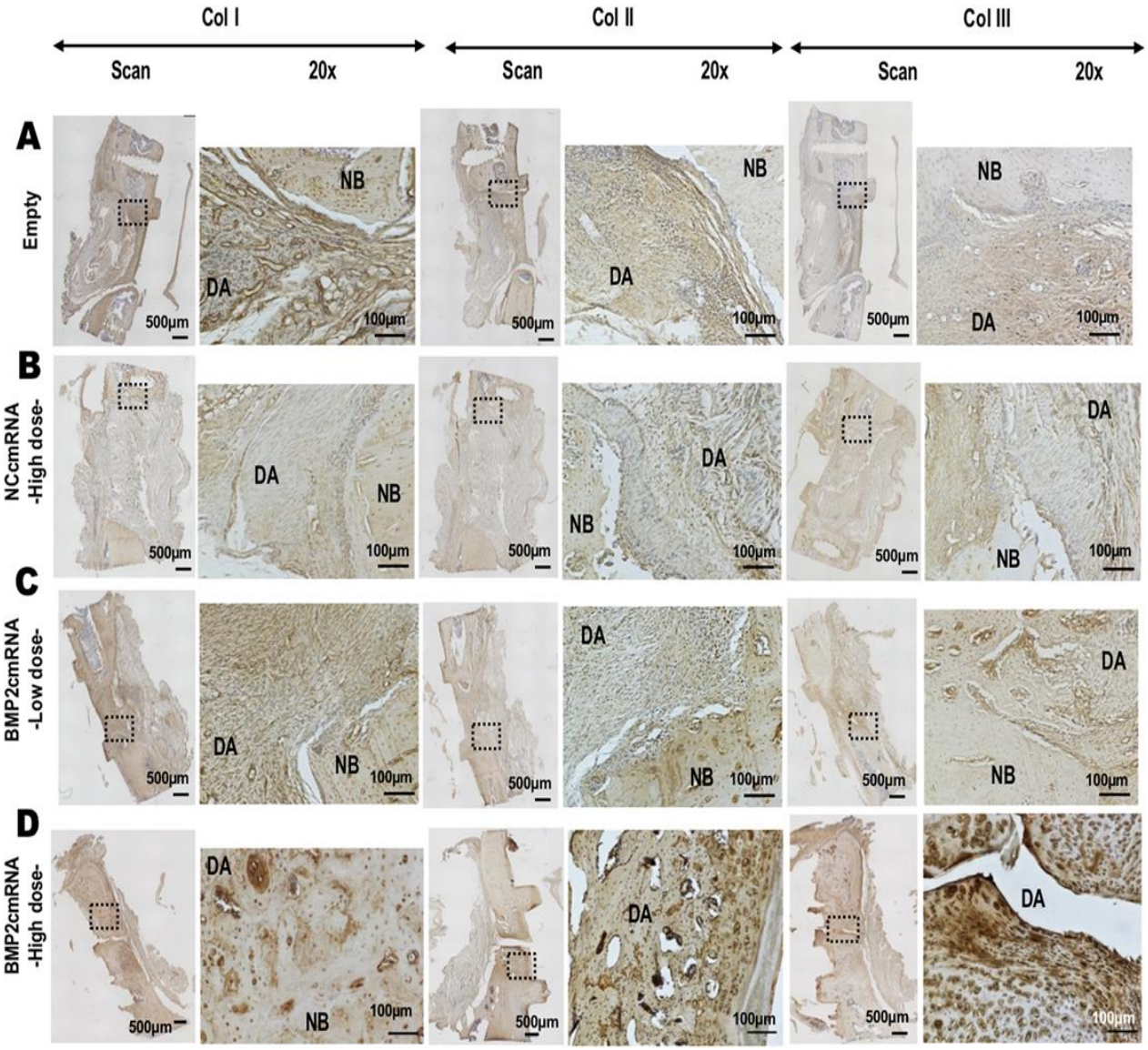

Fig. 12. Immunohistochemistry for Col I, Col II and Col III deposition in bone defects after 8 weeks. Groups: (**A**) empty and (**B**) NC cmRNA control groups as well as (**C**) low dose BMP-2 cmRNA (3.75 µg/defect) and (**D**) high dose BMP-2 cmRNA (15 µg/defect) were evaluated. From left to right, Col I, then Col II followed by Col III images are represented. For each staining, a general scan of the entire section as well as 20x magnifications images are shown. Inserts in scans are indicative of the area where the high magnification picture was taken. In the pictures, native bone is indicated by NB and defect area by DA. Figure reproduced from Zhang et. al. [115] with permission from Mary Ann Liebert Inc.

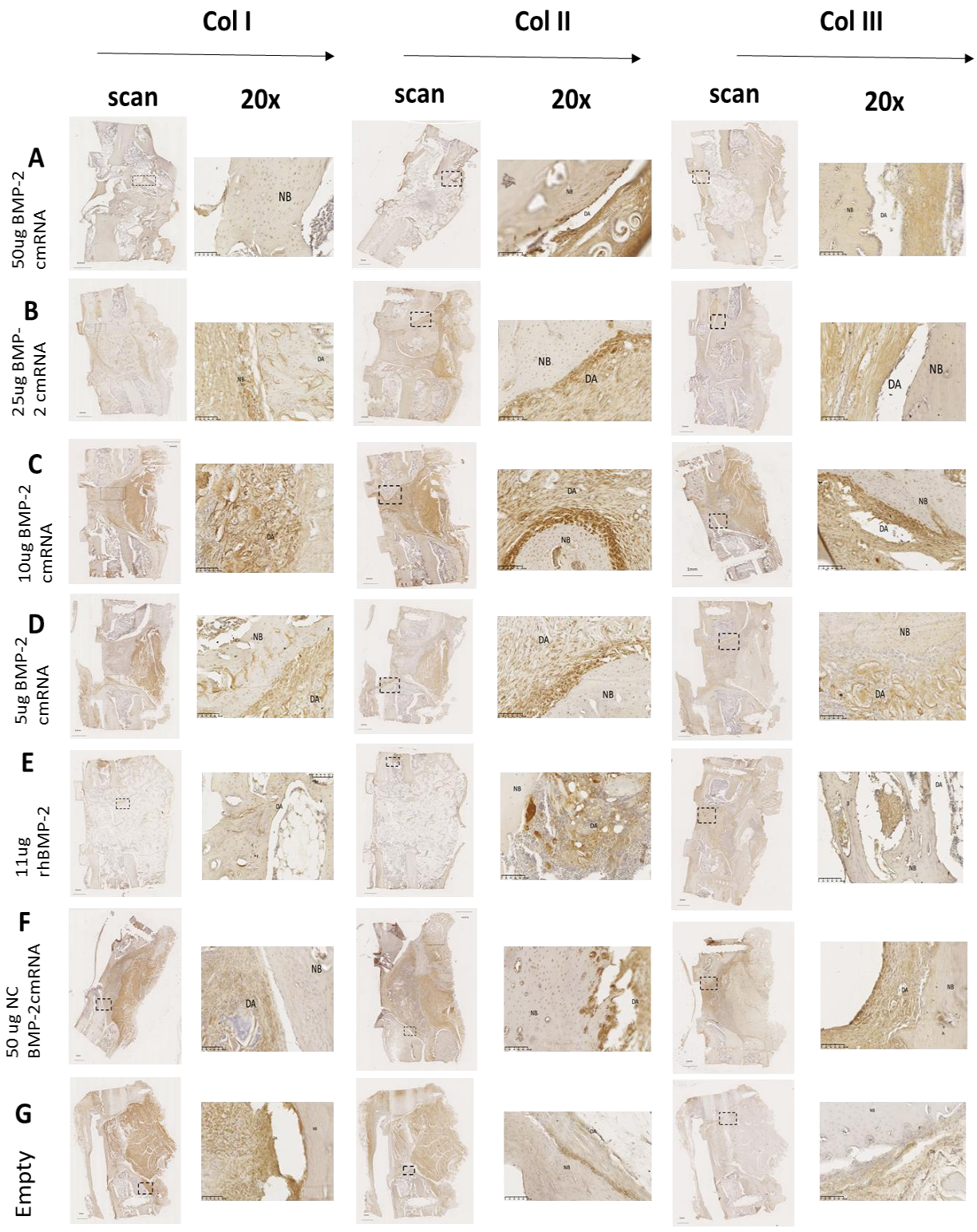

Fig. 13. Immunohistochemistry for Col I, Col II and Col III deposition in bone defects collected from dosage study at 4weeks and 8 weeks. Groups: (**A**) Highest dose BMP-2 cmRNA (50 μg/defect); (**B**) 25 μg/defect; (**C**) 10 μg/defect and (**D**) 5μg/defect as well as (**F**) NC cmRNA and (**G**) NC cmRNA empty control groups were evaluated.

From left to right, Col I, then Col II followed by Col III images are represented. For each staining, a general scan of the entire section as well as 20x magnifications images are shown. Inserts in scans are indicative of the area where the high magnification picture was taken. In the pictures, native bone is indicated by NB and defect area by DA.

To investigate angiogenesis progress, IHC for two important angiogenic biomarkers — CD31 and VEGF — was performed to detect any difference in vascular infiltration into the defect area among the different treatment groups. CD31-positive staining in endothelial lining of the newly formed blood vessels is shown in the right panel of Fig. 14. In the TISU BMP-2 cmRNA-treated groups (Fig. 14 C and D), relatively more new vessels were present inside of the newly formed bone tissue. Interestingly, more intense CD31-positive staining was observed in the empty group compared to the non-coding BMP-2 cmRNA group (Fig. 14B), although this was still considerably lower than that of the high-dose TISU BMP-2 cmRNA group (Fig. 14D).

Varying levels of leukocyte infiltration were found. Because of this, IHC for CD45 was performed to detect how many CD45+ cells infiltrated in all the groups (Fig. 14, left panels). The greatest CD45+ cell infiltration was observed in the TISU BMP-2 cmRNA-treated groups inside the active bone regenerating area (Fig. 14C and D). The lowest infiltration levels were found in the NC cmRNA group (Fig. 14B).

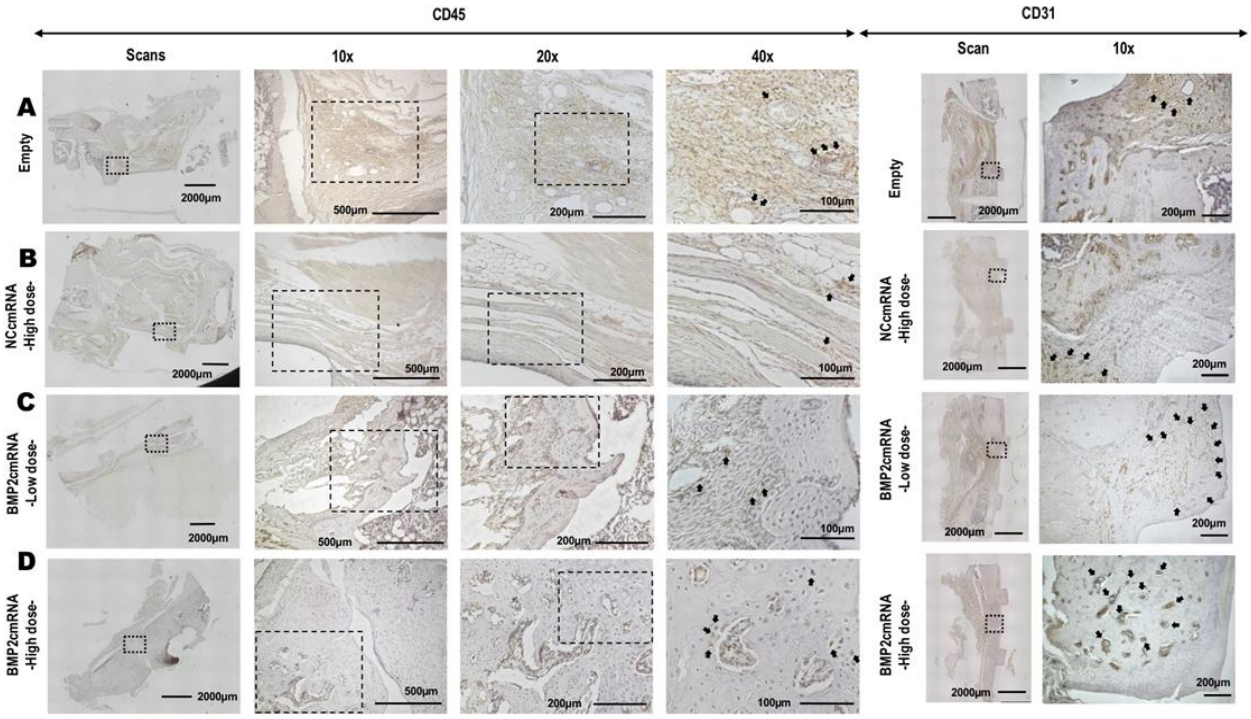

Fig. 14. Immunohistochemistry for CD45 and CD31 expression in bone defects after 8 weeks. Groups: (**A**) empty (**B**) NC cmRNA control groups (**C**) low dose BMP-2 cmRNA (3.75 µg/defect) (**D**) high dose BMP-2 cmRNA (15 µg/defect). For CD45 staining, a general scan of the entire section as well as 10x, 20x and 40x magnification images are shown. Examples of leukocyte infiltration are indicated with arrows. For CD31, a general scan of the entire section as well as 10x magnification images are shown. Examples of new vessel growth are indicated with arrows. Inserts in scans indicate the area where the high magnification picture was taken. Figure reproduced from Zhang et. al. [115] with permission from Mary Ann Liebert Inc.

5. 7 Osteoimmunogenic response *in vivo*

From the animals that were treated with 50µg TISU BMP-2 cmRNA, 50µg NC BMP-2 cmRNA, 11µg rhBMP-2, or empty sponge, plasma samples were taken at 1, 3, and 10 days for multiplex ELISA determinations (Fig. 15).

The results indicated that TISU BMP-2cmRNA had a strong osteo-immunogenic ability in terms of the expression of all the cytokines. Differences between TISU BMP-2 cmRNA and 11 µg rhBMP-2 were statistically significant. Only for TNF-α at day 1 post-application was

greater activation observed with11 μg rhBMP-2 compared with TISU BMP-2 cmRNA, but this was not statistically significant.

For all 14 cytokines evaluated, no significant differences were observed between the TISU and NC groups, even though the expression levels were quite high in the TISU group. For seven of the cytokines (IL-1α, IL-2, IL-4, IL-5, IL-13, IL-17A, and TNF-α) at day 10 post-application, no significant differences were detected among all four treatment groups. The NC and BMP-2 groups displayed strong cytokine-stimulating effects compared to the empty group, but only six cytokines (GM-CSF, TNF-α, IL-6, IL-13, and IL-17A) showed a significant difference.

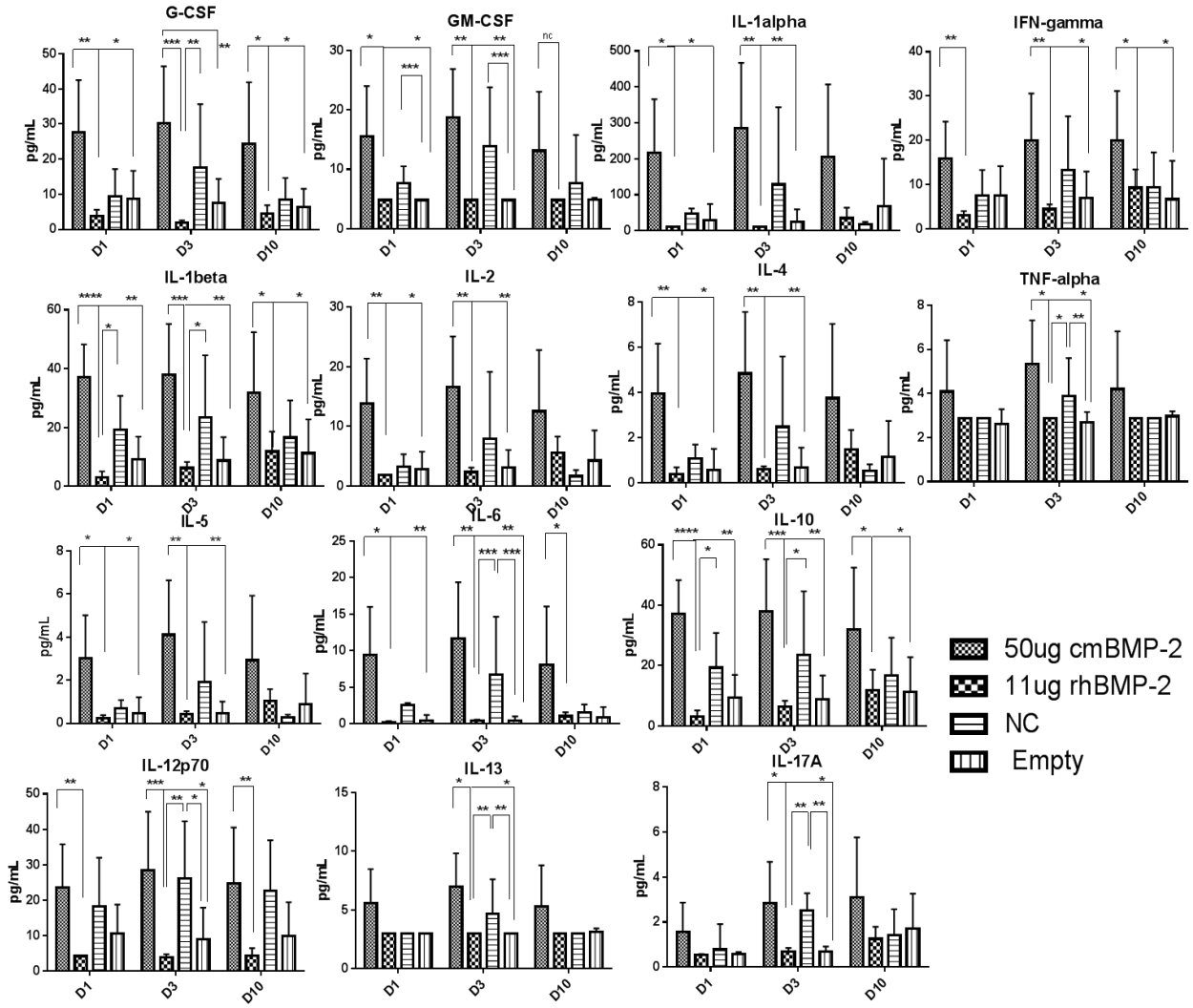

Fig.15. Osteoimmunogenic cytokines detection using Multiple ELISA. 14 cytokines (G-CSF, GM-CSF, IL-1α and β, IL-2, IL-4, IL-5, IL-6, IL-10, IL-12p70, IL-13, IL-17A, IFN-γ and TNF-α) were

analyzed from the plasma taken from the rats after treated with 4 different groups. Obtained p-values are indicated as follows: *p≤0.05, **p≤0.01, ***p≤0.001 and ****p≤0.0001. N=6 animals for each group, mean ± SD.

5. 8 Localization of cmRNA after implantation

Following implantation of TAMs loaded with Luc cmRNA, a strong luminescence signal was detected in the defect area in the rats (Fig. 16A). The luminescence from the defect area could still be detected up to 72 h (Fig. 16B). The anti-luciferase staining images showed an intracellular localization of the translated luciferase from the cmRNA (Fig. 16C).

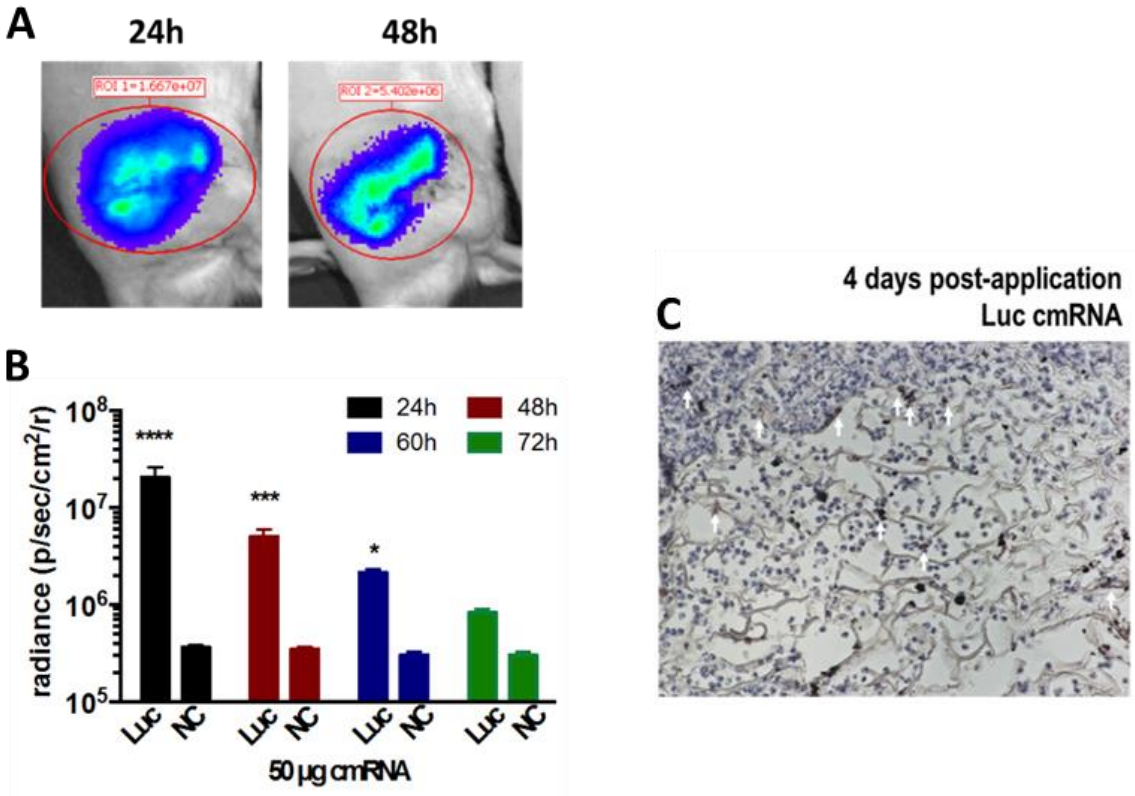

Fig.16. Localization of Luciferase cmRNA after implantation. (A)Live imaging of fluorescence signal in surgery area; (B) Quantification of signal radiance during 72h post-surgery; (C) Immunohistochemistry staining of Luciferase localization at cell level, 4 days post-application. Obtained p-values are indicated as **p≤0.01 and ****p≤0.0001. N=6 animals per group.

6. Discussion

RNA transcript therapy has promising conceptual advantages over gene and protein-replacement therapies. However, the development of transcript therapy still faces many challenges. How to improve the mRNA translation efficacy and cmRNA stability remains as two of the most important factors determining the success of transcript therapy. To date, numerous studies have addressed the elongation of the poly (A) tail, inclusion of chemically modified nucleotides, enhancement of capping efficiency, and insertion of UTRs to achieve the goals indicated above.

In the present study, two different cmBMP-2 RNA constructs were selected and investigated with respect to translation and mRNA stability. Furthermore, with the best-performing candidate, the ability to accelerate bone healing *in vitro* and *in vivo* in a critical bone defect model was studied. Therefore, chemically modified mRNAs with a long poly (A) tail, various cellular UTR combinations, and sequential modifications were designed.

6. 1 Optimizations of UTRs and BMP-2 sequence

The goal of this study was to investigate elements in the mRNA structure that are necessary for efficient *in vitro* transcription and cellular translation. In addition, we aimed to test the newly developed constructs' functionality in comparison with previously used cmBMP-2 constructs. In this regard, we designed synthetic RNA molecules consisting of slightly different minimalistic 5'-UTRs upstream of the gene of interest (GOI) and a 3' poly (A) tail.

In the meantime, we investigated the BMP-2 gene sequence in detail, and found two regulatory areas within the BMP-2 gene that can lead to reduced protein expression and mRNA stability, that is, a uORF in the 5' UTR and an AU-rich element in the 3' UTR. uORF is a mRNA element located in the 5' UTR and is defined by a start codon in the 5' UTR that is out-of-frame with the main coding sequence. These kind of elements can regulate mRNA post-transcription. Because

eukaryotic ribosomes normally load on the 5'cap of mRNA transcripts and scan for the presence of the first AUG start codon, uORFs can disrupt the efficient translation of the downstream coding sequence, which can further lead to reduced mRNA stability and protein expression [116-118]. It was shown that uORFs are present in approximately 50% of human and mouse protein-encoding genes and correlate with reduced protein expression across thousands of mammalian genes in a variety of tissues and conditions [119]. These studies regarding uORFs indicate that they can affect mRNA stability by approximately 30% and reduce protein expression levels by 30–80%. This suggests that uORFs act mostly by reducing translational efficiency, and more modestly by affecting mRNA levels.

The other negative regulatory element is an AU-rich element present after the polyadenylation signal. This AU-rich sequence located in 3'UTRs is associated with mRNA degradation as well as reduced translation [120]. Furthermore, the AU-rich sequence at the 3’ end was removed to make the mRNA more stable.

Besides deleting elements which could interfere with the translational efficiency and mRNA stability, we also incorporated a special sequence trying to further increase the function of BMP-2 mRNA. TISU element is a translation regulator originally discovered in the non-coding region of genes with extremely short 5'-UTRs [88]. From previous study, we found out that the mRNA incorporated with TISU element showed not only enhanced translation efficiency, but also the cell type independency *in vitro* experiments. Similar patterns were found in mice [113]. The TISU element, first identified by Elfakess and Dikstein [88], has a fixed position close to the 5' end of the mRNA molecule and regulates both transcription and translation [121]. This unique initiator is cap dependent, with the best results for the m7G cap [87]. Moreover, when the TISU is present, no scanning of the mRNA occurs [121]. These characteristics are different from the Kozak sequence, where the localization of the sequence is dispersed and not necessarily close to the 5' end.

The Kozak regulates only translation and depends on scanning of the mRNA [121]. Regarding the modified nucleotides used, the 5-iodo substitution provided the best results when compared to several alternative nucleotide modifications [113].

In the present study, two minimalistic synthetic 5'-UTR sequences (minimal UTR and TISU) were investigated with respect to their effect on protein levels post-mRNA delivery. In addition to the sequence modifications, chemical modifications that finally led to the new BMP-2 cmRNA described here, that is, nucleotides 5IU(0.35)5IC(0.075), and inclusion of a TISU sequence, clearly showed a robust improvement in protein translation. TISU BMP-2 was compared with our previously reported cmRNA (pVAX120 BMP-2 cmRNA, s2U (0.25) m5C (0.25)) [35, 89, 92] and we confirmed a significantly higher BMP-2 production (approx. four times) *in vitro* in 24h post-transfection. Furthermore, in both cell lines (HEK293 and MC3T3), the inclusion of a TISU sequence led to the same tendency for much higher BMP-2 production levels up to 72 h post-transfection compared with the minimal UTR constructs. On the basis of these results, we selected TISU cmBMP-2 as the target mRNA for further studies.

6.2 mRNA Immunology

One of the challenges in mRNA therapy is the relatively high immunogenic response that is induced after application. Therefore, we investigated the immunogenicity of the developed TISU-BMP-2 cmRNA construct. Previously, it was demonstrated that the modification s2U (0.25) m5C (0.25) abolished mRNA interaction with TLRs and decreased TNF-α, IFN-γ, and IL-12 expression *in vivo* [86]. *In vitro*, the modified cmRNA clearly decreased activation of immune-relevant cytokines when transfecting hPBMCs compared to unmodified mRNA. Our results showed that moderate TNF-α and IFN-γ activation by TISU cmRNA was much lower than that induced by unmodified mRNA at early time points and was insufficient to initiate the secondary response represented by increased IL-1 and IL-6 expression. Our results are in

accordance with previously published data. Kariko et al.[91] found that modifying mRNA with specific nucleotides reduced TLRs-mediated cytokine secretion, including of TNF-α, IL-1, and IL-6. Warren et al.[122] subsequently demonstrated that complete substitution of cytidine and uridine by modified homologues dramatically attenuated IFN signaling.

6. 3 Osteoimmunology

Natural bone healing after fracture involves an inflammatory phase which presumably is even more pronounced in the very invasive critical bone defect model used in this study, and which may be potentiated by the implantation of o-TAMs.

The natural inflammatory response after fracture normally starts immediately, peaking at 24 h, then continues for approximately one week [123]. During this phase, a complex cascade of proinflammatory signals and growth factors are released in a temporally and spatially controlled manner [124]. IL-1, IL-6, IL-11, IL-18, and TNF-α as first-responding cytokines are significantly elevated within the first few days [124, 125]. The increase in these cytokines could act as signals to promote inflammatory cell recruitment and angiogenesis [124]. After 7–10 days, a new phase - renewal and remodeling - starts. During this phase, osteoprogenitor cells differentiate into osteoblasts and osteoclasts. The cytokines expressed by these cells can either promote or inhibit the process of renewal and resorption to reform the initial woven bone structure. At this stage, in addition to IL-1, IL-6, and IL-11, elevated levels of TNF-α, IL-12, and IFN-γ are also detectable at the fracture site [124, 125].

Increasing numbers of studies have revealed the effects of cytokines on osteoblast and osteoclast generation. It is known that IL-1α, IL-1β, IL-6 and other members of the gp130 cytokine family, IL-7, and TNF-α directly or indirectly promote osteoclastogenesis [126-129], whereas interferon-beta (IFN-β), IFN-γ, IL-3, IL-4, IL-10, IL-13, and IL-12 alone and in synergy with IL-18 inhibit osteoclast formation [130-132].

Our results showed elevated cytokine expression in the TISU BMP-2 cmRNA group compared to rhBM-2. On the basis of the results obtained from a dose-response study, TISU BMP-2 cmRNA still had a relatively strong immunogenic potentiality. Interestingly, for the same modification and dosage of NC BMP-2 and TISU-BMP-2 cmRNA, no significant difference was found among all 14 cytokines at any of the three time points, although an increasing expression level was observed in the TISU BMP-2 cmRNA group. This suggested that BMP-2 over-expression can somehow activate inflammatory cytokine expression. By contrast, a certain level of the cytokine activation can also stimulate bone formation [133].

TNF-α regulates the differentiation and function of both osteoblasts and osteoclasts via cell-surface receptors for TNF-α [134]. The effect of IL-1 on bone largely overlaps with that of TNF-α. These findings are consistent with our results. In our results, TNF-α and IL-1 shared almost the same activation pattern. IL-1 also stimulates angiogenesis and promotes formation of the cartilaginous callus inside the fracture site [123]. IL-6 regulates the differentiation of both osteoblasts and osteoclasts, and promotes angiogenesis by stimulating the release of VEGF. IL-4, a so-called inhibitory cytokine, targets both osteoclasts and osteoblasts, inhibiting *in vivo* bone remodeling [135]. Significantly increased bone formation was observed under IL-5 overexpression [136]. IL-17 enhanced bone formation in a drill-hole injury animal model [137]. In the present study, all the samples used were collected from whole blood; it would be interesting to combine this with the sample taken from the defect area to map the correlation of the immune response between local injury and the circulation.

When we consider cytokine function in detail, all the cytokines have different impacts on bone regeneration. With respect to all the studies related to osteoimmunology, all these cytokines can behave as regulators in balancing the osteoblast-osteoclast cross talk, further regulating bone regeneration and remodeling.

Therefore, in order to even further reduce the immune response after the application of the cmRNA therapy, development of better modifications should be continued conducting.

6. 4 Angiogenesis during bone healing

Another important challenge in bone healing remains adequate vascularization of the new tissue [138, 139]. Because the major cause for delayed fracture healing is an insufficient blood supply [140], achieving more effective vascularization during the regeneration of large bone defects has become an even more relevant issue [139]. VEGF, as one of the most extensively studied angiogenic growth factors, predominantly acts during the early stage of fracture healing [141, 142]. Our results showed the *in vitro* upregulation of CD31 and VEGF genes in BMP-2 cmRNA-transfected stem cells. IHC staining of *in vivo* samples also showed increased CD31 expression in the BMP-2 cmRNA-treated groups, where vessel formation was also observed in the neo-bone formation area. This indicates a certain level of angiogenesis induced by the BMP-2 cmRNA. This has not been previously reported for BMP-2 cmRNA, although several studies reported angiogenic responses *in vitro* and *in vivo* while investigating osteogenesis induced by BMP-2-encoding DNA plasmids [143, 144].

Some studies concluded that a combination of BMP-2 and VEGF plasmids produced better osteogenic results [145]. Therefore, it would be of interest to further investigate these effects using the relevant cmRNAs combination.

6. 5 Osteogenesis potentiality and bone healing *in vivo*

These promising *in vitro* properties were confirmed by *in vivo* experiments showing enhanced bone formation within an osseous critical-size defect in the rat. Having generated an effective lipoplex-cmRNA formulation loaded on a collagen sponge to form o-TAMs, an off-the-shelf

product for stimulating osteogenesis locally in human patients would be practical [35]. To improve the treatment following surgery, in the dose-response study, we directly thawed the lipids-cmRNA complex and loaded this directly on the sponge without overnight freeze drying.

When combined with 3D biomaterials, in the form of TAMs, sustained release of cmRNAs from the matrix may allow the continuous transfection of target cells. In previous work, our colleagues reported that BMP-2 cmRNA-loaded fibrin gel enhanced osteogenesis of bone marrow MSCs [92] *in vitro* and bone formation in a non-critical defect model in the rat [89]. In the present work, we proved that on the application of new TISU BMP-2 cmRNA-loaded o-TAMs, strong osteogenesis and angiogenesis effects occurred both *in vitro* and *in vivo*. When we further analyzed the data in greater detail, we interestingly found *in vitro* that the highest osteogenic capacity was obtained in the lower-dose cmRNA group. By contrast, *in vivo* the expected dose-dependent bone tissue formation was observed. A possible reason for this difference might be the high dose of 5 μg per well may be very toxic for *in vitro* cell transfection. The hPBMCs results also showed more cytokine induction in the higher-dose group compared with lower-dose.

In the present study, instead of a non-critical bone defect model as used previously (mono-cortical drill-hole) [35, 89], we generated a more clinically relevant bone defect model that could not heal unaided in the rats. Both μCT results and histology showed significantly higher de novo bone formation in the defects treated with TISU BMP-2 cmRNA-loaded TAMs compared with empty collagens and non-coding BMP-2 collagens, particularly when the highest dose was used (15 μg/defect). The almost bridging healing of the high-dose group here was only previously observed in the protein-treated defect model.

The Masson trichrome staining results not only provided a general overview of new tissue formation within the bone-defect area, but also indicated an endochondral ossification process with newly formed cartilaginous structures that mineralized towards the native bone borders.

Furthermore, in IHC for Col II and Col III, staining deposits were observed at the fracture area and mostly localized in the interphase of the bridging area, where cartilaginous tissue was observed. Intense areas of Col I were observed in the mineralized new tissue, which indicated the formation of a more mature osseous structure.

In accordance with our results, Elangovan et al. and Khorsand et al. demonstrated that BMP-2 cmRNA stimulated *in vivo* ossification that could follow either of the two mechanisms observed during bone development, endochondral or intramembranous ossification [146, 147]. In their studies, up to 50 μg of a 100% nucleotide-substituted mRNA, via polyethylenimine (PEI), was delivered to a calvarial defect in rats.

Our results collectively demonstrated the *in vivo* osteogenic potential of a newly designed BMP-2 cmRNA and indicated a possible dose dependency. To investigate the dose-response, experiments over a wider dose range were conducted. From the results, we clearly saw that the extent of bone formation was related to the dose level. More convincing evidence for mRNA therapy as an alternative treatment was at 8 weeks after surgery, where the highest dose group (50 μg) showed significantly higher BV/TV compared to the rhBMP-2 group, while at 4 weeks no significant difference was observed. Additionally, at both time points, the TISU-BMP-2 groups displayed greater bone formation compared to protein treatment. From the Masson staining in the dose-response study, another interesting observation was that the 50 μg/defect and recombinant protein groups appeared to share the same regeneration pattern — endochondral bone formation. An intense staining called the bone collar along the diaphysis wall was formed on the outer layer of the defect area. In the staining at 8 weeks, the formation of spongy bone inside the defect area was shown. At the same time, in the lower-dose groups, it appears that regeneration is more likely via intramembranous ossification. When looking, for example, at the staining of the 25 μg/defect at 8 weeks, clear formation of an ossification center was shown. During the bone fracture-healing process, both intramembranous and endochondral

ossification occurred. Here with different dosages and at different time points, different bone regeneration patterns were observed. As understood in general, intramembranous ossification occurred earlier than endochondral ossification. One possible explanation for this phenomenon could be that with 50 μg cmRNA and 11 μg recombinant protein, more mesenchymal stem cells were recruited during the early stage and accelerated the process of intramembranous ossification. It will be interesting for further investigation of the ossification mechanism in the future.

Even with a treatment dose up to 50 μg, bone formation (BV/TV) was still mainly located in the ascending curve, thus it would be very interesting to include additional doses to cover the entire dosage curve and gain greater insight for potential future clinical application. In addition, on the application of our TISU BMP-2 cm RNA, a normally non-healing critical femur bone defect was totally bridged after the 8-week observation period, with a similar BV compared to the recombinant protein group. These results give us great confidence for future follow-up research regarding transcript therapy.

7. Conclusion and Outlook

In this thesis, several modifications were incorporated into BMP-2 cmRNA: chemically modified nucleotides including 5-iodo-uridine and 5-iodo-cytidine, 120nt poly (A) tail and the insertion of TISU in 5'UTR, and deletion of upstream ORF and AU-rich regions after the polyadenylation signal. Consequently, the modified TISU BMP-2 mRNA resulted in not only enhanced protein translation, but was also less immunogenic compared to the BMP-2 cmRNA used previously. For the first time, this newly modified TISU BMP-2 cmRNA has been applied in a critical bone defect rat model. On the application of up to 50 μg TISU BMP-2 cmRNA, the bone regeneration in a critical bone defect clearly demonstrated dose dependency. At 8 weeks after treatment, TISU BMP-2 cmRNA showed a significantly higher BV compared with the rhBMP-2 protein group ($p<0.001$). From the 3D reconstructed images, a bridged healing pattern, the same as for recombinant BMP-2 protein, was detected. Histology and IHC staining confirmed the μCT results.

The osteo-immunogenic experiments demonstrated the relatively high immunogenicity of cmRNA. This is a major challenge for future mRNA therapeutics. In future development of transcript therapy, greater effort will be needed regarding the immunogenic response to cmRNA.

8. References

1. Chiapasco, M., M. Zaniboni, and L. Rimondini, *Autogenous onlay bone grafts vs. alveolar distraction osteogenesis for the correction of vertically deficient edentulous ridges: a 2-4-year prospective study on humans.* Clin Oral Implants Res, 2007. **18**(4): p. 432-40.
2. Moses, O., et al., *Severely resorbed mandible treated with iliac crest autogenous bone graft and dental implants: 17-year follow-up.* Int J Oral Maxillofac Implants, 2007. **22**(6): p. 1017-21.
3. Burkus, J.K., et al., *Anterior lumbar interbody fusion using rhBMP-2 with tapered interbody cages.* J Spinal Disord Tech, 2002. **15**(5): p. 337-49.
4. Carragee, E.J., E.L. Hurwitz, and B.K. Weiner, *A critical review of recombinant human bone morphogenetic protein-2 trials in spinal surgery: emerging safety concerns and lessons learned.* Spine J, 2011. **11**(6): p. 471-91.
5. Haid, R.W., Jr., et al., *Posterior lumbar interbody fusion using recombinant human bone morphogenetic protein type 2 with cylindrical interbody cages.* Spine J, 2004. **4**(5): p. 527-38; discussion 538-9.
6. Mroz, T.E., et al., *Complications related to osteobiologics use in spine surgery: a systematic review.* Spine (Phila Pa 1976), 2010. **35**(9 Suppl): p. S86-104.
7. Bodalia, P.N., et al., *Effectiveness and safety of recombinant human bone morphogenetic protein-2 for adults with lumbar spine pseudarthrosis following spinal fusion surgery: A systematic review.* Bone Joint Res, 2016. **5**(4): p. 145-52.
8. Gibbs, D.M., et al., *Hope versus hype: what can additive manufacturing realistically offer trauma and orthopedic surgery?* Regen Med, 2014. **9**(4): p. 535-49.
9. Tang, D., et al., *Biofabrication of bone tissue: approaches, challenges and translation for bone regeneration.* Biomaterials, 2016. **83**: p. 363-82.
10. Orciani, M., et al., *Biofabrication and Bone Tissue Regeneration: Cell Source, Approaches, and Challenges.* Front Bioeng Biotechnol, 2017. **5**: p. 17.
11. Mueller-Klieser, W., *Three-dimensional cell cultures: from molecular mechanisms to clinical applications.* Am J Physiol, 1997. **273**(4 Pt 1): p. C1109-23.
12. Huh, D., G.A. Hamilton, and D.E. Ingber, *From 3D cell culture to organs-on-chips.* Trends Cell Biol, 2011. **21**(12): p. 745-54.
13. Pampaloni, F., E.G. Reynaud, and E.H. Stelzer, *The third dimension bridges the gap between cell culture and live tissue.* Nat Rev Mol Cell Biol, 2007. **8**(10): p. 839-45.
14. Haycock, J.W., *3D cell culture: a review of current approaches and techniques.* Methods Mol Biol, 2011. **695**: p. 1-15.
15. Lee, J., M.J. Cuddihy, and N.A. Kotov, *Three-dimensional cell culture matrices: state of the art.* Tissue Eng Part B Rev, 2008. **14**(1): p. 61-86.
16. Carletti, E., A. Motta, and C. Migliaresi, *Scaffolds for tissue engineering and 3D cell culture.* Methods Mol Biol, 2011. **695**: p. 17-39.
17. Langer, R. and D.A. Tirrell, *Designing materials for biology and medicine.* Nature, 2004. **428**(6982): p. 487-92.
18. Chevallay, B. and D. Herbage, *Collagen-based biomaterials as 3D scaffold for cell cultures: applications for tissue engineering and gene therapy.* Med Biol Eng Comput, 2000. **38**(2): p. 211-8.
19. Lee, C.H., A. Singla, and Y. Lee, *Biomedical applications of collagen.* Int J Pharm, 2001. **221**(1-2): p. 1-22.
20. Hansbrough, J.F., et al., *Burn wound closure with cultured autologous keratinocytes and fibroblasts attached to a collagen-glycosaminoglycan substrate.* JAMA, 1989. **262**(15): p. 2125-30.
21. Harriger, M.D., et al., *Glutaraldehyde crosslinking of collagen substrates inhibits degradation in skin substitutes grafted to athymic mice.* J Biomed Mater Res, 1997. **35**(2): p. 137-45.

22. Takaoka, K., et al., *Ectopic bone induction on and in porous hydroxyapatite combined with collagen and bone morphogenetic protein.* Clin Orthop Relat Res, 1988(234): p. 250-4.
23. Murata, M., et al., *Bone augmentation by recombinant human BMP-2 and collagen on adult rat parietal bone.* Int J Oral Maxillofac Surg, 1999. **28**(3): p. 232-7.
24. Flanagan, T.C., et al., *A collagen-glycosaminoglycan co-culture model for heart valve tissue engineering applications.* Biomaterials, 2006. **27**(10): p. 2233-46.
25. Auger, F.A., et al., *Tissue-engineered human skin substitutes developed from collagen-populated hydrated gels: clinical and fundamental applications.* Med Biol Eng Comput, 1998. **36**(6): p. 801-12.
26. Pitaru, S., et al., *Partial regeneration of periodontal tissues using collagen barriers. Initial observations in the canine.* J Periodontol, 1988. **59**(6): p. 380-6.
27. Ceballos, D., et al., *Magnetically aligned collagen gel filling a collagen nerve guide improves peripheral nerve regeneration.* Exp Neurol, 1999. **158**(2): p. 290-300.
28. Friess, W., *Collagen--biomaterial for drug delivery.* Eur J Pharm Biopharm, 1998. **45**(2): p. 113-36.
29. Unterman, S.R., et al., *Collagen shield drug delivery: therapeutic concentrations of tobramycin in the rabbit cornea and aqueous humor.* J Cataract Refract Surg, 1988. **14**(5): p. 500-4.
30. Seeherman, H., J. Wozney, and R. Li, *Bone morphogenetic protein delivery systems.* Spine (Phila Pa 1976), 2002. **27**(16 Suppl 1): p. S16-23.
31. Dang, J.M. and K.W. Leong, *Natural polymers for gene delivery and tissue engineering.* Adv Drug Deliv Rev, 2006. **58**(4): p. 487-99.
32. McKay, W.F., S.M. Peckham, and J.M. Badura, *A comprehensive clinical review of recombinant human bone morphogenetic protein-2 (INFUSE Bone Graft).* Int Orthop, 2007. **31**(6): p. 729-34.
33. Bartus, R.T., et al., *Sustained delivery of proteins for novel therapeutic agents.* Science, 1998. **281**(5380): p. 1161-2.
34. Khan, A., et al., *Sustained polymeric delivery of gene silencing antisense ODNs, siRNA, DNAzymes and ribozymes: in vitro and in vivo studies.* J Drug Target, 2004. **12**(6): p. 393-404.
35. Badieyan, Z.S., et al., *Transcript-activated collagen matrix as sustained mRNA delivery system for bone regeneration.* J Control Release, 2016. **239**: p. 137-48.
36. Hanamura, H. and M.R. Urist, *Osteogenesis and chondrogenesis in transplants of Dunn and Ridgway osteosarcoma cell cultures.* Am J Pathol, 1978. **91**(2): p. 277-98.
37. Wozney, J.M., et al., *Novel regulators of bone formation: molecular clones and activities.* Science, 1988. **242**(4885): p. 1528-34.
38. Carlisle, E. and J.S. Fischgrund, *Bone morphogenetic proteins for spinal fusion.* Spine J, 2005. **5**(6 Suppl): p. 240S-249S.
39. Bianco, P., P.G. Robey, and P.J. Simmons, *Mesenchymal stem cells: revisiting history, concepts, and assays.* Cell Stem Cell, 2008. **2**(4): p. 313-9.
40. Moustakas, A., S. Souchelnytskyi, and C.H. Heldin, *Smad regulation in TGF-beta signal transduction.* J Cell Sci, 2001. **114**(Pt 24): p. 4359-69.
41. Gazzerro, E. and E. Canalis, *Bone morphogenetic proteins and their antagonists.* Rev Endocr Metab Disord, 2006. **7**(1-2): p. 51-65.
42. Maeda, S., et al., *Endogenous TGF-beta signaling suppresses maturation of osteoblastic mesenchymal cells.* EMBO J, 2004. **23**(3): p. 552-63.
43. Li, X., et al., *Smad6 is induced by BMP-2 and modulates chondrocyte differentiation.* J Orthop Res, 2003. **21**(5): p. 908-13.
44. Hassel, S., et al., *Initiation of Smad-dependent and Smad-independent signaling via distinct BMP-receptor complexes.* J Bone Joint Surg Am, 2003. **85-A Suppl 3**: p. 44-51.
45. Xiao, G., et al., *Bone morphogenetic proteins, extracellular matrix, and mitogen-activated protein kinase signaling pathways are required for osteoblast-specific gene expression and differentiation in MC3T3-E1 cells.* J Bone Miner Res, 2002. **17**(1): p. 101-10.

46. Hu, Y., et al., *Activation of p38 mitogen-activated protein kinase is required for osteoblast differentiation.* Endocrinology, 2003. **144**(5): p. 2068-74.
47. Lee, K.S., et al., *Runx2 is a common target of transforming growth factor beta1 and bone morphogenetic protein 2, and cooperation between Runx2 and Smad5 induces osteoblast-specific gene expression in the pluripotent mesenchymal precursor cell line C2C12.* Mol Cell Biol, 2000. **20**(23): p. 8783-92.
48. Javed, A., et al., *runt homology domain transcription factors (Runx, Cbfa, and AML) mediate repression of the bone sialoprotein promoter: evidence for promoter context-dependent activity of Cbfa proteins.* Mol Cell Biol, 2001. **21**(8): p. 2891-905.
49. Karsenty, G., *Transcriptional regulation of osteoblast differentiation during development.* Front Biosci, 1998. **3**: p. d834-7.
50. Nakashima, K., et al., *The novel zinc finger-containing transcription factor osterix is required for osteoblast differentiation and bone formation.* Cell, 2002. **108**(1): p. 17-29.
51. Milona, M.A., J.E. Gough, and A.J. Edgar, *Expression of alternatively spliced isoforms of human Sp7 in osteoblast-like cells.* BMC Genomics, 2003. **4**: p. 43.
52. Lee, M.H., et al., *BMP-2-induced Osterix expression is mediated by Dlx5 but is independent of Runx2.* Biochem Biophys Res Commun, 2003. **309**(3): p. 689-94.
53. Argintar, E., S. Edwards, and J. Delahay, *Bone morphogenetic proteins in orthopaedic trauma surgery.* Injury, 2011. **42**(8): p. 730-4.
54. Einhorn, T.A., et al., *A single percutaneous injection of recombinant human bone morphogenetic protein-2 accelerates fracture repair.* J Bone Joint Surg Am, 2003. **85-A**(8): p. 1425-35.
55. Boden, S.D., et al., *The use of rhBMP-2 in interbody fusion cages. Definitive evidence of osteoinduction in humans: a preliminary report.* Spine (Phila Pa 1976), 2000. **25**(3): p. 376-81.
56. Grauer, J.N., et al., *2000 Young Investigator Research Award winner. Evaluation of OP-1 as a graft substitute for intertransverse process lumbar fusion.* Spine (Phila Pa 1976), 2001. **26**(2): p. 127-33.
57. Cunningham, B.W., et al., *Osseointegration of autograft versus osteogenic protein-1 in posterolateral spinal arthrodesis: emphasis on the comparative mechanisms of bone induction.* Spine J, 2002. **2**(1): p. 11-24.
58. Vaccaro, A.R., et al., *The safety and efficacy of OP-1 (rhBMP-7) as a replacement for iliac crest autograft for posterolateral lumbar arthrodesis: minimum 4-year follow-up of a pilot study.* Spine J, 2008. **8**(3): p. 457-65.
59. Matsui, A., et al., *Messenger RNA-based therapeutics for the treatment of apoptosis-associated diseases.* Sci Rep, 2015. **5**: p. 15810.
60. Russell, D.W. and M. Grompe, *Adeno-associated virus finds its disease.* Nat Genet, 2015. **47**(10): p. 1104-5.
61. Zou, S., et al., *Lipid-mediated delivery of RNA is more efficient than delivery of DNA in non-dividing cells.* Int J Pharm, 2010. **389**(1-2): p. 232-43.
62. Oberli, M.A., et al., *Lipid Nanoparticle Assisted mRNA Delivery for Potent Cancer Immunotherapy.* Nano Lett, 2017. **17**(3): p. 1326-1335.
63. Pascolo, S., *Messenger RNA-based vaccines.* Expert Opin Biol Ther, 2004. **4**(8): p. 1285-94.
64. Midoux, P. and C. Pichon, *Lipid-based mRNA vaccine delivery systems.* Expert Rev Vaccines, 2015. **14**(2): p. 221-34.
65. Richner, J.M., et al., *Modified mRNA Vaccines Protect against Zika Virus Infection.* Cell, 2017. **169**(1): p. 176.
66. Pardi, N., et al., *Zika virus protection by a single low-dose nucleoside-modified mRNA vaccination.* Nature, 2017. **543**(7644): p. 248-251.
67. Barrett, L.W., S. Fletcher, and S.D. Wilton, *Regulation of eukaryotic gene expression by the untranslated gene regions and other non-coding elements.* Cell Mol Life Sci, 2012. **69**(21): p. 3613-34.

68. Pichon, X., et al., *RNA binding protein/RNA element interactions and the control of translation.* Curr Protein Pept Sci, 2012. **13**(4): p. 294-304.
69. Cheneval, D., et al., *A review of methods to monitor the modulation of mRNA stability: a novel approach to drug discovery and therapeutic intervention.* J Biomol Screen, 2010. **15**(6): p. 609-22.
70. Ingolia, N.T., *Ribosome Footprint Profiling of Translation throughout the Genome.* Cell, 2016. **165**(1): p. 22-33.
71. Wethmar, K., *The regulatory potential of upstream open reading frames in eukaryotic gene expression.* Wiley Interdiscip Rev RNA, 2014. **5**(6): p. 765-78.
72. Wethmar, K., et al., *uORFdb--a comprehensive literature database on eukaryotic uORF biology.* Nucleic Acids Res, 2014. **42**(Database issue): p. D60-7.
73. Johnstone, T.G., A.A. Bazzini, and A.J. Giraldez, *Upstream ORFs are prevalent translational repressors in vertebrates.* EMBO J, 2016. **35**(7): p. 706-23.
74. Vattem, K.M. and R.C. Wek, *Reinitiation involving upstream ORFs regulates ATF4 mRNA translation in mammalian cells.* Proc Natl Acad Sci U S A, 2004. **101**(31): p. 11269-74.
75. Brewer, G. and J. Ross, *Poly(A) shortening and degradation of the 3' A+U-rich sequences of human c-myc mRNA in a cell-free system.* Mol Cell Biol, 1988. **8**(4): p. 1697-708.
76. Zhang, X., A. Virtanen, and F.E. Kleiman, *To polyadenylate or to deadenylate: that is the question.* Cell Cycle, 2010. **9**(22): p. 4437-49.
77. Fuke, H. and M. Ohno, *Role of poly (A) tail as an identity element for mRNA nuclear export.* Nucleic Acids Res, 2008. **36**(3): p. 1037-49.
78. Tudek, A., M. Lloret-Llinares, and T.H. Jensen, *The multitasking polyA tail: nuclear RNA maturation, degradation and export.* Philos Trans R Soc Lond B Biol Sci, 2018. **373**(1762).
79. Shaw, G. and R. Kamen, *A conserved AU sequence from the 3' untranslated region of GM-CSF mRNA mediates selective mRNA degradation.* Cell, 1986. **46**(5): p. 659-67.
80. Caput, D., et al., *Identification of a common nucleotide sequence in the 3'-untranslated region of mRNA molecules specifying inflammatory mediators.* Proc Natl Acad Sci U S A, 1986. **83**(6): p. 1670-4.
81. Kariko, K., et al., *Incorporation of pseudouridine into mRNA yields superior nonimmunogenic vector with increased translational capacity and biological stability.* Mol Ther, 2008. **16**(11): p. 1833-40.
82. Jopling, C., S. Boue, and J.C. Izpisua Belmonte, *Dedifferentiation, transdifferentiation and reprogramming: three routes to regeneration.* Nat Rev Mol Cell Biol, 2011. **12**(2): p. 79-89.
83. Nguyen, P.D., et al., *Fabrication of Magnetic Upconversion Nanohybrid for Luminescent Resonance Energy Transfer-Based Detection of Glutathione.* J Nanosci Nanotechnol, 2015. **15**(10): p. 7950-4.
84. Li, B., X. Luo, and Y. Dong, *Effects of Chemically Modified Messenger RNA on Protein Expression.* Bioconjug Chem, 2016. **27**(3): p. 849-53.
85. Uchida, S., K. Kataoka, and K. Itaka, *Screening of mRNA Chemical Modification to Maximize Protein Expression with Reduced Immunogenicity.* Pharmaceutics, 2015. **7**(3): p. 137-51.
86. Kormann, M.S., et al., *Expression of therapeutic proteins after delivery of chemically modified mRNA in mice.* Nat Biotechnol, 2011. **29**(2): p. 154-7.
87. Elfakess, R., et al., *Unique translation initiation of mRNAs-containing TISU element.* Nucleic Acids Res, 2011. **39**(17): p. 7598-609.
88. Elfakess, R. and R. Dikstein, *A translation initiation element specific to mRNAs with very short 5'UTR that also regulates transcription.* PLoS One, 2008. **3**(8): p. e3094.
89. Ferizi, M., et al., *Human cellular CYBA UTR sequences increase mRNA translation without affecting the half-life of recombinant RNA transcripts.* Sci Rep, 2016. **6**: p. 39149.
90. Holtkamp, S., et al., *Modification of antigen-encoding RNA increases stability, translational efficacy, and T-cell stimulatory capacity of dendritic cells.* Blood, 2006. **108**(13): p. 4009-17.
91. Kariko, K., et al., *Suppression of RNA recognition by Toll-like receptors: the impact of nucleoside modification and the evolutionary origin of RNA.* Immunity, 2005. **23**(2): p. 165-75.

92. Balmayor, E.R., et al., *Modified mRNA for BMP-2 in Combination with Biomaterials Serves as a Transcript-Activated Matrix for Effectively Inducing Osteogenic Pathways in Stem Cells.* Stem Cells Dev, 2017. **26**(1): p. 25-34.
93. Heiser, A., et al., *Autologous dendritic cells transfected with prostate-specific antigen RNA stimulate CTL responses against metastatic prostate tumors.* J Clin Invest, 2002. **109**(3): p. 409-17.
94. Weide, B., et al., *Results of the first phase I/II clinical vaccination trial with direct injection of mRNA.* J Immunother, 2008. **31**(2): p. 180-8.
95. Kyte, J.A., et al., *Phase I/II trial of melanoma therapy with dendritic cells transfected with autologous tumor-mRNA.* Cancer Gene Ther, 2006. **13**(10): p. 905-18.
96. Mu, L.J., et al., *Immunotherapy with allotumour mRNA-transfected dendritic cells in androgen-resistant prostate cancer patients.* Br J Cancer, 2005. **93**(7): p. 749-56.
97. Hoerr, I., et al., *In vivo application of RNA leads to induction of specific cytotoxic T lymphocytes and antibodies.* Eur J Immunol, 2000. **30**(1): p. 1-7.
98. Martinon, F., et al., *Induction of virus-specific cytotoxic T lymphocytes in vivo by liposome-entrapped mRNA.* Eur J Immunol, 1993. **23**(7): p. 1719-22.
99. Brazzoli, M., et al., *Induction of Broad-Based Immunity and Protective Efficacy by Self-amplifying mRNA Vaccines Encoding Influenza Virus Hemagglutinin.* J Virol, 2016. **90**(1): p. 332-44.
100. Petsch, B., et al., *Protective efficacy of in vitro synthesized, specific mRNA vaccines against influenza A virus infection.* Nat Biotechnol, 2012. **30**(12): p. 1210-6.
101. Van Gulck, E., et al., *mRNA-based dendritic cell vaccination induces potent antiviral T-cell responses in HIV-1-infected patients.* AIDS, 2012. **26**(4): p. F1-12.
102. Nair, S.K., et al., *Induction of primary carcinoembryonic antigen (CEA)-specific cytotoxic T lymphocytes in vitro using human dendritic cells transfected with RNA.* Nat Biotechnol, 1998. **16**(4): p. 364-9.
103. Anderson, D.M., et al., *Stability of mRNA/cationic lipid lipoplexes in human and rat cerebrospinal fluid: methods and evidence for nonviral mRNA gene delivery to the central nervous system.* Hum Gene Ther, 2003. **14**(3): p. 191-202.
104. Glenn, J.S., H. Ellens, and J.M. White, *Delivery of liposome-encapsulated RNA to cells expressing influenza virus hemagglutinin.* Methods Enzymol, 1993. **221**: p. 327-39.
105. Rudolph, C., et al., *In vivo gene delivery to the lung using polyethylenimine and fractured polyamidoamine dendrimers.* J Gene Med, 2000. **2**(4): p. 269-78.
106. Jayaraman, M., et al., *Maximizing the potency of siRNA lipid nanoparticles for hepatic gene silencing in vivo.* Angew Chem Int Ed Engl, 2012. **51**(34): p. 8529-33.
107. Yamamoto, A., et al., *Current prospects for mRNA gene delivery.* Eur J Pharm Biopharm, 2009. **71**(3): p. 484-9.
108. Semple, S.C., et al., *Efficient encapsulation of antisense oligonucleotides in lipid vesicles using ionizable aminolipids: formation of novel small multilamellar vesicle structures.* Biochim Biophys Acta, 2001. **1510**(1-2): p. 152-66.
109. Dong, Y., et al., *Poly(glycoamidoamine) Brushes Formulated Nanomaterials for Systemic siRNA and mRNA Delivery in Vivo.* Nano Lett, 2016. **16**(2): p. 842-8.
110. Khan, O.F., et al., *Ionizable amphiphilic dendrimer-based nanomaterials with alkyl-chain-substituted amines for tunable siRNA delivery to the liver endothelium in vivo.* Angew Chem Int Ed Engl, 2014. **53**(52): p. 14397-401.
111. Uchida, H., et al., *Modulated protonation of side chain aminoethylene repeats in N-substituted polyaspartamides promotes mRNA transfection.* J Am Chem Soc, 2014. **136**(35): p. 12396-405.
112. Jarzebinska, A., et al., *A Single Methylene Group in Oligoalkylamine-Based Cationic Polymers and Lipids Promotes Enhanced mRNA Delivery.* Angew Chem Int Ed Engl, 2016. **55**(33): p. 9591-5.

113. Trepotec, Z., et al., *Maximizing the Translational Yield of mRNA Therapeutics by Minimizing 5'-UTRs.* Tissue Eng Part A, 2019. **25**(1-2): p. 69-79.
114. Schrom, E., et al., *Translation of Angiotensin-Converting Enzyme 2 upon Liver- and Lung-Targeted Delivery of Optimized Chemically Modified mRNA.* Mol Ther Nucleic Acids, 2017. **7**: p. 350-365.
115. Zhang, W., et al., *An Improved, Chemically Modified RNA Encoding BMP-2 Enhances Osteogenesis In Vitro and In Vivo.* Tissue Eng Part A, 2019. **25**(1-2): p. 131-144.
116. Kozak, M., *Structural features in eukaryotic mRNAs that modulate the initiation of translation.* J Biol Chem, 1991. **266**(30): p. 19867-70.
117. Morris, D.R. and A.P. Geballe, *Upstream open reading frames as regulators of mRNA translation.* Mol Cell Biol, 2000. **20**(23): p. 8635-42.
118. Matsui, M., et al., *Bioinformatic analysis of post-transcriptional regulation by uORF in human and mouse.* FEBS Lett, 2007. **581**(22): p. 4184-8.
119. Calvo, S.E., D.J. Pagliarini, and V.K. Mootha, *Upstream open reading frames cause widespread reduction of protein expression and are polymorphic among humans.* Proc Natl Acad Sci U S A, 2009. **106**(18): p. 7507-12.
120. Chen, C.Y. and A.B. Shyu, *AU-rich elements: characterization and importance in mRNA degradation.* Trends Biochem Sci, 1995. **20**(11): p. 465-70.
121. Dikstein, R., *Transcription and translation in a package deal: the TISU paradigm.* Gene, 2012. **491**(1): p. 1-4.
122. Warren, L., et al., *Highly efficient reprogramming to pluripotency and directed differentiation of human cells with synthetic modified mRNA.* Cell Stem Cell, 2010. **7**(5): p. 618-30.
123. Cho, T.J., L.C. Gerstenfeld, and T.A. Einhorn, *Differential temporal expression of members of the transforming growth factor beta superfamily during murine fracture healing.* J Bone Miner Res, 2002. **17**(3): p. 513-20.
124. Gerstenfeld, L.C., et al., *Fracture healing as a post-natal developmental process: molecular, spatial, and temporal aspects of its regulation.* J Cell Biochem, 2003. **88**(5): p. 873-84.
125. Rundle, C.H., et al., *Microarray analysis of gene expression during the inflammation and endochondral bone formation stages of rat femur fracture repair.* Bone, 2006. **38**(4): p. 521-9.
126. Kudo, O., et al., *Proinflammatory cytokine (TNFalpha/IL-1alpha) induction of human osteoclast formation.* J Pathol, 2002. **198**(2): p. 220-7.
127. Palmqvist, P., et al., *IL-6, leukemia inhibitory factor, and oncostatin M stimulate bone resorption and regulate the expression of receptor activator of NF-kappa B ligand, osteoprotegerin, and receptor activator of NF-kappa B in mouse calvariae.* J Immunol, 2002. **169**(6): p. 3353-62.
128. Toraldo, G., et al., *IL-7 induces bone loss in vivo by induction of receptor activator of nuclear factor kappa B ligand and tumor necrosis factor alpha from T cells.* Proc Natl Acad Sci U S A, 2003. **100**(1): p. 125-30.
129. Sabokbar, A., O. Kudo, and N.A. Athanasou, *Two distinct cellular mechanisms of osteoclast formation and bone resorption in periprosthetic osteolysis.* J Orthop Res, 2003. **21**(1): p. 73-80.
130. Fox, S.W., et al., *The possible role of TGF-beta-induced suppressors of cytokine signaling expression in osteoclast/macrophage lineage commitment in vitro.* J Immunol, 2003. **170**(7): p. 3679-87.
131. Bendixen, A.C., et al., *IL-4 inhibits osteoclast formation through a direct action on osteoclast precursors via peroxisome proliferator-activated receptor gamma 1.* Proc Natl Acad Sci U S A, 2001. **98**(5): p. 2443-8.
132. Horwood, N.J., et al., *IL-12 alone and in synergy with IL-18 inhibits osteoclast formation in vitro.* J Immunol, 2001. **166**(8): p. 4915-21.
133. Ibarra Urizar, A., et al., *Inflammatory Cytokines Stimulate Bone Morphogenetic Protein-2 Expression and Release from Pancreatic Beta Cells.* J Interferon Cytokine Res, 2016. **36**(1): p. 20-9.

134. Kon, T., et al., *Expression of osteoprotegerin, receptor activator of NF-kappaB ligand (osteoprotegerin ligand) and related proinflammatory cytokines during fracture healing.* J Bone Miner Res, 2001. **16**(6): p. 1004-14.
135. Lee, S.K. and J. Lorenzo, *Cytokines regulating osteoclast formation and function.* Curr Opin Rheumatol, 2006. **18**(4): p. 411-8.
136. Macias, M.P., et al., *Expression of IL-5 alters bone metabolism and induces ossification of the spleen in transgenic mice.* J Clin Invest, 2001. **107**(8): p. 949-59.
137. Ono, T., et al., *IL-17-producing gammadelta T cells enhance bone regeneration.* Nat Commun, 2016. **7**: p. 10928.
138. Grosso, A., et al., *It Takes Two to Tango: Coupling of Angiogenesis and Osteogenesis for Bone Regeneration.* Front Bioeng Biotechnol, 2017. **5**: p. 68.
139. Roux, B.M., M.H. Cheng, and E.M. Brey, *Engineering clinically relevant volumes of vascularized bone.* J Cell Mol Med, 2015. **19**(5): p. 903-14.
140. Glowacki, J., *Angiogenesis in fracture repair.* Clin Orthop Relat Res, 1998(355 Suppl): p. S82-9.
141. Street, J., et al., *Vascular endothelial growth factor stimulates bone repair by promoting angiogenesis and bone turnover.* Proc Natl Acad Sci U S A, 2002. **99**(15): p. 9656-61.
142. Peng, H., et al., *Synergistic enhancement of bone formation and healing by stem cell-expressed VEGF and bone morphogenetic protein-4.* J Clin Invest, 2002. **110**(6): p. 751-9.
143. Samee, M., et al., *Bone morphogenetic protein-2 (BMP-2) and vascular endothelial growth factor (VEGF) transfection to human periosteal cells enhances osteoblast differentiation and bone formation.* J Pharmacol Sci, 2008. **108**(1): p. 18-31.
144. Wang, C.J., et al., *pCMV-BMP-2-transfected cell-mediated gene therapy in anterior cruciate ligament reconstruction in rabbits.* Arthroscopy, 2010. **26**(7): p. 968-76.
145. Peng, H., et al., *VEGF improves, whereas sFlt1 inhibits, BMP2-induced bone formation and bone healing through modulation of angiogenesis.* J Bone Miner Res, 2005. **20**(11): p. 2017-27.
146. Elangovan, S., et al., *Chemically modified RNA activated matrices enhance bone regeneration.* J Control Release, 2015. **218**: p. 22-8.
147. Khorsand, B., et al., *A Comparative Study of the Bone Regenerative Effect of Chemically Modified RNA Encoding BMP-2 or BMP-9.* AAPS J, 2017. **19**(2): p. 438-446.

9. List of publication

1. Zhang W[1,2], De La Vega RE[3], Coenen MJ[3], Müller SA[3,4], Peniche Silva CJ[1], Aneja MK[5], Plank C[2,5], van Griensven M[1,3], Evans CH[3], Balmayor ER[1,3].(2019). An Improved, Chemically Modified RNA Encoding BMP-2 Enhances Osteogenesis In Vitro and *In Vivo*. Tissue Eng Part A, 25(1-2):131-144.

10. Appendix

10.1 Publication

Tissue Engineering

DOI: 10.1089/ten.TEA.2018.0112

An improved, chemically modified RNA encoding BMP-2 enhances osteogenesis in vitro and in vivo

Wen Zhang[1,2], Rodolfo E. De La Vega[3], Michael J. Coenen[3], Carlos J. Peniche Silva[1], Manish K. Aneja[4], Christian Plank[2,4], Martijn van Griensven[1,3], Christopher H. Evans[3], Elizabeth R. Balmayor[1,3,*]

[1] Department of Experimental Trauma Surgery, Klinikum rechts der Isar, Technical University of Munich, Munich, Germany

[2] Institute of Molecular Immunology and Experimental Oncology, Klinikum rechts der Isar, Technical University of Munich, Munich, Germany

[3] Rehabilitation Medicine Research Center, Mayo Clinic, Rochester, MN, USA

[4] Ethris GmbH, Planegg, Germany

Full contact information for each author:

Wen Zhang, MD – phone: +49-89-4140-6249; e-mail: Wen.Zhang@tum.de

Rodolfo E. De La Vega, MD – phone: +1-507-266-0436; e-mail: Delavega.Rodolfo@mayo.edu

Michael J. Coenen – phone: +1-507-284-9564; e-mail: Coenen.Michael@mayo.edu

Carlos J. Peniche Silva – phone: +49-89-4140-6249; e-mail: Carlos.Peniche@tum.de

Manish K. Aneja, PhD – phone: +49 89 89 55 788 13; e-mail: Aneja@ethris.com

Christian Plank, PhD – phone: +49-89-4140-4453; e-mail: Christian.Plank@tum.de

Martijn van Griensven, MD, PhD – phone: +49-89-4140-6310; e-mail: Martijn.vanGriensven@tum.de

Christopher H. Evans, PhD – phone: +1-507-255-0099; e-mail: Evans.Christopher@mayo.edu

Elizabeth R. Balmayor, PhD – phone: +49-89-4140-9754; e-mail: Elizabeth.Rosado-Balmayor@tum.de

Tissue Engineering
An improved, chemically modified RNA encoding BMP-2 enhances osteogenesis in vitro and in vivo (DOI: 10.1089/ten.TEA.2018.0112)

***Corresponding author:**

Elizabeth Rosado Balmayor, PhD

Assistant Professor for Experimental Trauma Surgery

Department of Experimental Trauma Surgery

Klinikum rechts der Isar

Technical University of Munich

Ismaningerstr 22

81675 Munich, Germany

Phone: +49-89-4140-9754; Fax: +49-89-4140-7526

e-mail: Elizabeth.Rosado-Balmayor@tum.de

Tissue Engineering
An improved, chemically modified RNA encoding BMP-2 enhances osteogenesis in vitro and in vivo (DOI: 10.1089/ten.TEA.2018.0112)

Abstract

The first therapeutic application of mRNA was suggested over two decades ago. However, its application was constrained by the ability of mRNA to activate the innate immune response, cytotoxicity and poor potency. We and others recently demonstrated that these undesirable properties of mRNA may be overcome by alterating its structure. In this study, we developed a new chemically modified mRNA coding for BMP-2 with improved osteogenic features. To develop this new construct, we removed from the mRNA sequence the following undesirable elements: an upstream ORF in the 5'UTR and a polyadenylation element together with an AU-rich tract in the 3'UTR. In addition, a translation initiator of short UTRs (TISU) was introduced together with 5-iodo modified pyrimidine nucleotides. The new TISU BMP-2 cmRNA showed robust BMP-2 production *in vitro* in cell lines (HEK293 and MC3T3) and primary cells (muscle-derived mesenchymal stem cells). Stem cells additionally showed upregulation of osteogenic and angiogenic genes as result of the TISU BMP-2 cmRNA transfection. The in vivo osteogenic properties of TISU BMP-2 cmRNA were explored in a critical-sized femoral defect in the rat. For this, the TISU BMP-2 cmRNA was loaded into collagen sponges to form transcript-activated matrices. Animals treated with TISU BMP-2 cmRNA showed superior bone formation that seemed to recapitulate endochondral ossification. The higher of the two doses examined in this model showed more robust new tissue formation. Finally, improved vascularization was detected in the healing area for animals treated with TISU BMP-2 cmRNA.

Keywords: transcript therapy, mRNA, modified mRNA, BMP-2, bone healing, vascularization

Tissue Engineering
An improved, chemically modified RNA encoding BMP-2 enhances osteogenesis in vitro and in vivo (DOI: 10.1089/ten.TEA.2018.0112)

Impact statement

The use of cmRNA with increased stability using TISU offers the prospect of finally allowing us to unlock the potent osteogenic properties of BMP-2 in a clinically expedient manner. As noted, delivery of recombinant BMP-2 protein has had modest clinical efficacy, while gene delivery is effective but very difficult to translate into human clinical use. This study shows the great potential of cmRNA encoding BMP-2 with TISU in an long bone critical size rat model.

Introduction

There is much interest in the use of mRNA as an alternative to protein delivery and gene therapy for certain indications. Unlike DNA, RNA does not need to traffic to the nucleus of the cell and there is no possibility of mutation, integration or other undesirable genetic events. Regenerative medicine provides attractive opportunities for the application of mRNA therapies because the necessary duration and level of expression may well match those achieved with mRNA.

Native mRNA, however, is unsuitable for this purpose because it is unstable, inflammatory and cytotoxic. The basic components of the native mRNA molecule are shown in figure 1A. Chemically-modified RNA (cmRNA) is being developed in response to the challenges of using mRNA therapeutically. Previous research has identified a number of alterations to mRNA that address one or more of its shortcomings that prevent it from becoming a therapeutic agent (1-3). For example, extending the 3' poly(A) tail to 120 nucleotides increases the metabolic stability of the RNA (2). Pyrimidine substitution inhibits the interaction of the RNA with toll-like receptors (TLRs) and retinoid-inducible gene 1 (RIG-1), thereby reducing inflammation (3). As first demonstrated elegantly by Kariko *et al.* (4), pseudouridine substituted mRNA has reduced binding to TLRs. Our group also reported that substituting 25% of uridine and cytidine with 2-thiouridine and 5-methylcytidine, respectively, decreased mRNA interactions with TLRs and RIG-1 in human peripheral blood mononuclear cells (PBMCs) (3). Another modification of interest includes the use of non-native 5'- and 3'- untranslated regions (UTRs). In our previous study, we could demonstrate that the use of human cellular cytochrome b-245 alpha polypeptide

(CYBA) UTR sequence increased mRNA translation while maintaining stability of the recombinant RNA transcripts (1).

Few previous publications explore the use of cmRNA as an agent of osteogenesis. Elangovan *et al.* developed a cmRNA encoding BMP-2, in which pyrimidines were 100% substituted with pseudouridine and 5-methylcytosine (5). Bone marrow mesenchymal stem cells (MSCs) transfected with these constructs remained viable and secreted substantial amounts of BMP-2 into their culture media, expressed certain transcripts associated with osteogenesis and deposited a mineralized matrix. In these regards, transfection with BMP-2 cmRNA was more effective than transfection with a plasmid encoding BMP-2. Plasmid and BMP-2 cmRNA were loaded onto collagen scaffolds and compared in a rat cranial defect model, under which conditions defects treated with cmRNA deposited more bone. By means of the same pyrimidine substitution, the authors recently developed a BMP-9 cmRNA that induced osteogenic responses in bone marrow MSCs and in a rat cranial defect model (6).

Our group has been following a different approach in order to develop a highly stable, non-toxic and osteogenic cmRNA. This involves combining different sequence alterations into a single cmRNA molecule. The first osteogenic BMP-2 cmRNA developed by us contained a poly(A) tail of 120 nucleotides with only 25% of pyrimidines substituted with 2-thiouridine and 5-methylcytosine (1, 7, 8). Human adipose-derived MSCs and rat bone marrow MSCs transfected with these constructs secreted substantial amounts of BMP-2 for at least 10 days, expressed genes associated with osteogenesis and deposited a mineralized matrix (1, 8). Similar results were obtained with explants of human fat tissue (1). This cmRNA construct also accelerated bone healing in a rat, femoral, cortical drill-hole (1, 7).

We have dedicated considerable research to the study of alterations to mRNA and their combinations, aiming to develop a cmRNA that features maximal stability. As a consequence, higher stability may increase the cmRNA persistence inside the cell, which in turn results in increased protein production and prolonged secretion time. Thus, the present communication describes several novel modifications designed to improve the

Tissue Engineering
An improved, chemically modified RNA encoding BMP-2 enhances osteogenesis in vitro and in vivo (DOI: 10.1089/ten.TEA.2018.0112)
This paper has been peer-reviewed and accepted for publication, but has yet to undergo copyediting and proof correction. The final published version may differ from this proof.

Tissue Engineering
An improved, chemically modified RNA encoding BMP-2 enhances osteogenesis in vitro and in vivo (DOI: 10.1089/ten.TEA.2018.0112)

performance of BMP-2 cmRNA. These include the substitution of 35% of uridine with 5-iodo-uridine and 7.5% of cytidine with 5-iodo-cytidine. The new construct also includes a translation initiator of short 5'UTR (TISU) sequence to improve translational efficiency, as well as deletion of an upstream open reading frame (ORF) and an extra polyadenylation signal followed by an AU rich region that were detected in the BMP-2 sequence. The ability of this new construct to induce BMP-2 production was evaluated in cell lines and primary cells. Moreover, cytokine induction was assessed in human PBMCs after their contact with the newly developed BMP-2 cmRNA. This assessment provided an indication of the immunogenicity of the developed construct. The osteogenic properties of this new construct were evaluated *in vitro* and *in vivo*. For this, an osteogenic transcript activated matrix (o-TAM) was developed by loading the new BMP-2 cmRNA into collagen sponges. A previous report from our group indicates the enhancement of the osteogenic potential of BMP-2 cmRNA when formulated in a three-dimensional (3D) matrix or TAM (8). Moreover, the combination of an osteogenic cmRNA with a clinically used biomaterial may produce a superior material for bone healing applications.

Materials and Methods

Generation of cmRNAs encoding human BMP-2

In our previous studies (1, 7, 8), BMP-2 cmRNA was produced from a plasmid pVAXA120 BMP-2, which contained codon optimized human BMP-2 sequence (optimized using GeneOptimizer, Thermo Fischer Scientific, MA, USA) but also included certain undesirable features, namely an upstream ORF in the 5'UTR and cytoplasmic polyadenylation element together with an AU-rich tract in the 3'UTR (Fig. 1B). In the present study, only the BMP-2 coding sequence (corresponding to the annotation in NCBI database: NM_001200.2) was used in combination with different 5'UTR elements, namely a minimal UTR sequence (Fig. 1C) (9, 10) and the TISU element (Fig. 1D) (11). The recombinant constructs were synthetized by GeneScript and provided in pUC57-Kana vector. In addition to the BMP-2 coding construct, a non-coding (NC) plasmid was produced, in which the Kozak element (GCCACC) was scrambled (CGCACC) and all in-frame ATGs were converted to stop codons (TGA).

Tissue Engineering
An improved, chemically modified RNA encoding BMP-2 enhances osteogenesis in vitro and in vivo (DOI: 10.1089/ten.TEA.2018.0112)

To generate the templates for *in vitro* transcription (IVT), plasmids were linearized and purified with chloroform – ethanol. IVT reactions were carried out using T7 RNA polymerase (Thermo Fischer Scientific, MA, USA), following manufacturer's instructions. For production of cmRNAs defined, chemically modified ribonucleotides were added to the IVT mix. Thus, 35% of uridine residues were replaced with 5-iodo-uridine and 7.5% of cytidine residues with 5-iodo-cytidine; these constructs are referred to as $5IU_{(0.35)}5IC_{(0.075)}$. In addition, for comparison purposes, a cmRNA was produced using our previously published modification i.e. 25% of pyrimidines were substituted with 2-thiouridine and 5-methylcytosine ($s2U_{(0.25)}m5C_{(0.25)}$) (1, 7, 8). The chemically modified nucleotides were obtained from Jena Biosciences (Jena, Germany). The complete IVT mix was incubated for 2 hours at 37°C with later addition of DNase I (Thermo Fisher Scientific, MA, USA) and further incubation for 45 min. Purification of resulting cmRNAs was performed by ammonium acetate precipitation. A m7G cap structure was added to the 5' end, while the 3' end was subjected to enzymatic polyadenylation of approximately 120 nucleotides. The employed enzymes, both from New England Biolabs (MA, USA), were Vaccinia Virus Capping Enzyme and *E. coli* poly(A) polymerase, respectively. The concentration and quality of all produced cmRNAs were measured on a NanoDrop2000C (Thermo Fisher Scientific, MA, USA). The purity and size were confirmed by automated capillary electrophoresis (Fragment Analyzer, Advanced Analytical, IA, USA). A schematic representation of the structure of cmRNAs generated for the study is shown in Fig. 1B-D.

Unmodified mRNA was produced by the methodology described above using only natural ribonucleotides.

BMP-2 cmRNA transfection screening using HEK293 and MC3T3 cell lines

All materials used for cell culture were purchased from Gibco Life Technologies, Paisley, UK unless otherwise stated.

HEK293 cells (ATCC® CRL 1573™, VA, USA) were cultured in Dulbecco's modified Eagle's medium (DMEM). MC3T3-E1 cells (ATCC® CRL-2593™, VA, USA) were cultured in complete alpha minimum essential medium (α-MEM). Both culture media were

supplemented with 10% fetal bovine serum (FBS) and 1% penicillin/streptomycin (P/S). Both cell lines were maintained at 37°C and 5% CO_2 in a humidified atmosphere.

Cells were transfected using Lipofectamine® 2000 (Thermo Fisher Scientific, MA, USA) for cmRNA screening purposes and according to the manufacturer's instructions. In brief, $6.25x10^4$ cells/cm^2 were seeded into 96-well plates and incubated for 24 hours before transfection. BMP-2 cmRNA doses in the range from 500 to 7.5 ng/well were used for HEK293 and a single dose of 500 ng/well for MC3T3-E1. BMP-2 cmRNA complexes were formed by using 2 µl Lipofectamine® 2000 per 1 µg cmRNA. Following 20 min of incubation at room temperature, the complexes were added to the cells and incubated for 24, 48 and 72 hours. At each time point cell culture supernatants were collected for BMP-2 quantification by ELISA (R&D Systems, MN, USA) following the manufacturer's instructions.

Formation and characterization of lipoplex transfection complexes

The transfection reagent comprised a cationic lipid N,N'-Bis(2-aminoethyl)-1,3-propanediamine modified with C12 alkylchains (C12-(2-3-2)) along with 1,2-dipalmitoyl-sn-glycero-3-phosphocholine (DPPC) and cholesterol as helper lipids. Moreover, 1,2-dimyristoyl-sn-glycerol methoxypolyethylene glycol (DMG-PEG2k) was included as a PEGylated lipid. The preparation methodology for this in-house transfection reagent has been described elsewhere (9, 12). Lipoplexes were formed using a solvent exchange method also described in (9, 12) ensuring a final cmRNA concentration of 200 µg/ml. An N/P ratio (molar ratio of amino groups of the lipid to phosphate groups of cmRNA) of 8 was used. Lipoplexes were then dialyzed against double distilled water using dialysis cassettes with molecular weight cut-off of 7 kDa (Pierce™, Thermo Fisher Scientific, MA, USA). The particle sizes, polydispersity index and electrokinetic potential of the obtained lipoplexes were measured by dynamic light scattering (DLS) using a Zetasizer Nano ZS (Malvern Instruments, Worcester, UK).

Loading of BMP-2 cmRNA lipoplexes into collagen sponges to obtain o-TAMs

After formulation, the BMP-2 mRNA lipoplexes were loaded into collagen sponges. The collagen biomaterial used was KOLLAGEN resorb™ (equine origin) from Resorba Medical GmbH (Nuremberg, Germany). The methodology used for the loading of BMP-2

Tissue Engineering
An improved, chemically modified RNA encoding BMP-2 enhances osteogenesis in vitro and in vivo (DOI: 10.1089/ten.TEA.2018.0112)
This paper has been peer-reviewed and accepted for publication, but has yet to undergo copyediting and proof correction. The final published version may differ from this proof.

Tissue Engineering
An improved, chemically modified RNA encoding BMP-2 enhances osteogenesis in vitro and in vivo (DOI: 10.1089/ten.TEA.2018.0112)

mRNA lipoplexes into the sponge has been recently published (7). In brief, 6 mm diameter disks (punched from the original collagen sponge) were placed in the wells of a 96-well-plates. Next, 50 µl of lipoplexes in 2% sucrose were slowly added to the collagen disks. Once the sponges were completely soaked with the lipoplexes, the BMP-2 mRNA loaded sponges were dried in high vacuum for at least 2 hours at 0.05 mbar, after which the o-TAMs were ready to use for *in vitro* and *in vivo* applications. Two cmRNA loading doses were used to produce the o-TAMs, a low dose containing 1.25 µg cmRNA/sponge and a high dose with 5 µg cmRNA/sponge. The o-TAMs structure and surface topography were characterized using a VHX-900F microscope with its software (version 1.6.1.0) and the VH-Z20R objective.

Isolation of human peripheral blood mononuclear cells (hPBMCs) for immunogenicity evaluation of BMP-2 cmRNA o-TAMs

Blood collection and further experiments described inhere involving human material was approved (#5870/13) by the ethical committee of the Faculty of Medicine at the Technical University of Munich. In accordance with this approval, blood was collected with previous written patient informed consent and adhering to the newest guidelines of the declaration of Helsinki.

hPBMCs were isolated from fresh human blood (n=3 donors) by using Lymphocyte Separation Medium (LSM, density 1077 kg/m^3, Biowest, Nuaillé, France) following the manufacturer's recommendations. Next, hPBMCs were re-suspended in RPMI-GlutaMax containing 10% FBS and 1% P/S. hPBMCs were incubated with o-TAMs containing BMP-2 cmRNA as well as its unmodified mRNA homologue at two different concentrations (low dose (1.25 µg) and high dose (5 µg)). Cells were seeded on the loaded sponges (o-TAM) at a concentration of 1x10^5 cells/sponge, and incubated for 6, 12 and 24 hours. At these time points supernatants were collected and cytokine production (TNF-α, IFN-γ, IL-1β and IL-6) was evaluated by ELISA. All ELISA kits were purchased from PeproTech (NJ, USA) and used following the manufacturer's instructions.

Tissue Engineering
An improved, chemically modified RNA encoding BMP-2 enhances osteogenesis in vitro and in vivo (DOI: 10.1089/ten.TEA.2018.0112)

Isolation and BMP-2 cmRNA transfection of rat, muscle-derived mesenchymal stem cells

The harvest of rat tissue for stem cell isolation was performed according the approval from the Mayo Clinic Institutional Animal Care and Use Committee (IACUC) #A00001567-16. Primary, muscle-derived MSCs were isolated from the hind limb muscles of male Fischer F344 rats (n=3, 14-week-old, Charles River Laboratory (Wilmington, MA, USA)). following a previously reported protocol with slight modifications (13).

The rats were euthanized using CO_2 exposure. The tibialis anterior and gastrocnemius muscles were excised from both hind limbs. Following careful removal of extraneous tissues such as fat and tendon, the muscles were washed in Dulbecco's Phosphate-Buffered Saline (DPBS), diced and the pieces incubated in 0.2% collagenase type II solution at 37°C for 1 hour on an orbital shaker with frequent re-suspension. Supernatants were pooled and filtered through a 40 µm cell strainer and centrifuged at 1000g for 10 min. After counting the cells, they were plated at a density of $2x10^4$ cells/cm^2 in a gelatin coated flask. Cells were sub-cultured using high glucose DMEM supplemented with 20% FBS, 10% heat-inactivated horse serum (HS, HyClone, UT, USA), 1% chicken embryo extract (CEE, USBiological, MA, USA) and 1% P/S. Cells of passages between 2 – 4 were utilized for this study.

Three different o-TAMs were used for transfection: collagen sponges loaded with non-coding cmRNA (5 µg NC cmRNA); low dose (1.25 µg BMP-2 cmRNA); high dose (5 µg BMP-2 cmRNA). Cells were seeded from a cell suspension of $1x10^5$ cells in 50 µl non-supplemented DMEM. After 2 hours incubation, 200 µl supplemented DMEM (5% FBS + 5% HS + 0.5% CEE + 1% P/S) was added to each well. Cell culture supernatants were collected 6, 12, 24, 48 and 72 hours post-transfection; 6 days post-transfection, both cell culture supernatants and cell lysates were harvested. Samples were stored at –80°C until further examination. ELISA was performed with a commercial kit (R&D Systems, MN, USA) following the manufacturer's instructions; results are reported as ng BMP-2 per ml sample.

Expression of osteogenic markers by transfected rat, muscle-derived MSCs

As a functional assay, rat, muscle-derived MSCs were seeded onto two different matrices: plain collagen sponges (without cmRNA) and low dose BMP-2 cmRNA o-TAMs.

Tissue Engineering
An improved, chemically modified RNA encoding BMP-2 enhances osteogenesis in vitro and in vivo (DOI: 10.1089/ten.TEA.2018.0112)

The culture medium was supplemented with 10 mM β-glycerophosphate and 50 µg/ml L-ascorbic acid (both reagents from Sigma Aldrich, MO, USA). Media were renewed every two to three days. Rat, muscle-derived MSCs seeded onto plain collagen sponges without cmRNA, were used as controls. After 7, 14 and 21 days, cells were examined for expression of osteogenic marker genes by RT-PCR.

To extract total RNA, cell-seeded sponges were collected with TRI-reagent (Life Technologies, Darmstadt, Germany) and total RNA was isolated by the phenol/chloroform method. RNA concentration and purity were determined spectrophotometrically using a BioPhotometer plus UV spectrophotometer (Eppendorf AG, Hamburg, Germany). Total RNA was reverse-transcribed using a First Strand cDNA Synthesis Kit (Thermo Scientific, MA, USA) with random primers. SsoFast Eva Green Supermix (Bio-Rad Laboratories, CA, USA) was used and the PCR reactions were carried out in a Bio-Rad CFX96 thermal cycler (Bio-Rad Laboratories, CA, USA). The expression of RunX2, collagen type I (Col I), osteocalcin (OCN), osteopontin (OPN), CD31 and VEGF was evaluated. Details on the rat amplification primers used can be found elsewhere (1). Rat β-tubulin was used as housekeeping gene and results were reported relative to untransfected, rat, muscle-derived MSCs seeded onto plain collagen sponges by means of the $2^{-\Delta\Delta CT}$ method.

Rat critical size femoral bone defect model

Male Fischer F344 rats were purchased from Charles River Laboratory (Wilmington, MA). All animals were housed in a central animal care facility with 12 hours light cycles and given chow and water *ad libitum*. Animal care and experimental protocols were followed in accordance with National Institutes of Health guidelines and approved by the Mayo Clinic Institutional Animal Care and Use Committee (#A00002349-16).

Rats (n=24) were 14-weeks-old at the time of surgery. A 5 mm, critical-sized, mid-femoral defect was created in the right hind limb of each rat. Rats were anesthetized with 2.5% isoflurane inhalation (induction and maintenance) at 1 L/min of oxygen flow. Under sterile conditions, a 4 cm incision was made in the right posterolateral thigh. The lateral intermuscular septum with respect to the femur was dissected to expose the diaphysis of the femur. Care was taken to preserve the periosteum and the surrounding soft tissues.

Tissue Engineering
An improved, chemically modified RNA encoding BMP-2 enhances osteogenesis in vitro and in vivo (DOI: 10.1089/ten.TEA.2018.0112)

Using a polyacetal plate (Special Designs, TX, USA) as a guide, four holes were drilled along the mid-diaphysis using a 0.79 mm drill bit. The plate was then secured carefully to the femur using four hand-driven 0.9 mm threaded K-wires (MicroAire Surgical Instruments, VA, USA), which allowed the construct to act as a locked plate. A 5 mm osteotomy was made precisely equidistant from each of the inner wires using a 0.22 mm Gigli wire saw (RISystem AG, Davos, Switzerland) and a precision saw guide. After completion of the osteotomy, the site was irrigated with saline and the defect was left either empty or three collagen sponges loaded with NC cmRNA (5 µg), low (1.25 µg) or high (5 µg) dose BMP-2 cmRNA were placed in the 5 mm gap. A soft tissue pouch was created using the adjacent muscles to ensure that the collagen sponges would stay in place. The wound was closed in layers with 4-0 Vicryl sutures and the incision site closed using 9 mm wound clips. The animals were allowed to recover at 37°C in a recovery box before being returned to their cages. Analgesic treatment with slow release Buprenorphine at a dose of 0.6 mg/kg was administered subcutaneously pre-operatively and at day three after surgery to ensure continuous analgesia for a minimum of six days after surgery. Eight weeks after surgery, euthanasia was performed (CO_2 asphyxiation) and the right femora were harvested. Bone explants were fixed in 10% v/v neutral buffered formalin (Thermo Fisher Scientific, MA, USA) for 48 hours. Subsequently, the samples were transferred to ethanol 70% and stored at 4°C until further processing.

Images in Fig. 5A show the polyacetal plate used for stabilization as well as the bone defect. The experimental outline along with the experimental groups included in the study are presented in Fig. 5B. Six animals were included in each experimental group.

Radiographic evaluation

In vivo bone healing was monitored by performing radiographic images of the right femur using a digital x-ray cabinet (Faxitron Bioptics, AZ, USA) under general isoflurane inhalation anesthesia. Rats were ventrally positioned inside the cabinet with the hind limbs abducted at a 90° angle from rat body. Radiographs were obtained at 42 kV energy and 10 seconds exposure time on days 10, 28, 42 and 56. Two observers analyzed the images looking for fractures, failure of fixation and bone formation.

Tissue Engineering
An improved, chemically modified RNA encoding BMP-2 enhances osteogenesis in vitro and in vivo (DOI: 10.1089/ten.TEA.2018.0112)

Micro-computed tomography (μ-CT) analysis

Bone explants were scanned using a Skyscan 1176 μCT (Bruker, Kontich, Belgium) at 65 kV and 385 uA with a voxel size of 9 μm. Image reconstruction was performed using NRecon (Bruker, Version1.7.3), and analysis was performed using CTAn (Bruker, Version 1.13). Briefly, a region of interest (ROI) was selected, representing the entire area of the defect. Then, global thresholding was implemented for the binarization of images. Finally, using a built-in algorithm in CTAn, the bone volume (BV, cm^3), tissue volume (TV, cm^3) and the ratio BV/TV (%) were calculated for each sample.

Histology and immunohistochemistry (IHC)

After μCT, femoral explants were subjected to decalcified tissue histology. Samples were decalcified in 10% buffered EDTA (Sigma Aldrich, MO, USA), dehydrated in an ascending ethanol series and embedded in paraffin. Longitudinal cross-sections with a thickness of 7 μm were stained with Masson-Goldner Trichrome (Carl Roth GmbH, Karlsruhe, Germany) using the protocol provided by the manufacturer. For IHC, dewaxed and rehydrated sections were incubated with 3% hydrogen peroxide (Sigma Aldrich, MO, USA) for 15 min to block endogenous peroxidase activity. For antigen retrieval, sections for collagen and CD31 staining were incubated with proteinase K (Dako, Glostrup, Denmark) for 7 min at room temperature. In the case of CD45, antigen retrieval was performed by incubating in 10 mM citrate buffer (pH 6) for 20 min at 90°C. After blocking with 2% BSA (Sigma Aldrich, MO, USA) for 60 min, the sections were incubated with the primary antibodies solutions in blocking buffer overnight at 4°C. Primary antibodies were all purchased from Abcam (Cambridge, UK): collagen type I, ab34710, 1:200; collagen type II, ab34712, 1:200; collagen type III, ab7778, 1:200; CD31, ab182981, 1:1000; CD45, ab10558, 1:1000; rabbit isotype control IgG, ab27478, 1:200. Subsequently, slides were incubated with EnVision+ Dual Link System-HRP Rabbit/Mouse (Dako, Glostrup, Denmark) for 1 hour at room temperature. Color development was performed with liquid diaminobenzidine chromogen (Dako, Glostrup, Denmark) and sections were counterstained with Mayer's hematoxylin (Carl Roth GmbH, Karlsruhe, Germany).

Tissue Engineering
An improved, chemically modified RNA encoding BMP-2 enhances osteogenesis in vitro and in vivo (DOI: 10.1089/ten.TEA.2018.0112)

All stained slides were observed and photographed with a microscope (Biorevo BZ9000, Keyence, Osaka, Japan) at 10x and 20x magnifications. A general picture of the entire histological section was performed using the software BZ-II Viewer and BZ-II Analyzer (Keyence, Osaka, Japan).

Statistical analysis

Transfections in cell lines were performed in triplicates. Transfections of rat, muscle-derived MSCs and hPBMCs using the 3D (o-)TAMs were performed using N=3 individual donors. For each donor, the experiments were performed in triplicate (n=3). Data are reported as mean ± standard deviation. Statistical analysis was performed using GraphPad Prism Version 7.00 (GraphPad Software, CA, USA). Normal distribution of the data was analyzed by D'Agostino-Pearson test. One- and two-way ANOVA were performed to analyze comparison of multiple groups. ANOVA analyses were corrected for multiple comparison by Tukey (Gaussian distribution) and Kruskal-Wallis or Dunn's (non-Gaussian distribution) tests. P values were reported using the GraphPad style as follows: $p>0.05$ was considered not significant and indicated with "ns", $p\leq0.05$ was indicated with *, $p\leq0.01$ was indicated with **, $p\leq0.001$ was indicated with *** and $p\leq0.0001$ was indicated with ****.

Results

BMP-2 cmRNA transfected cells secrete high levels of hBMP-2

Two different BMP-2 cmRNA constructs modified with $5IU_{(0.35)}5IC_{(0.075)}$, with and without the TISU sequence, were compared. As shown in Fig. 1E and F, cells transfected with either of the two modified BMP-2 constructs (i.e. TISU and minimal UTR) gave significantly higher expression of BMP-2 than cells transfected with the pVAXA120 BMP-2 cmRNA construct ($p<0.0001$). The later included $s2U_{(0.25)}m5C_{(0.25)}$ and no TISU element. Moreover, the inclusion of the TISU sequence considerably enhanced BMP-2 expression ($p<0.0001$). The NC BMP-2 construct gave no expression (Fig. 1E). Expression of BMP-2 persisted for at least 72 hours in cultures of HEK293 and MC3T3-E1 cells (Fig. 1F).

Tissue Engineering
An improved, chemically modified RNA encoding BMP-2 enhances osteogenesis in vitro and in vivo (DOI: 10.1089/ten.TEA.2018.0112)

Osteogenic Transcript Activated Matrix, o-TAMs, were produced using TISU BMP-2 cmRNA

TISU element containing sequence was selected to be loaded into a 3D scaffold by lipoplex formation and vacuum drying onto collagen sponges with addition of sucrose for lyo-protection (Fig. 2A). The lipoplexes used for loading were about 80 nm in diameter and featured a positive charge (Table 1). The obtained o-TAMs were structurally stable, characterized by circular shape (Fig. 2B) and smooth surfaces (Fig. 2C and D). The interior of the o-TAMs was porous (Fig. 2E and F).

Reduced immunogenicity of TISU BMP-2 cmRNA compared to its unmodified mRNA homologue

TISU BMP-2 cmRNA and unmodified BMP-2 mRNA were incubated with hPBMCs using the 3D o-TAM structures. Cytokine production as result of cmRNA stimulation is presented in Fig. 3. Release of TNF-α and IFN-γ occurred primarily, followed by IL-1β and IL-6. In most cases, there was a dose-dependency in the induction of cytokines by both TISU BMP-2 cmRNA and unmodified BMP-2 mRNA.

Analyzing each evaluated cytokine in detail, for TNF-α and IFN-γ (Fig. 3A and B) lower expression was obtained that gradually declined over a period of 24 hours in the cmRNA groups. This result was more noticeable for IFN-γ (high dose, $p<0.001$ cmRNA vs. unmodified mRNA, all observation times assayed). Interestingly, the lowest levels of TNF-α and IFN-γ (<200 pg/ml) were obtained when hPBMCs were incubated with low dose cmRNA, which remained consistent over time ($p>0.05$). IL-1β and IL-6 production (Fig. 3C and D) increased as result of the unmodified mRNA transfection. Concentrations higher than 600 pg/ml were detected for both cytokines at 24 hours post-hPBMCs exposure. In contrast, when cmRNA was used, levels of IL-1β remained lower than 100 pg/ml and invariable over time ($p>0.05$). Remarkably, no differences were found between low and high dose cmRNA regarding IL-1β and IL-6 induction ($p>0.05$).

Transfection of rat, muscle-derived MSCs with TISU BMP-2 cmRNA o-TAM

Rat, muscle-derived MSCs transfected with either dose of TISU BMP-2 cmRNA o-TAM gave significantly higher expression of BMP-2 than cells transfected on NC cmRNA

Tissue Engineering
An improved, chemically modified RNA encoding BMP-2 enhances osteogenesis in vitro and in vivo (DOI: 10.1089/ten.TEA.2018.0112)

TAM (Fig. 4A, $p<0.01$). Remarkable, BMP-2 production persisted for 6 days, the end point of the evaluation. Interestingly, the lower dose TISU BMP-2 cmRNA o-TAM gave significantly higher expression of BMP-2 than the higher dose between 12 and 72 hours post-transfection ($p<0.0001$). At 6 days post-transfection, there were no significant differences in the amount of BMP-2 secreted by cells transfected with either cmRNA dose ($p>0.05$). However, a higher amount of BMP-2 could be detected in the lysates of cells transfected with the high dose in comparison to the low dose ($p<0.01$).

TISU BMP-2 cmRNA o-TAM promotes the expression of osteogenic genes by rat, muscle-derived MSCs

Expression of osteogenesis and angiogenesis related genes were quantified at different time points by RT-PCR (Fig. 4B-G). RunX2, collagen type I (Col1), and osteopontin (OPN), markers of osteogenesis, were significantly induced by BMP-2 cmRNA. Expression of osteocalcin (OCN) also trended higher but, unlike the other markers, this did not reach statistical significance. The upregulation of RunX2 and Col1 occurred 14 days post-transfection, effectively matching the early-middle expression of these genes during osteogenesis (14). Notable the induction of OPN occurred as early as 7 days post-transfection, which is interesting considering that OPN is usually considered a late marker for osteogenesis. Expression of vascular endothelial growth factor (VEGF) and CD31, markers of angiogenesis, also increased over time, although neither increase reached statistical significance (Fig. 4F and G). NC cmRNA lacked these inductive effects (results not shown).

Osteogenic properties of TISU BMP-2 cmRNA in vivo in skeletally mature rats

The X-ray and μCT data clearly show more abundant neo-tissue formation within the defect area in the groups that were treated with the TISU BMP-2 cmRNA o-TAMs (Fig. 5C and D). The higher dose of TISU BMP-2 cmRNA (15 μg/defect) produced approximately twice as much new bone as the lower dose (3.75 μg/defect) (Fig. 5D, % BV/TV).

μCT data were confirmed by Masson trichrome staining that also detected bone tissue (compact green) only in the presence of TISU BMP-2 cmRNA (Fig. 6). In contrast, the

Tissue Engineering
An improved, chemically modified RNA encoding BMP-2 enhances osteogenesis in vitro and in vivo (DOI: 10.1089/ten.TEA.2018.0112)

formation of new bone tissue was negligible in the empty group and NC BMP-2 group (Fig. 6A and B). Interestingly, a cartilage-like tissue could be observed at the bridging point of the bone defects treated with the high dose of TISU BMP-2 cmRNA (Fig. 6D, 10x and 20x magnifications). A gradient of mineralizing tissue (stained as solid green) was then observed from the bridging area towards the old bone.

Collagen deposition was confirmed by IHC for Col I, Col II and Col III. For Col I (Fig. 7, left panels), intense deposition was shown in the newly formed bone area around cells (Fig. 7D). There is a clear concentration dependence between TISU BMP-2 cmRNA low and high dose (Fig. 7C and D). In contrast, the NC cmRNA hardly shows any Col I staining except for the native bone part (Fig. 7B). In the empty group, many vessel-like structures are seen, in which the borders are positive for Col I (Fig. 7A). The fracture area shows high deposition of Col II (Fig. 7, middle panels), dose dependently, for TISU BMP-2 cmRNA (Fig. 7C and D). Considerably less Col II is present in the NC cmRNA and empty groups (Fig. 7A and B). A similar pattern to that of Col II is observed for Col III (Fig. 7, right panels).

To detect different vascular infiltration into the defect area among different treatment groups, CD31 staining was performed (Fig. 8, right panel). The endothelial lining of the new blood vessels was confirmed by CD31 staining. In TISU BMP-2 cmRNA treated groups (Fig. 8 C and D), relatively more new vessels grew inside of the newly formed bone tissue. The NC cmRNA (Fig. 8B) showed few vessels, whereas the empty group (Fig. 8A) had more intense staining, although considerably lower than that of the high dose TISU BMP-2 cmRNA group (Fig. 8D).

Concerning leukocyte infiltration, as indicated by CD45 staining, minimal cell infiltrates were seen in all groups (Fig. 8, left panels). Most infiltration is observed in the TISU BMP-2 cmRNA treated groups (Fig. 8C and D), in the active healing area. Lowest infiltration levels were found in the NC cmRNA group (Fig. 8B).

Discussion

These data confirm the enhanced osteogenic properties of the novel TISU BMP-2 cmRNA construct described here. In particular, the inclusion of a TISU sequence led to much higher levels of BMP-2 production by both cell lines and primary cultures of MSCs,

Tissue Engineering
An improved, chemically modified RNA encoding BMP-2 enhances osteogenesis in vitro and in vivo (DOI: 10.1089/ten.TEA.2018.0112)
This paper has been peer-reviewed and accepted for publication, but has yet to undergo copyediting and proof correction. The final published version may differ from this proof.

while reducing the secretion of inflammatory cytokines by human PBMCs. These promising *in vitro* properties were confirmed by *in vivo* experiments showing enhanced bone formation within an osseous critical-size defect in the rat. The ability to produce an effective lipoplex-cmRNA formulation, successfully delivered on a collagen sponge to form a o-TAM, raises the possibility of eventually developing an off-the-shelf product for stimulating osteogenesis locally in human patients. It might be interesting to further investigate how final drying steps impact the function of loaded TISU BMP-2 cmRNA.

The modifications that led to the new BMP-2 cmRNA described here, i.e. nucleotides $5IU_{(0.35)}5IC_{(0.075)}$ and inclusion of a TISU sequence, clearly showed a robust improvement on protein translation. We have compared this new TISU BMP-2 cmRNA to our previously reported cmRNA (pVAX120 BMP-2 cmRNA, $s2U_{(0.25)}m5C_{(0.25)}$ (1, 7, 8)) and confirmed a significantly higher production of BMP-2 *in vitro*. TISU element, first identified by Elfakess and Dikstein (15), has a strict position close to the 5' end of the mRNA molecule and regulates transcription as well as translation (16). This is cap dependent with the best results for the m7G cap (11). Moreover, when TISU is present, no scanning of the mRNA takes place (16). These characteristics are different from the Kozak sequence, where the localization of the sequence is dispersed and not necessarily close to the 5' end. Kozak regulates only translation and depends on scanning of the mRNA (16). As for the modified nucleotides used, the 5-iodo substitution provided the best results when compared to several alternative nucleotide modifications (10). Furthermore, the AU-rich sequence at the 3' end was removed in order to make the mRNA more stable. This AU-rich sequence located in 3'UTRs is associated with fast mRNA degradation as well as reduced translation (17).

In addition to protein translation, the modifications made here to the cmRNA clearly decreased activation of immune-relevant cytokines by hPBMCs *in vitro* compared to unmodified mRNA. Our results show that the initial, mild activation of TNF-α and IFN-γ by cmRNA was much lower than that induced by unmodified mRNA and insufficient to initiate the secondary response represented by increased IL-1β and IL-6 expression. Previously, we have demonstrated that the modification $s2U_{(0.25)}m5C_{(0.25)}$ abolished mRNA interaction with TLRs and decreased expression of TNF-α, IFN-γ and IL-12 *in vivo* (3). Our results are in

Tissue Engineering
An improved, chemically modified RNA encoding BMP-2 enhances osteogenesis in vitro and in vivo (DOI: 10.1089/ten.TEA.2018.0112)

accordance to previously published data. Kariko *et al.* (4) found that modifying mRNA with specific nucleotides reduced toll-like receptors (TLR) mediated secretion of cytokines such as TNF-α, IL-1β and IL-6. Warren *et al.* (18) subsequently demonstrated that complete substitution of cytidine and uridine by modified homologues dramatically attenuated IFN-signaling.

Collectively, these results demonstrate the improved protein translation and reduced immunogenicity of the newly developed TISU BMP-2 cmRNA construct. When combined with 3D biomaterials, in the form of TAMs, sustained release of cmRNAs from the matrix may be obtained that allows the continuous transfection of target cells. In our case, this may enhance osteogenesis when stem cells are used in combination with BMP-2 cmRNA. We have previously reported that loading BMP-2 cmRNA into a fibrin gel enhanced *in vitro* osteogenesis of bone marrow MSCs (8) and *in vivo* bone formation in a non-critical defect model in the rat (1). In the present work, our results indicate strong *in vitro* and *in vivo* osteogenesis in response to the new TISU BMP-2 cmRNA loaded into a collagen sponge. Interestingly, the lowest dose cmRNA used was the most efficient in terms of BMP-2 production by rat, muscle-derived MSCs. This was not seen when MetLuc cmRNA was used to transfect established cell lines *in vitro* (7), suggesting an influence of the collagen sponge or a different response from primary cell cultures. Nevertheless, when the two doses were compared *in vivo*, the highest dose tested showed stronger osteoinductive capacity, supporting superior neo-tissue formation.

In vivo, the cmRNA was administered to a critical-sized bone defect in a rat femur. In the past, we have used a mono-cortical drill-hole defect model to demonstrate the *in vivo* osteogenic properties of BMP-2 cmRNA (1, 7). Here, we used a more clinically-relevant bone defect model that does not heal by itself. µCT analysis clearly showed *de novo* bone formation in the animals treated with the TISU BMP-2 cmRNA, particularly when the highest dose was used. These results were confirmed by histology. The Masson trichrome staining beautifully showed the formation of new tissue within the area of the bone defect. This contained cartilagenous structures that mineralized towards the native bone borders, indicating an endochondral ossification process. Furthermore, Col III and Col II deposits were observed at the fracture area and mostly within the bridging point where

Tissue Engineering
An improved, chemically modified RNA encoding BMP-2 enhances osteogenesis in vitro and in vivo (DOI: 10.1089/ten.TEA.2018.0112)
This paper has been peer-reviewed and accepted for publication, but has yet to undergo copyediting and proof correction. The final published version may differ from this proof.

cartilagenous tissue was observed. Intense areas of Col I were observed in the mineralized new tissue, which indicated a more mature osseous structure forming. Our results collectively demonstrate the *in vivo* osteogenic potential of a newly developed BMP-2 cmRNA, and indicate a possible dose dependency.

Elangovan *et al.* and Khorsand *et al.* also demonstrated the osteogenic properties of nucleotide-modified mRNAs coding for BMP-2 and BMP-9 (5, 6). The authors delivered up to 50 μg of a 100% nucleotide substituted mRNA, via PEI, to a calvarial defect in rats. Four weeks post-administration, the groups treated with the BMP cmRNA showed superior ossification when compared to empty controls. Calvarial ossification occurs via intramembranous ossification (mesenchymal condensation with subsequent differentiation) (19, 20). Hence our results, together with those of Elangovan *et al.* and Khorsand *et al.*, demonstrate that BMP-2 cmRNA stimulates *in vivo* ossification that can follow either of the two mechanisms observed during bone development, endochondral ossification or intramembranous ossification.

An important challenge during bone healing remains adequate vascularization of the new tissue (21, 22). This becomes even more relevant when the reconstruction of large bone defects is needed (22). Our results showed the *in vitro* upregulation of CD31 and VEGF in BMP-2 cmRNA transfected stem cells. *In vivo*, CD31 was expressed in the BMP-2 cmRNA treated groups, where vessel formation was also observed. This indicates a certain level of angiogenesis induced by the BMP-2 cmRNA. This has not been reported before for BMP-2 cmRNA, although several studies reported angiogenic responses *in vitro* and *in vivo* while studying osteogenesis induced by DNA plasmids encoding BMP-2 (23, 24). Nevertheless, some studies concluded that a combination of BMP-2 and VEGF plasmids gave better osteogenic results (23, 25). It would be interesting to study this using the relevant cmRNAs.

Acknowledgements

The support received from the *Deutsche Forschungsgemeinschaft* (DFG) via the Excellence Cluster "Nanosystems Initiative Munich (NIM)" (grant number: EXC 4/3) is greatly appreciated. WZ acknowledges the support received by the PhD program "Medical

Life Science and Technology" at the Technical University of Munich. The authors would like to thank the valuable assistance of Zeljka Trepotec with drafting the mRNA sequences, and Johannes Geiger during the cmRNAs production.

Author Disclosure Statement

No competing financial interest exists for all authors, except MKA and CP. MKA and CP are employees of Ethris GmbH. CP is shareholder of Ethris GmbH.

Tissue Engineering
An improved, chemically modified RNA encoding BMP-2 enhances osteogenesis in vitro and in vivo (DOI: 10.1089/ten.TEA.2018.0112)

Tissue Engineering
An improved, chemically modified RNA encoding BMP-2 enhances osteogenesis in vitro and in vivo (DOI: 10.1089/ten.TEA.2018.0112)

References

1. Ferizi, M., Aneja, M.K., Balmayor, E.R., Badieyan, Z.S., Mykhaylyk, O., Rudolph, C., and Plank, C. Human cellular CYBA UTR sequences increase mRNA translation without affecting the half-life of recombinant RNA transcripts. Sci Rep **6**, 39149, 2016.

2. Holtkamp, S., Kreiter, S., Selmi, A., Simon, P., Koslowski, M., Huber, C., Tureci, O., and Sahin, U. Modification of antigen-encoding RNA increases stability, translational efficacy, and T-cell stimulatory capacity of dendritic cells. Blood **108**, 4009, 2006.

3. Kormann, M.S., Hasenpusch, G., Aneja, M.K., Nica, G., Flemmer, A.W., Herber-Jonat, S., Huppmann, M., Mays, L.E., Illenyi, M., Schams, A., Griese, M., Bittmann, I., Handgretinger, R., Hartl, D., Rosenecker, J., and Rudolph, C. Expression of therapeutic proteins after delivery of chemically modified mRNA in mice. Nature biotechnology **29**, 154, 2011.

4. Kariko, K., Buckstein, M., Ni, H., and Weissman, D. Suppression of RNA recognition by Toll-like receptors: the impact of nucleoside modification and the evolutionary origin of RNA. Immunity **23**, 165, 2005.

5. Elangovan, S., Khorsand, B., Do, A.V., Hong, L., Dewerth, A., Kormann, M., Ross, R.D., Sumner, D.R., Allamargot, C., and Salem, A.K. Chemically modified RNA activated matrices enhance bone regeneration. J Control Release **218**, 22, 2015.

6. Khorsand, B., Elangovan, S., Hong, L., Dewerth, A., Kormann, M.S., and Salem, A.K. A Comparative Study of the Bone Regenerative Effect of Chemically Modified RNA Encoding BMP-2 or BMP-9. AAPS J **19**, 438, 2017.

7. Badieyan, Z.S., Berezhanskyy, T., Utzinger, M., Aneja, M.K., Emrich, D., Erben, R., Schuler, C., Altpeter, P., Ferizi, M., Hasenpusch, G., Rudolph, C., and Plank, C. Transcript-activated collagen matrix as sustained mRNA delivery system for bone regeneration. J Control Release **239**, 137, 2016.

8. Balmayor, E.R., Geiger, J.P., Koch, C., Aneja, M.K., van Griensven, M., Rudolph, C., and Plank, C. Modified mRNA for BMP-2 in Combination with Biomaterials Serves as a Transcript-Activated Matrix for Effectively Inducing Osteogenic Pathways in Stem Cells. Stem Cells Dev **26**, 25, 2017.

9. Schrom, E., Huber, M., Aneja, M., Dohmen, C., Emrich, D., Geiger, J., Hasenpusch, G., Herrmann-Janson, A., Kretzschmann, V., Mykhailyk, O., Pasewald, T., Oak, P., Hilgendorff,

A., Wohlleber, D., Hoymann, H.G., Schaudien, D., Plank, C., Rudolph, C., and Kubisch-Dohmen, R. Translation of Angiotensin-Converting Enzyme 2 upon Liver- and Lung-Targeted Delivery of Optimized Chemically Modified mRNA. Mol Ther Nucleic Acids **7**, 350, 2017.

10. Trepotec, Z., Aneja, M., Geiger, J., Hasenpusch, G., Plank, C., and Rudolph, C. Maximizing the translational yield of mRNA therapeutics by minimizing 5'-UTRs. Tissue Eng Part A 2018.

11. Elfakess, R., Sinvani, H., Haimov, O., Svitkin, Y., Sonenberg, N., and Dikstein, R. Unique translation initiation of mRNAs-containing TISU element. Nucleic Acids Res **39**, 7598, 2011.

12. Jarzebinska, A., Pasewald, T., Lambrecht, J., Mykhaylyk, O., Kummerling, L., Beck, P., Hasenpusch, G., Rudolph, C., Plank, C., and Dohmen, C. A Single Methylene Group in Oligoalkylamine-Based Cationic Polymers and Lipids Promotes Enhanced mRNA Delivery. Angew Chem Int Ed Engl **55**, 9591, 2016.

13. Gharaibeh, B., Lu, A., Tebbets, J., Zheng, B., Feduska, J., Crisan, M., Peault, B., Cummins, J., and Huard, J. Isolation of a slowly adhering cell fraction containing stem cells from murine skeletal muscle by the preplate technique. Nat Protoc **3**, 1501, 2008.

14. Aubin, J.E. Mesenchymal Stem Cells and Osteoblast Differentiation. In: Bilezikian J.P., Raisz L.G., Martin T.J., eds. Principles of Bone Biology. Third Edition ed. San Diego, CA, USA: Academic Press. Inc. (Elsevier); 2008. pp. 85.

15. Elfakess, R., and Dikstein, R. A translation initiation element specific to mRNAs with very short 5'UTR that also regulates transcription. PLoS One **3**, e3094, 2008.

16. Dikstein, R. Transcription and translation in a package deal: the TISU paradigm. Gene **491**, 1, 2012.

17. Chen, C.Y., and Shyu, A.B. AU-rich elements: characterization and importance in mRNA degradation. Trends Biochem Sci **20**, 465, 1995.

18. Warren, L., Manos, P.D., Ahfeldt, T., Loh, Y.H., Li, H., Lau, F., Ebina, W., Mandal, P.K., Smith, Z.D., Meissner, A., Daley, G.Q., Brack, A.S., Collins, J.J., Cowan, C., Schlaeger, T.M., and Rossi, D.J. Highly efficient reprogramming to pluripotency and directed differentiation of human cells with synthetic modified mRNA. Cell Stem Cell **7**, 618, 2010.

19. Balmayor, E.R., and van Griensven, M. Stem Cell Therapy for Bone Disorders. In: Chase L.G., Vemuri M.C., eds. Mesenchymal Stem Cell Therapy. New York: Humana Press; 2012. pp. 101.

Tissue Engineering
An improved, chemically modified RNA encoding BMP-2 enhances osteogenesis in vitro and in vivo (DOI: 10.1089/ten.TEA.2018.0112)
This paper has been peer-reviewed and accepted for publication, but has yet to undergo copyediting and proof correction. The final published version may differ from this proof.

20. Clines, G.A. Prospects for osteoprogenitor stem cells in fracture repair and osteoporosis. Curr Opin Organ Transplant **15**, 73, 2010.

21. Grosso, A., Burger, M.G., Lunger, A., Schaefer, D.J., Banfi, A., and Di Maggio, N. It Takes Two to Tango: Coupling of Angiogenesis and Osteogenesis for Bone Regeneration. Front Bioeng Biotechnol **5**, 68, 2017.

22. Roux, B.M., Cheng, M.H., and Brey, E.M. Engineering clinically relevant volumes of vascularized bone. J Cell Mol Med **19**, 903, 2015.

23. Samee, M., Kasugai, S., Kondo, H., Ohya, K., Shimokawa, H., and Kuroda, S. Bone morphogenetic protein-2 (BMP-2) and vascular endothelial growth factor (VEGF) transfection to human periosteal cells enhances osteoblast differentiation and bone formation. Journal of pharmacological sciences **108**, 18, 2008.

24. Wang, C.J., Weng, L.H., Hsu, S.L., Sun, Y.C., Yang, Y.J., Chan, Y.S., and Yang, Y.L. pCMV-BMP-2-transfected cell-mediated gene therapy in anterior cruciate ligament reconstruction in rabbits. Arthroscopy **26**, 968, 2010.

25. Peng, H., Usas, A., Olshanski, A., Ho, A.M., Gearhart, B., Cooper, G.M., and Huard, J. VEGF improves, whereas sFlt1 inhibits, BMP2-induced bone formation and bone healing through modulation of angiogenesis. J Bone Miner Res **20**, 2017, 2005.

Tissue Engineering
An improved, chemically modified RNA encoding BMP-2 enhances osteogenesis in vitro and in vivo (DOI: 10.1089/ten.TEA.2018.0112)

Table 1. Characteristic size, polydispersity index and electrokinetic potential of the TISU BMP-2 cmRNA and NC cmRNA lipoplexes. Each value represents the mean ± SD.

Lipoplex LF92	Assembling medium	Mean hydrated diameter Dh (nm)	Polydispersity index, PdI	Electrokinetic potential ξ (mV)
TISU BMP2cmRNA	Water	80.89 ± 1.09	0.211 ± 0.007	+18.1 ± 3.7
TISU NCcmRNA		82.45 ± 0.44	0.209 ± 0.001	+20.0 ± 4.2

Tissue Engineering
An improved, chemically modified RNA encoding BMP-2 enhances osteogenesis in vitro and in vivo (DOI: 10.1089/ten.TEA.2018.0112)
This paper has been peer-reviewed and accepted for publication, but has yet to undergo copyediting and proof correction. The final published version may differ from this proof.

Tissue Engineering
An improved, chemically modified RNA encoding BMP-2 enhances osteogenesis in vitro and in vivo (DOI: 10.1089/ten.TEA.2018.0112)

Figure Legends

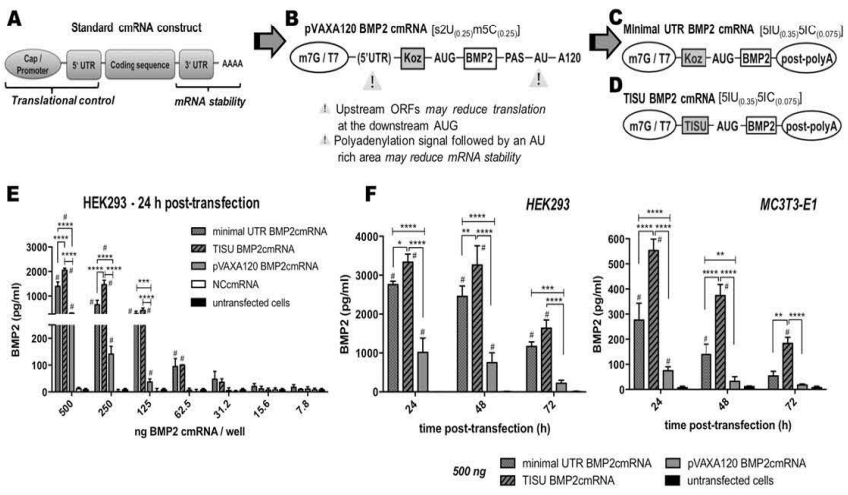

Fig. 1. Schematic representation of cmRNA constructs and BMP-2 production in cell lines. (**A**) Standard cmRNA structures include cap and 5'UTR for recognition and translation, a coding sequence, and a 3'UTR followed by the poly (A) tail. Both last elements are responsible for RNA stability. (**B**) Sequence of the BMP-2 cmRNA previously reported by us and produced from a pVAXA120 plasmid. Undesirable features such as upstream ORF in the 5'UTR, polyadenylation element and AU-rich tract in the 3'UTR are indicated. New BMP-2 cmRNAs produced here included 5-iodo modified nucleotides and different 5'UTR elements, either (**C**) Minimal UTR or (**D**) TISU element. The BMP-2 production in cells transfected with the newly produced BMP-2 cmRNAs was evaluated and compared to the pVAXA120 BMP-2 cmRNA. (**E**) BMP-2 production 24 hours after HEK293 transfection with 7.8 ng - 500 ng BMP-2 cmRNAs/well. (**F**) BMP-2 production over time for transfected HEK293 and MC3T3-E1 (500 ng/well). In all transfections, NC cmRNA transfected and untransfected cells were analyzed as controls. Obtained p-values are indicated as follows: *p≤0.05, **p≤0.01, ***p≤0.001 and ****p≤0.0001. In addition, the symbol # is used to indicate p-values ≤0.05 obtained when analyzed groups were compared with untransfected cells. n=3, mean ± SD.

Tissue Engineering
An improved, chemically modified RNA encoding BMP-2 enhances osteogenesis in vitro and in vivo (DOI: 10.1089/ten.TEA.2018.0112)

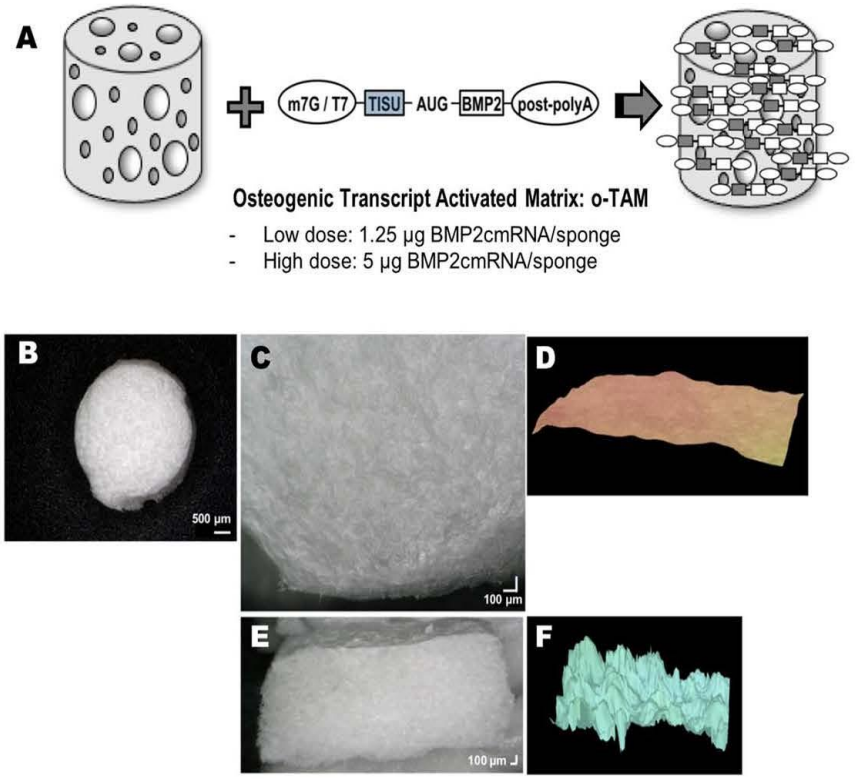

Fig. 2. (**A**) Fabrication of the osteogenic transcript activated matrix (o-TAM) by loading two doses of TISU BMP-2 cmRNA into collagen sponges. o-TAMs with either low dose (1.25 µg) or high dose (5 µg) cmRNA were produced. (**B, C**) Digital light microscopy images showing the appearance of the obtained o-TAMs. (**D**) Surface characteristics of the o-TAMs. (**E, F**) Transversal section showing higher porosity features that characterizes the interior of the o-TAMs.

Tissue Engineering
An improved, chemically modified RNA encoding BMP-2 enhances osteogenesis in vitro and in vivo (DOI: 10.1089/ten.TEA.2018.0112)
This paper has been peer-reviewed and accepted for publication, but has yet to undergo copyediting and proof correction. The final published version may differ from this proof.

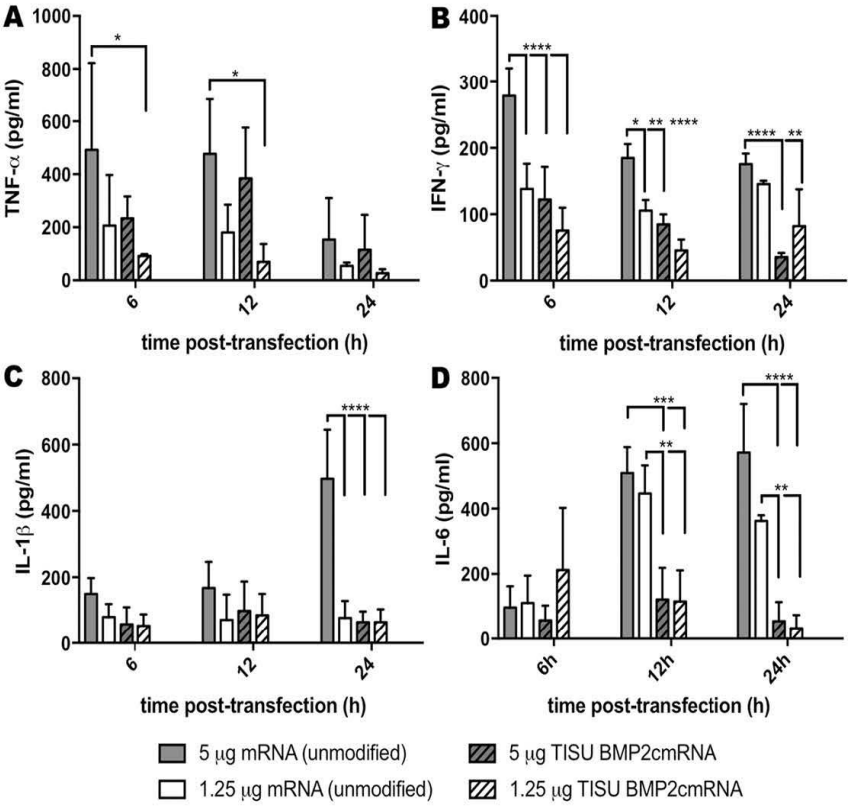

Fig. 3. Inflammatory cytokine production by hPBMCs *in vitro* up to 24 hours post-exposure to low or high dose TISU BMP-2 cmRNA o-TAMs. Unmodified BMP-2 cmRNA, also loaded into collagen sponges, was used as control. (**A**) TNF-α, (**B**) IFN-γ, (**C**) IL-1β and (**D**) IL-6 were evaluated. Obtained p-values are indicated as follows: *p≤0.05, **p≤0.01, ***p≤0.001 and ****p≤0.0001. N=3 donors and n=3 triplicate for each donor, mean ± SD.

Tissue Engineering
An improved, chemically modified RNA encoding BMP-2 enhances osteogenesis in vitro and in vivo (DOI: 10.1089/ten.TEA.2018.0112)

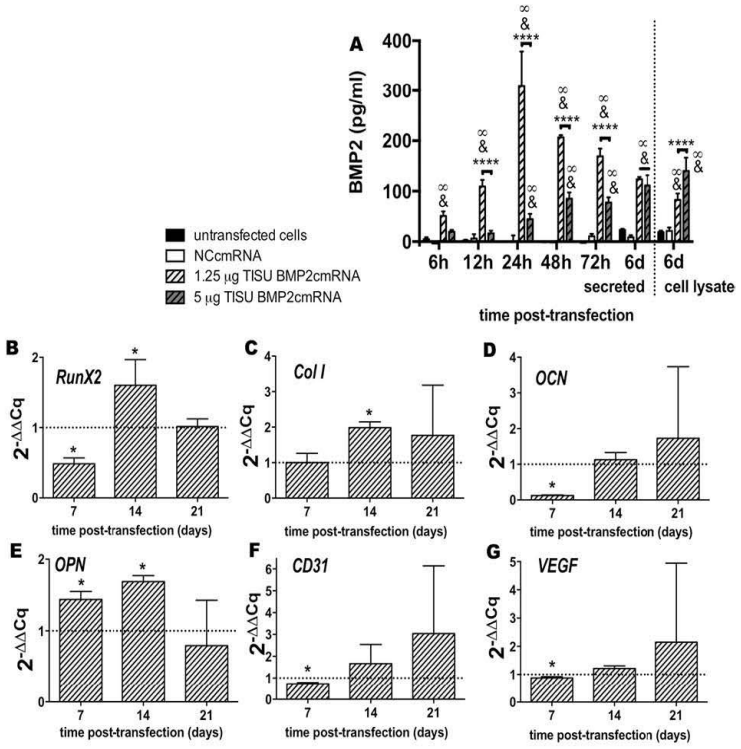

Fig. 4. BMP-2 production by rat, muscle-derived MSCs and resulting gene expression as consequence of TISU BMP-2 cmRNA o-TAM transfection. (**A**) BMP-2 production is shown for up to 6 days post-transfection. Either low dose (1.25 μg/sponge) or high dose (5 μg/sponge) TISU BMP-2 cmRNA was used for transfection. Additionally, NC cmRNA (1.25 μg/sponge) was used as a control. Untransfected cells were also evaluated as controls. Obtained p-values are indicated as ****p≤0.0001. In addition, the symbol & is used to indicate p-values ≤0.05 obtained when TISU BMP-2 cmRNA was compared with NC cmRNA. Similarly, the symbol ∞ is used to indicate p-values ≤0.05 obtained when TISU BMP-2 cmRNA was compared with untransfected cells. N=3 donors and n=3 triplicate for each donor, mean ± SD. Expression of osteogenic [(**B**) RunX2, (**C**) Col I, (**D**) OCN and (**E**) OPN] and angiogenic genes [(**F**) CD31 and (**G**) VEGF] at 7, 14 and 21 days post-TISU BMP-2 cmRNA transfections by using the low dose o-TAM. Obtained p-values are indicated as *p≤0.05. Results are normalized to the housekeeping gene (rat β-tubulin) and to the untransfected cells. N=3 donors and n=3 triplicate for each donor, mean ± SD.

Tissue Engineering
An improved, chemically modified RNA encoding BMP-2 enhances osteogenesis in vitro and in vivo (DOI: 10.1089/ten.TEA.2018.0112)

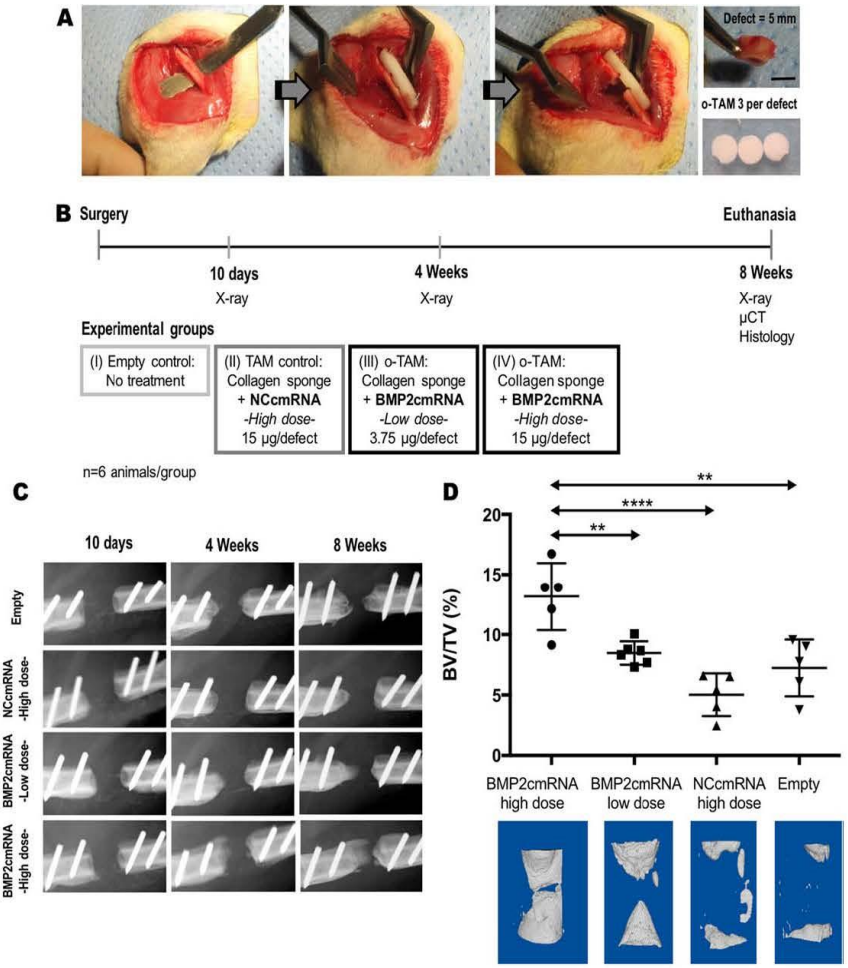

Fig. 5. Schematic representation of (**A**) surgical approach and (**B**) surgery time line and experimental groups tested *in vivo* in a femoral critical-sized defect in rats. (**C**) x-ray evaluation at 10 days, 4 weeks and 8 weeks after treatment. (**D**) Representative 3D reconstruction of the µCT images obtained for each group at 8 weeks after treatment. BV/TV (%) as calculated by the CTAn software. The values obtained for each individual sample are shown. Obtained p-values are indicated as **p≤0.01 and ****p≤0.0001. N=6 animals per group.

Tissue Engineering
An improved, chemically modified RNA encoding BMP-2 enhances osteogenesis in vitro and in vivo (DOI: 10.1089/ten.TEA.2018.0112)

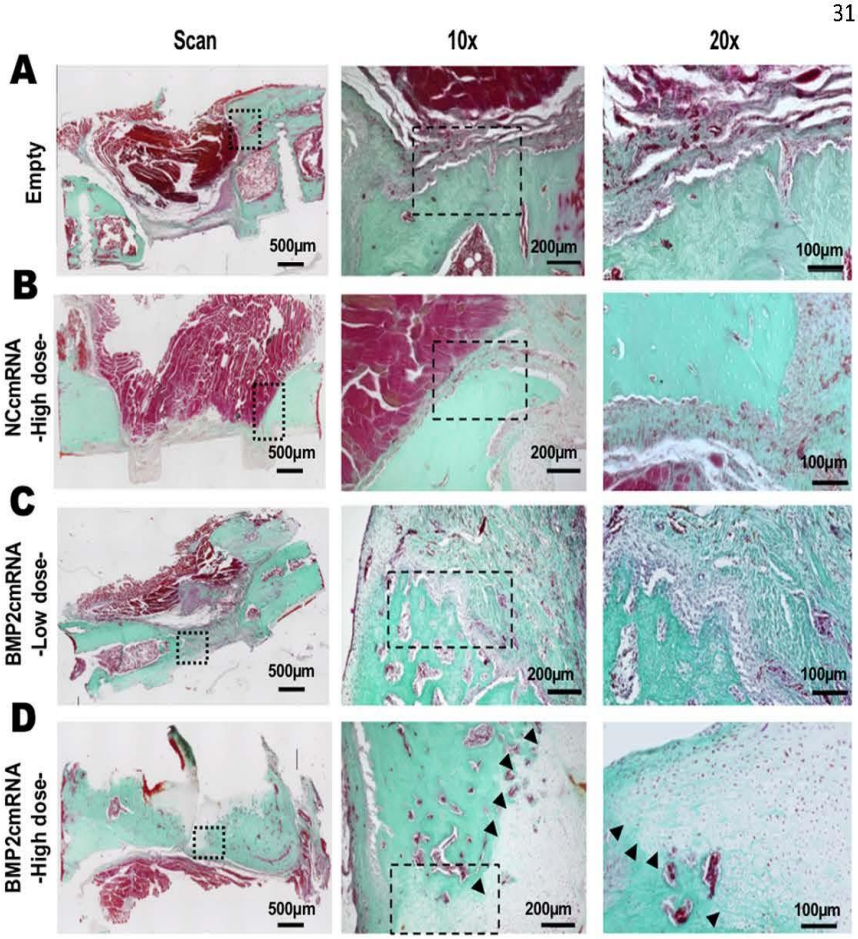

Fig. 6. Histological analysis of bone defects after 8 weeks. Masson trichrome staining for (**A**) empty and (**B**) NC cmRNA control groups as well as (**C**) low dose BMP-2 cmRNA (3.75 µg/defect) and (**D**) high dose BMP-2 cmRNA (15 µg/defect). From left to right, a general scan of the entire section, 10x and 20x magnifications images are displayed. Red staining = muscle, Green staining = collagen (bony tissue)

Tissue Engineering
An improved, chemically modified RNA encoding BMP-2 enhances osteogenesis in vitro and in vivo (DOI: 10.1089/ten.TEA.2018.0112)

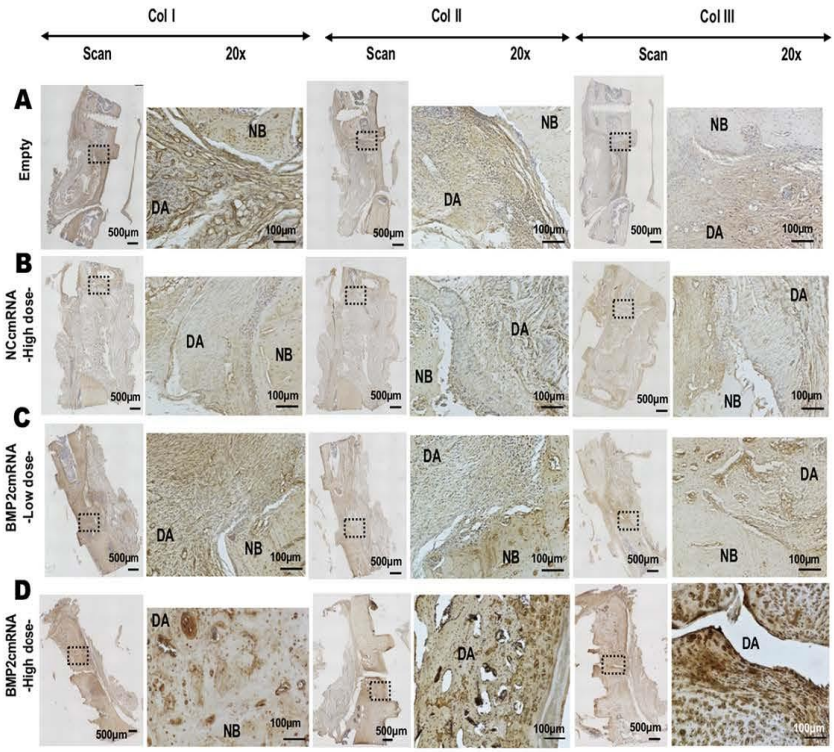

Fig. 7. Immunohistochemistry for Col I, Col II and Col III deposition in bone defects after 8 weeks. Groups: (**A**) empty and (**B**) NC cmRNA control groups as well as (**C**) low dose BMP-2 cmRNA (3.75 µg/defect) and (**D**) high dose BMP-2 cmRNA (15 µg/defect) were evaluated. From left to right, Col I, then Col II followed by Col III images are represented. For each staining, a general scan of the entire section as well as 20x magnifications images are shown. Inserts in scans are indicative of the area where the high magnification picture was taken. In the pictures, native bone is indicated by NB and defect area by DA.

Tissue Engineering
An improved, chemically modified RNA encoding BMP-2 enhances osteogenesis in vitro and in vivo (DOI: 10.1089/ten.TEA.2018.0112)
This paper has been peer-reviewed and accepted for publication, but has yet to undergo copyediting and proof correction. The final published version may differ from this proof.

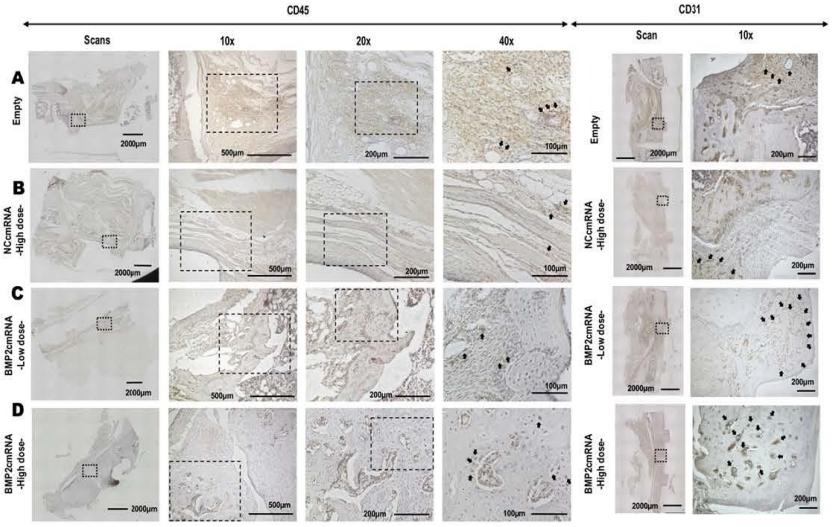

Fig. 8. Immunohistochemistry for CD45 and CD31 expression in bone defects after 8 weeks. Groups: (**A**) empty (**B**) NC cmRNA control groups (**C**) low dose BMP-2 cmRNA (3.75 μg/defect) (**D**) high dose BMP-2 cmRNA (15 μg/defect). For CD45 staining, a general scan of the entire section as well as 10x, 20x and 40x magnification images are shown. Examples of leukocyte infiltration are indicated with arrows. For CD31, a general scan of the entire section as well as 10x magnification images are shown. Examples of new vessel growth are indicated with arrows. Inserts in scans indicate the area where the high magnification picture was taken.

10.2 Abbreviations

o-TAMs	osteo-inductive transcript-activated matrix
cmRNA	chemically modified mRNA
uOPF	Upstream open reading frame
UTR	Untranslated Regions
TISU	translation initiator of short UTRs
BMP	Bone Morphogenetic Protein
µCT	Micro-Computed Tomography
PGA	Poly glycolic acid
PLA	Poly lactic acid
FDA	Food and Drug Administration
TGF	Transforming growth factor
BMPR-I	BMP-I receptor
BMPR-II	BMP-II receptor
GS region	glycine- and serine-rich region
MAPKs	Mitogen-activated protein kinases
BSP	bone sialoprotein
Cbfa1	core-binding factor-1
OSE2	osteoblast-specific cis-acting element 2
OPN	osteopontin
Osx	Osterix
rhBMPs	human recombinant BMPs
ALIF	anterior lumbar interbody fusion
AUE	AU-rich elements

PIC	pre-initiation complex
IVT	*in vitro* transcription
GM-CSF	granulocyte/ macrophage colony-stimulating factor
hPBMCs	human peripheral blood mononuclear cells
CYBA	cytochrome b-245 alpha polypeptide
DMEM	Dulbecco's Modified Eagle's Medium
α-MEM	alpha Minimum essential medium
FBS	Fetal Bovine Serum
MSCs	Mesenchymal stem cells
DPBS	Dulbecco's Phosphate-Buffered Saline without Calcium and Magnesium
NC	non-coding
ELISA	Enzyme-linked immunosorbent assay
DPPC	1,2-dipalmitoyl-snglycero-3-phosphocholine
DMG-PEG2k	1, 2-dimyristoyl-sn-glycerol methoxy polyethylene glycol
DLS	dynamic light scattering
RT	Room Temperature
TNF- α	tumor necrosis factor alpha
IFN- γ	Interferon gamma
IL-1 α	Interleukin 1 alpha
IL-6	Interleukin 6
RT-qPCR	real-time polymerase chain reaction
VEGF	Vascular endothelial growth factor
RUNX2	Runt-related transcription factor 2
Col I	Collagen I

Col II	Collagen II
Col III	Collagen III
BV	bone volume
TV	tissue volume
IHC	Immunohistochemistry
EDTA	Ethylenediaminetetraacetic acid
H & E	Hematoxylin and Eosin

10.3 List of Figures and Tables

Acknowledgements

Since Oct 2015, I have started an adventure here in Technical University of Munich (TUM). After four years, this PhD study is finally coming to an end. Now in my heart, there is no more words but thanks. So here I am sincerely writing down all my gratefulness to everyone who participated in my exiting journey of PhD study.

The work summarized in this thesis was carried out during the years 2015-2019 at the company Ethris GmbH, Department of Experimental Trauma Surgery – TUM and at the Mayo Clinic, Rochester (MN) USA.

First, I am deeply grateful to PD Carsten Rudolph and Prof. Christian Plank, owners of the company Ethris GmbH in Planegg, who provided me with this great opportunity to pursue my scientific carrier in the field of RNA therapeutics. Especially my supervisor Prof. Christian Plank, during four years, his patient guidance, encouragement and enthusiasm supported me to explore and overcome difficulties in my research.

I would like to express my deepest appreciation to my second mentor, Prof. Martijn van Griensven. He allowed me to have a space in the Experimental Trauma Surgery and perform most of my sample analyses. Without his support, I would have not been able to perform most of the studies comprised in this thesis work.

I would also like to thank Prof. Percy Knolle, director of the Institute of Molecular Immunology – Experimental Oncology (IMI-Experimental Oncology) for financially supporting me and constructive suggestions during the institute seminars.

Furthermore, I owe my deepest heartfelt gratitude to PD Elizabeth Rosado Balmayor, who has been extraordinarily patient and supportive. Without her, both my thesis and publication would not have been possible. Dear Elizabeth, I cannot thank you more for all your constructive comments, patient guidance and help during my PhD study. It was a big pleasure for me to work with you together in the past years. Thank you also for the amazing amount of work you carried out for my thesis at the Mayo Clinic during several stays. In this context, I would like to present my sincere thanks to Prof. Christopher H. Evans and his amazing team at the Mayo clinic. Particularly, to Dr. Rodolfo de la Vega Amador for performing all the surgeries described in this thesis and Mike Coenen for assisting. There was no other chance for me to have all those nice in vivo experiment results without their hard work.

Many thanks to all the teammates who helped me with my PhD work for their support and insightful comments and suggestions during work. Dear Dr. Manish K. Aneja and Dr. Johannes Geiger, thanks for taking care of me during the time of my research in Ethris. I really felt welcome and enjoyed working with you. A special thanks also to Carlos Peniche Silva for his tremendous help with the immunohistochemistry.

Last but not the least I would like to thank my family members and friends.

I would like to thank my parents for their understanding and support during my thesis, most importantly for letting me live my dream. I might not be able to be there whenever they need me; however, I will not stop trying to make them proud. Moreover, for my friends, I know that it was not always easy for me to stick to every appointment. Thank you, people, for being so tolerant with me.

Again, thanks for everything!